axioms

IMPACT FACTOR 1.6

Article

Quantum Field Theory of 3+1 Dimensional BTZ Gravity: Graviton Self-Energy, Axion Interactions, and Dark Matter in the Ultrahyperfunction Framework

Hameeda Mir, Angelo Plastino, Behnam Pourhassan and Mario Carlos Rocca

MDPI

https://doi.org/10.3390/axioms14110810

axioms

MDPI

Article

Quantum Field Theory of 3+1 Dimensional BTZ Gravity: Graviton Self-Energy, Axion Interactions, and Dark Matter in the Ultrahyperfunction Framework

Hameeda Mir [1,2,3], Angelo Plastino [4,5,6], Behnam Pourhassan [1,7,8] and Mario Carlos Rocca [1,4,5,9,*]

[1] School of Physics, Damghan University, Damghan 3671641167, Iran; hameeda@candqrc.ca (H.M.); b.pourhassan@du.ac.ir (B.P.)
[2] Department of Physics, Government Degree College, Tangmarg 193402, Kashmir, India
[3] Inter University Center for Astronomy and Astrophysics, Pune 411007, Maharashtra, India
[4] Departamento de Física, Universidad Nacional de La Plata, La Plata 1900, Argentina; plastino@fisica.unlp.edu.ar
[5] Consejo Nacional de Investigaciones Científicas y Tecnológicas, (IFLP-CCT-CONICET)-C. C. 727, La Plata 1900, Argentina
[6] Academia de Ciencias de America Latina, Caracas 1012, Venezuela
[7] Centre of Research Impact and Outcome, Chitkara University, Rajpura 140417, Punjab, India
[8] Center for Theoretical Physics, Khazar University, 41 Mehseti Street, Baku AZ1096, Azerbaijan
[9] Departamento de Matemática, Universidad Nacional de La Plata, La Plata 1900, Argentina
* Correspondence: mariocarlosrocca@candqrc.ca

Abstract

We present a comprehensive quantum field theoretical analysis of graviton self-energy and mass generation in 3+1 dimensional BTZ black hole spacetime, incorporating axion interactions within the framework of dark matter theory. Using a novel mathematical approach based on ultrahyperfunctions, generalizations of Schwartz tempered distributions to the complex plane, we derive exact quantum relativistic expressions for graviton and axion self-energies without requiring ad hoc regularization procedures. Our approach extends the Gupta–Feynman quantization framework to BTZ gravity while introducing a new constraint that eliminates unitarity violations inherent in previous formulations, thereby avoiding the need for ghost fields. Through systematic application of generalized Feynman parameters, we evaluate both bradyonic and tachyonic graviton modes, revealing distinct quantum correction patterns that depend critically on momentum, energy, and mass parameters. Key findings include (1) natural graviton mass generation through cosmological constant interactions, yielding $m^2 = 2|\Lambda|/\kappa(1-\kappa)$; (2) qualitatively different quantum behaviors between bradyonic and tachyonic modes, with bradyonic corrections reaching amplitudes 6 times larger than their tachyonic counterparts; (3) the discovery of momentum-dependent quantum dissipation effects that provide natural ultraviolet regulation; and (4) the first explicit analytical expressions and graphical representations for 17 distinct graviton self-energy contributions. The ultrahyperfunction formalism proves essential for handling the non-renormalizable nature of the theory, providing mathematically rigorous treatment of highly singular integrals while maintaining Lorentz invariance. Our results suggest observable consequences in gravitational wave propagation through frequency-dependent dispersive effects and modifications to black hole thermodynamics, potentially bridging theoretical quantum gravity with experimental constraints.

Keywords: quantum field theory; Einstein gravity; axions; dark matter; non-renormalizable theories; unitarity; ultrahyperfunctions

Academic Editor: Wilson A. Zuniga-Galindo

Received: 23 September 2025
Revised: 14 October 2025
Accepted: 18 October 2025
Published: 31 October 2025

Citation: Mir, H.; Plastino, A.; Pourhassan, B.; Rocca, M.C. Quantum Field Theory of 3+1 Dimensional BTZ Gravity: Graviton Self-Energy, Axion Interactions, and Dark Matter in the Ultrahyperfunction Framework. *Axioms* **2025**, *14*, 810. https://doi.org/10.3390/axioms14110810

MSC: 46A11; 46F15; 46F20; 81T20; 83C35; 83C47; 83C56

1. Introduction

The quantum nature of gravity remains one of the most profound and enduring challenges in theoretical physics, fundamentally reshaping our understanding of how quantum mechanical principles interact with and modify classical gravitational phenomena. This challenge becomes particularly acute when attempting to reconcile the smooth, continuous nature of Einstein's general relativity with the discrete, probabilistic framework of quantum mechanics. The BTZ (Bañados–Teitelboim–Zanelli) black hole [1], as an exact solution to $(2+1)$-dimensional gravity with a negative cosmological constant $\Lambda < 0$, has emerged as an invaluable theoretical laboratory for exploring the intricate interplay between quantum field theory and gravitational dynamics. This remarkable spacetime configuration provides a unique window into quantum gravitational effects while maintaining sufficient mathematical tractability to permit detailed analytical investigation.

While the BTZ black hole has been extensively studied within the framework of the AdS/CFT correspondence [2,3] and holographic duality principles, revealing deep connections between gravitational physics in the bulk and conformal field theories on the boundary, the quantum properties of gravitons within BTZ spacetime, particularly when extended to higher-dimensional analogues, remain incompletely understood and present numerous unresolved questions. The extension to $(3+1)$-dimensional BTZ-like geometries introduces additional complexity while preserving many of the advantageous features that make the original BTZ solution so amenable to analytical treatment. This dimensional enhancement allows for a more direct connection to our four-dimensional universe while maintaining the essential geometric and topological properties that render BTZ spacetimes so theoretically valuable [4].

A fundamental and longstanding question in quantum gravity concerns the intrinsic properties of gravitons, the hypothetical quantum mediators of the gravitational force, whose existence is predicted by quantum field theory but whose direct detection remains beyond current experimental capabilities. Of particular theoretical and phenomenological significance is the possibility of graviton mass generation through purely quantum mechanical effects, a phenomenon that could arise naturally from the interaction between quantum fluctuations and the background spacetime geometry. The relationship between such quantum-induced mass generation and the cosmological constant Λ presents both profound theoretical implications for our understanding of quantum gravity and potentially observable consequences for gravitational wave propagation, black hole thermodynamics, and large-scale cosmological evolution [5–8].

The BTZ black hole, with its relatively simple yet non-trivial geometric structure combined with remarkably rich physical content, provides an ideal theoretical setting for investigating these quantum gravitational phenomena in a controlled and mathematically tractable environment. Unlike more complex black hole solutions in higher dimensions, the BTZ geometry allows for exact analytical treatment of quantum field theory in curved spacetime while preserving the essential features of event horizons, thermodynamic properties, and causal structure that characterize genuine black hole physics. This unique combination of mathematical simplicity and physical richness makes BTZ spacetimes particularly suitable for developing and testing new approaches to quantum gravity, serving as a bridge between the well-understood flat spacetime quantum field theory and the more challenging arena of quantum gravity in realistic astrophysical environments [9,10].

Previous studies have primarily focused on the classical aspects of BTZ black holes, examining their geometric properties, thermodynamic behavior, and causal structure, or, alternatively, on their profound holographic implications within the context of the AdS/CFT correspondence [11,12]. These investigations have yielded significant insights into the nature of black hole entropy, Hawking radiation, and the holographic principle, establishing BTZ black holes as paradigmatic examples of the deep connections between gravity and quantum field theory. However, while quantum field theory in curved spacetime has been successfully applied to various black hole geometries, revealing important phenomena such as particle creation near event horizons and the emergence of thermodynamic properties from quantum effects, a comprehensive and systematic analysis of graviton self-energy and its far-reaching implications for mass generation mechanisms in BTZ spacetime has been conspicuously lacking in the literature.

This gap in our understanding becomes particularly pronounced and theoretically significant when considering the context of $(3+1)$-dimensional extensions of BTZ gravity, where the interplay between quantum effects and the underlying geometric structure becomes substantially more intricate and mathematically challenging. The transition from the relatively well-understood $(2+1)$-dimensional case to the more physically relevant $(3+1)$-dimensional scenario introduces additional degrees of freedom and complexity in the gravitational field, necessitating more sophisticated analytical techniques and a deeper understanding of how quantum corrections modify classical gravitational dynamics. Furthermore, the higher-dimensional setting allows for a more direct connection to realistic astrophysical scenarios while preserving many of the mathematical advantages that make BTZ-type solutions so amenable to detailed theoretical investigation [13,14].

In this paper, we present a comprehensive quantum field theoretical investigation of graviton properties in $(3+1)$-dimensional BTZ black holes, with particular emphasis on the detailed computation of graviton self-energy contributions and their profound implications for quantum mass generation mechanisms. Our theoretical approach builds systematically upon the well-established Gupta–Feynman quantization framework, a formalism that has proven particularly effective for handling gauge theories with constraint structures similar to those encountered in gravitational physics. We incorporate both gravitational self-interactions and cosmological constant contributions in a unified and mathematically rigorous manner that naturally reveals their intricate quantum interplay and demonstrates how these fundamental interactions conspire to generate observable physical effects.

Through careful and systematic analysis of the graviton propagator structure and the evaluation of higher-order self-energy contributions using advanced techniques from quantum field theory in curved spacetime, we demonstrate how the inclusion of a cosmological constant Λ leads naturally and inevitably to graviton mass generation through purely quantum mechanical processes. Our analysis yields the explicit result $m^2 = \frac{2|\Lambda|}{\kappa(1-\kappa)}$, where κ represents the gravitational coupling constant, providing a direct and quantitative connection between the cosmological constant and the emergent graviton mass scale. This relationship not only represents a significant theoretical advance in our understanding of quantum gravity but also suggests potential observational signatures that could be detected through precision measurements of gravitational wave propagation or modifications to black hole thermodynamics [15–19].

Our investigation employs the powerful mathematical framework of generalized Feynman parameters, a sophisticated technique that extends beyond conventional Feynman parametrization to handle the complex multi-loop integrals and singular behavior that naturally arise in quantum gravitational calculations. This advanced methodology proves particularly well-suited for evaluating both bradyonic modes, corresponding to conventional massive particle excitations with positive energy–momentum dispersion

relations, and tachyonic modes, representing the more exotic excitations characterized by imaginary mass parameters and superluminal phase velocities that can emerge in certain quantum field theoretical contexts. Through systematic application of this parametrization scheme, we obtain fully explicit analytical expressions for various components of the graviton self-energy tensor, capturing the complete tensor structure that reflects the spin-2 nature of gravitational interactions and the underlying diffeomorphism symmetries of the theory [20–22].

This comprehensive analysis reveals remarkably distinct and physically meaningful behavioral patterns across different kinematic regimes, each characterized by unique signatures when explored through multiple interconnected parameter spaces that encompass mass dependencies, momentum transfer characteristics, and energy scale variations. The mass dependence exhibits particularly intriguing features, showing how quantum corrections scale with the emergent graviton mass and demonstrating clear distinctions between the light graviton limit, where classical general relativity should be recovered, and the massive graviton regime, where quantum effects become increasingly prominent. The momentum dependence reveals unexpected dissipative quantum effects that grow systematically with increasing momentum transfer, suggesting the presence of natural ultraviolet regulation mechanisms that could potentially address some of the notorious divergence problems that plague attempts at quantum gravity. Meanwhile, the energy scale dependence illuminates the transition between different physical regimes, from the low-energy domain where classical gravitational physics dominates to the high-energy quantum regime where graviton self-interactions become the primary determinant of physical behavior [23–25].

These results provide fundamentally new insights into the quantum nature of gravity within BTZ spacetimes, revealing how quantum mechanical effects modify classical gravitational dynamics in ways that are both mathematically precise and potentially observable. The analysis demonstrates that quantum gravitational effects in BTZ backgrounds exhibit a rich hierarchical structure, with different physical phenomena becoming dominant across various energy and length scales, thereby providing a detailed roadmap for understanding how classical general relativity emerges from an underlying quantum gravitational theory. Furthermore, our findings contribute significantly to the broader theoretical understanding of the fundamental relationship between cosmological constants and graviton mass generation mechanisms, establishing clear mathematical connections between these seemingly disparate aspects of gravitational physics and suggesting that the cosmological constant may play a more active and dynamic role in quantum gravitational dynamics than previously anticipated.

A crucial mathematical tool in our analysis is the sophisticated theory of ultradistributions, which provides a rigorously formulated and mathematically consistent framework for handling the notoriously challenging quantum field theoretical calculations that arise naturally in curved spacetime environments. Unlike conventional approaches to quantum field theory in flat spacetime, calculations in curved backgrounds frequently encounter severe mathematical difficulties associated with the non-trivial geometric structure of the underlying manifold, the presence of event horizons, and the complex interplay between quantum fluctuations and gravitational fields. Ultradistributions address these fundamental challenges by extending far beyond the scope of traditional distribution theory, encompassing a much broader class of highly singular functions and mathematical operations that arise unavoidably in quantum field theory when dealing with curved spacetime geometries and non-trivial topological configurations.

This powerful mathematical framework, originally developed by the pioneering work of Sebastião e Silva [26] and subsequently refined and extended through the fundamental

contributions of Hasumi [27], proves particularly valuable and indeed indispensable in our specific theoretical context. The framework allows for the systematic and mathematically rigorous treatment of divergent integrals that would otherwise render conventional analytical approaches ineffective or mathematically ill-defined while simultaneously providing the proper mathematical foundation for defining products of distributions that occur ubiquitously in the evaluation of graviton self-energy contributions. These products of distributions represent one of the most technically challenging aspects of quantum field theory in curved spacetime, as they involve mathematical operations that are typically undefined or divergent within the standard framework of Schwartz distribution theory.

The systematic application of ultradistributions in our analysis enables us to obtain finite, well-defined, and physically meaningful results without requiring the introduction of ad hoc regularization procedures that often obscure the underlying physical content and introduce artificial parameters that must be eliminated through renormalization schemes. This mathematical consistency represents a significant methodological advance, as it provides a genuinely fundamental foundation for our quantum gravitational analysis that respects both the mathematical rigor demanded by modern theoretical physics and the physical principles that govern gravitational interactions. The comprehensive theoretical development of ultradistributions has been extensively documented and systematically explored in the foundational References [28–30], which present a complete mathematical theory encompassing both the abstract theoretical foundations and the practical computational techniques necessary for applications to physical problems.

The practical utility and theoretical depth of ultrahyperfunctions have been demonstrated through numerous sophisticated applications across diverse areas of mathematical physics. Franco and Renoli, together with their collaborators, have made several groundbreaking applications of ultrahyperfunctions of remarkable mathematical depth to both pure mathematics and theoretical physics [31–33], establishing the framework as a powerful tool for addressing previously intractable problems in quantum field theory and mathematical analysis. Building upon these foundational developments, Plastino and Rocca have made significant mathematical advances through their systematic development of a simplified yet mathematically consistent version of convolution theory for ultrahyperfunctions [34], culminating in important applications to the quantization of fundamental fields, including gravitons, axions, and dark matter components.

The versatility and power of the ultrahyperfunction approach (see Appendix G) have been further demonstrated through extensive applications to various topics in statistical mechanics and quantum field theory [35–40], with the majority of these investigations focusing specifically on gravitational phenomena and their quantum mechanical manifestations. These applications have revealed the particular effectiveness of ultrahyperfunctions in handling the mathematical complexities associated with gravitational theories, where the non-linear nature of Einstein's equations and the gauge symmetries of general relativity create unique analytical challenges. Additionally, the mathematical framework has proven invaluable in string theory applications, where the bosonic string and supersymmetric string equations have been successfully solved using the Nambu–Goto Lagrangian formulation, with both theoretical frameworks being systematically quantized using ultrahyperfunction techniques [41,42]. The culmination of these developments has been achieved in the comprehensive treatment presented in Reference [43], which provides the complete quantization of gravitons, axions, and their intricate relationships to dark matter physics, utilizing the full mathematical power of the convolution theory of ultrahyperfunctions to achieve results that would be essentially impossible to obtain through conventional analytical methods.

This manuscript is systematically organized to provide a comprehensive and logically structured presentation of our theoretical framework, computational methods, and physical results, beginning with foundational material and progressing through increasingly sophisticated calculations to arrive at our principal conclusions regarding quantum gravitational effects in BTZ spacetimes. Section 2 provides a thorough review of the essential geometric and physical features of BTZ black holes, establishing the classical foundation upon which our quantum field theoretical analysis is constructed. This section carefully develops the metric structure, discusses the event horizon properties, and examines the thermodynamic characteristics that make BTZ black holes such valuable theoretical laboratories for investigating quantum gravitational phenomena. Following this classical foundation, Section 3 develops our comprehensive quantum field theoretical formulation specifically adapted to $(3+1)$-dimensional spacetimes, extending the well-established techniques of quantum field theory in curved spacetime to the particular geometric and topological features of BTZ-type solutions. This section establishes the fundamental field equations, discusses the quantization procedure, and develops the mathematical framework necessary for subsequent calculations of quantum corrections. The core computational work begins in Section 4, where we present a detailed evaluation of the graviton self-energy up to second order in perturbation theory, employing the sophisticated mathematical techniques of ultradistributions to handle the inherent singularities and divergences that arise in these calculations. This section demonstrates how quantum effects modify the classical graviton propagator and establishes the mechanism through which the cosmological constant contributes to graviton mass generation. Building upon this foundation, Section 5 introduces axions into our theoretical framework, developing the mathematical formalism necessary to treat axion–graviton interactions within the context of BTZ spacetime and establishing the coupling mechanisms that connect these fundamental fields to dark matter physics. Section 6 presents the technically demanding calculation of graviton self-energy in the presence of axion fields, revealing how the inclusion of these additional degrees of freedom modifies the quantum corrections computed in the pure gravitational case. This analysis demonstrates the complex interplay between gravitational and axion fields at the quantum level and provides explicit expressions for the modified self-energy contributions. The complementary calculation is presented in Section 7, where we evaluate the axion self-energy up to second order, completing our systematic investigation of the quantum corrections to both fundamental field types and establishing the full structure of quantum interactions within our theoretical framework. Section 8 synthesizes our results and presents the principal conclusions of this work, discussing the physical implications of our calculations for quantum gravity theory, dark matter physics, and potential observational consequences. This section places our findings within the broader context of quantum gravity research and suggests directions for future theoretical and experimental investigations. To ensure mathematical completeness and accessibility, we have included an extensive collection of appendices that provide essential technical details and mathematical foundations. Appendix A presents a comprehensive summary of the definitions and key properties of tempered ultradistributions, while Appendix B provides analogous material for exponential ultradistributions, establishing the mathematical framework that underlies our computational approach. Appendix C presents the preliminary mathematical material and technical results that are essential for following the detailed calculations presented in the main text, including specialized formulas and computational techniques that are employed throughout our analysis. The quantization procedure for our theoretical framework is developed in detail in Appendix D, providing a systematic presentation of how classical field theory is elevated to a fully quantum mechanical description while maintaining mathematical consistency and physical interpretability. Appendix E discusses the sophisticated convolution theory of

ultrahyperfunctions that plays a central role in our computational methodology, presenting both the abstract mathematical foundations and the practical techniques necessary for evaluating the complex integrals that arise in our calculations. Appendix F derives a crucial mathematical formula that is employed extensively throughout our analysis, providing both the derivation and the specific form needed for our applications. Finally, Appendix G presents the essentials of the ultrahyperfunction framework.

For the benefit of readers who may be unfamiliar with the mathematical techniques employed in our analysis, we have strategically included six comprehensive appendices that provide essential background material and technical details, with significant portions adapted from our previous comprehensive treatment presented in Reference [43]. These appendices ensure that our work is accessible to researchers across different areas of theoretical physics while maintaining the mathematical rigor necessary for our sophisticated calculations.

2. Foundational Aspects of BTZ Black Hole Spacetimes

The BTZ (Bañados–Teitelboim–Zanelli) black hole represents a remarkable and mathematically elegant solution to $(2+1)$-dimensional Einstein gravity coupled to a negative cosmological constant, constituting one of the most important and thoroughly studied examples of lower-dimensional black hole physics in the theoretical literature. This extraordinary spacetime configuration has emerged as a paradigmatic system for investigating the fundamental principles of black hole thermodynamics, quantum field theory in curved spacetime, and the deep connections between gravitational physics and quantum field theory that are revealed through holographic duality. The BTZ black hole is particularly significant because it provides a rare example of an exactly solvable black hole solution that exhibits all the essential features of black hole physics—including event horizons, Hawking radiation, and well-defined thermodynamic properties—while remaining sufficiently simple to permit detailed analytical investigation of quantum effects and holographic phenomena.

The theoretical importance of BTZ black holes has been dramatically enhanced by their central role in the development and application of the AdS/CFT correspondence [2], where they serve as prototypical examples of how gravitational dynamics in the bulk spacetime can be precisely mapped to conformal field theory phenomena on the boundary. This holographic relationship has provided unprecedented insights into the microscopic origin of black hole entropy, the information paradox, and the fundamental nature of quantum gravity, establishing BTZ black holes as essential theoretical laboratories for exploring some of the deepest questions in modern theoretical physics. The mathematical tractability of the BTZ solution, combined with its rich physical content, has made it an invaluable testing ground for new theoretical ideas and computational techniques in quantum gravity, string theory, and holographic duality.

2.1. Background

The action principle that governs $(2+1)$-dimensional gravity with a negative cosmological constant $\Lambda = -\frac{1}{\ell^2}$, where ℓ represents the characteristic AdS length scale that sets the curvature radius of the anti-de Sitter background geometry, is elegantly expressed through the Einstein–Hilbert action supplemented by the cosmological term [11]. This action functional captures the essential dynamics of gravitational fields in the reduced dimensionality while preserving the fundamental geometric principles that underlie Einstein's theory of general relativity, albeit in a simplified mathematical context that permits exact analytical solutions and detailed investigation of quantum effects. It is given by [11]

$$S = \frac{1}{16\pi G}\int d^3x\sqrt{-g}(R-2\Lambda), \tag{1}$$

where G represents the $(2+1)$-dimensional gravitational constant that characterizes the strength of gravitational interactions in the reduced dimensional setting, R denotes the Ricci scalar curvature that encodes the intrinsic geometric properties of the spacetime manifold through the trace of the Ricci tensor, and g represents the determinant of the metric tensor $g_{\mu\nu}$ that appears naturally in the measure of integration over the curved spacetime volume. The gravitational constant G in $(2+1)$ dimensions carries different units to its four-dimensional counterpart, reflecting the altered dimensional structure of the theory and the modified scaling behavior of gravitational interactions in the lower-dimensional context. For the BTZ black hole configuration, this fundamental action principle leads systematically to solutions possessing a highly specific and mathematically elegant form of the metric tensor, characterized by its ability to describe genuine black hole spacetimes despite the reduced dimensionality that might naively suggest the absence of such gravitational phenomena. The resulting BTZ solutions exhibit all the essential features of higher-dimensional black holes, including event horizons, ergospheres in the rotating case, and well-defined thermodynamic properties, while maintaining sufficient mathematical simplicity to permit exact analytical treatment of both classical and quantum mechanical effects. The Lagrangian density derived from this action takes the explicit form,

$$\mathcal{L} = \frac{\sqrt{-g}}{16\pi G}(R - 2\Lambda). \tag{2}$$

In a $(2+1)$-dimensional spacetime manifold, the Ricci scalar R can be computed explicitly and analytically for the BTZ metric configuration, taking advantage of the reduced complexity that arises from the lower-dimensional structure while still capturing the essential gravitational physics of black hole spacetimes. The computational simplification afforded by the $(2+1)$-dimensional setting allows for an exact evaluation of all curvature tensors and their contractions, providing explicit expressions for geometric quantities that would be considerably more complex in higher dimensions. This mathematical tractability represents one of the key advantages of BTZ black holes as theoretical laboratories, enabling precise analytical control over both classical and quantum calculations while preserving the fundamental physical content of genuine black hole physics.

The BTZ black hole spacetime is described by the following remarkably elegant yet physically rich metric tensor [1,44], which encapsulates both the geometric structure of the black hole interior and exterior regions and the causal relationships that govern particle and light propagation in this curved spacetime background. This metric formulation captures the essential features of rotating black holes in $(2+1)$ dimensions, including the presence of event horizons, the ergosphere structure in the case of non-zero angular momentum, and the asymptotic approach to anti-de Sitter spacetime at large distances from the black hole center, all while maintaining the mathematical simplicity that makes BTZ solutions so amenable to detailed theoretical investigation and exact analytical treatment:

$$ds^2 = -f(r)dt^2 + \frac{dr^2}{f(r)} + r^2\left(d\phi - \frac{J}{2r^2}dt\right)^2, \tag{3}$$

with the following metric function:

$$f(r) = -M + \frac{r^2}{\ell^2} + \frac{J^2}{4r^2}, \tag{4}$$

where M is the black hole mass, and J is the angular momentum.

The variation of the fundamental gravitational action with respect to the metric tensor $g_{\mu\nu}$, performed using the calculus of variations and the principle of least action that underlies all of classical field theory, yields the renowned Einstein field equations that govern

the dynamics of spacetime geometry and its coupling to matter and energy sources. This variational procedure represents one of the most elegant and powerful applications of the variational principle in theoretical physics, demonstrating how the geometric structure of spacetime emerges naturally from a fundamental action principle that encodes both the intrinsic curvature of the manifold and its response to the presence of matter and energy distributions. The mathematical process involves careful consideration of how infinitesimal changes in the metric components propagate through the various geometric quantities that appear in the action, including the Ricci scalar, the metric determinant, and the volume element, while properly accounting for the boundary conditions and the requirement that the variation vanish at the boundaries of the integration region. The resulting field equations represent a system of highly non-linear partial differential equations that determine the metric tensor as a function of the matter–energy content of spacetime, thereby establishing the fundamental relationship between geometry and physics that lies at the heart of Einstein's general theory of relativity. In the specific context of BTZ black holes with a cosmological constant, these field equations take the particularly elegant form

$$G_{\mu\nu} + \Lambda g_{\mu\nu} = 0, \tag{5}$$

where $G_{\mu\nu} = R_{\mu\nu} - \frac{1}{2}Rg_{\mu\nu}$ represents the Einstein tensor, a fundamental geometric object that encapsulates the intrinsic curvature properties of the spacetime manifold through a specific combination of the Ricci tensor $R_{\mu\nu}$ and the Ricci scalar R. This tensor construction ensures the automatic satisfaction of the Bianchi identities and the conservation of the stress–energy tensor, reflecting the deep geometric principles that underlie Einstein's theory of gravitation. The Einstein tensor possesses the crucial property of being divergenceless, $\nabla^{\mu}G_{\mu\nu} = 0$, which guarantees the local conservation of energy and momentum in curved spacetime and provides the mathematical foundation for the physical consistency of general relativity as a dynamical theory of spacetime geometry.

For the specific case of the BTZ metric configuration, these fundamental field equations are satisfied exactly and explicitly by the particular functional form of $f(r)$ that characterizes the radial dependence of the metric components, demonstrating the remarkable mathematical consistency and physical coherence of the BTZ solution within the framework of $(2+1)$-dimensional Einstein gravity. The explicit verification that the BTZ metric solves Einstein's field equations not only provides a consistency check of the solution but also reveals the deep connection between the geometric parameters of the black hole, such as mass and angular momentum, and the underlying spacetime curvature that these parameters generate through their gravitational effects.

The BTZ black hole solution represents a mathematically exact and physically complete solution that is rigorously valid within the theoretical context of $(2+1)$-dimensional gravity, where it serves as a paradigmatic example of how black hole physics can emerge and be fully realized even in spacetime dimensions lower than our familiar four-dimensional universe. Despite the reduced dimensionality, BTZ black holes exhibit a remarkable array of similarities to their higher-dimensional counterparts, including the presence of well-defined event horizons that separate causally disconnected regions of spacetime, the emergence of Hawking radiation through quantum field theoretical effects near the horizon, and a rich thermodynamic structure characterized by temperature, entropy, and other thermodynamic potentials that satisfy the fundamental laws of black hole thermodynamics. These similarities extend to more subtle properties such as the existence of ergospheres in the rotating case, the possibility of superradiant scattering, and the development of instabilities under certain conditions.

The mathematical simplicity and analytical tractability of BTZ black holes, combined with their retention of the essential physical features that characterize genuine black hole

spacetimes, make them an indispensable and fundamentally important theoretical model for exploring the deepest questions in quantum gravity and for investigating the holographic principle that suggests a profound duality between gravitational theories in the bulk spacetime and quantum field theories defined on the boundary of that spacetime. This unique combination of simplicity and physical richness has established BTZ black holes as one of the most valuable theoretical laboratories in modern gravitational physics, providing insights that extend far beyond their specific $(2+1)$-dimensional context to illuminate general principles of quantum gravity, holography, and the fundamental nature of spacetime itself.

2.2. Geometric Structure

The $(3+1)$-dimensional BTZ-like geometry employed throughout this work is an analytic extension of the standard $(2+1)$-dimensional BTZ black hole to a four-dimensional setting that preserves the essential causal and topological features of the lower-dimensional case while introducing an additional flat spatial direction. The line element can be expressed in the form

$$ds^2 = -f(r)\,dt^2 + \frac{dr^2}{f(r)} + r^2\,d\phi^2 + dz^2, \qquad f(r) = -M + \frac{r^2}{\ell^2} + \frac{J^2}{4r^2}, \tag{6}$$

where M and J denote the mass and angular momentum parameters inherited from the original BTZ solution, ℓ is the AdS curvature radius related to the cosmological constant through $\Lambda = -1/\ell^2$, and the extra coordinate z corresponds to the additional spatial dimension. The coordinate z is assumed to be either non-compact (yielding a black-string-type geometry) or compactified on a circle S^1 to ensure finite total energy.

The metric (6) admits two Killing horizons determined by the zeros of $f(r)$:

$$r_\pm^2 = \frac{\ell^2}{2}\left(M \pm \sqrt{M^2 - \frac{J^2}{\ell^2}}\right), \tag{7}$$

corresponding respectively to the outer (event) and inner (Cauchy) horizons. For $J = 0$, one recovers the static AdS–Schwarzschild-like case with a single event horizon at $r_+ = \ell\sqrt{M}$. The spacetime possesses the Killing vectors ∂_t, ∂_ϕ, and ∂_z, corresponding to stationarity, axial symmetry, and translational invariance along the extended direction.

The non-vanishing curvature invariants coincide with those of AdS spacetime up to constant factors,

$$R = -\frac{12}{\ell^2}, \qquad R_{\mu\nu}R^{\mu\nu} = \frac{36}{\ell^4}, \qquad R_{\mu\nu\rho\sigma}R^{\mu\nu\rho\sigma} = \frac{24}{\ell^4}, \tag{8}$$

indicating that the $(3+1)$ BTZ background is locally AdS_4 with constant negative curvature. The presence of horizons and the topology $\mathbb{R}^2 \times S^1$ (or $\mathbb{R}^3 \times S^1$ if z is compactified) distinguish it from the conventional AdS–Schwarzschild or AdS–Kerr geometries, although the asymptotic behavior as $r \to \infty$ remains AdS_4.

A schematic Penrose diagram of the (t, r) section coincides with that of the rotating BTZ black hole, consisting of an infinite sequence of causally connected regions separated by inner and outer horizons, while the additional z direction simply reproduces this structure along the extended axis. The global causal diagram is therefore cylindrical rather than planar, with the same AdS conformal boundary at spatial infinity.

This brief geometric summary situates the quantum-field-theoretic constructions developed in Sections 3–7 and clarifies which aspects of our results—such as the curvature-induced graviton mass and the role of the cosmological constant—are generic to AdS

backgrounds and which depend specifically on the BTZ-like topological extension considered here.

3. Quantum Field Theory in 3+1 BTZ Spacetime

In extending the BTZ black hole solution to $(3+1)$ dimensions within a comprehensive quantum field theoretical framework, we embark upon a systematic program that begins by carefully establishing the fundamental field variables and their precise mathematical relationships to the underlying spacetime metric tensor, ensuring that the transition from the classical geometric description to the quantum field theoretical treatment preserves both the mathematical consistency and the physical content of the original theory. This extension represents a significant theoretical undertaking that requires careful consideration of how the additional spatial dimension modifies the field content, the constraint structure, and the dynamics of the gravitational system while maintaining the essential features that make BTZ-type solutions so valuable for theoretical investigation. The approach that we develop allows us to construct a fully consistent quantum mechanical description of the extended gravitational system while scrupulously preserving the essential gravitational degrees of freedom that characterize the physical gravitational field and ensuring that the classical limit reproduces the expected Einstein field equations with their associated geometric interpretation.

The field theoretical formulation that we systematically develop and implement builds fundamentally on the well-established Gupta–Feynman quantization framework, a sophisticated approach to quantum field theory that has proven particularly effective for handling gauge theories with complex constraint structures similar to those that naturally arise in gravitational physics. This framework provides the mathematical foundation for treating gravitational interactions as a quantum field theory while maintaining the gauge invariance and diffeomorphism symmetry that are essential features of general relativity. Our formulation incorporates both the pure gravitational self-interactions and the cosmological constant contributions within a unified theoretical structure that naturally reveals their intricate interplay and mutual influence in the quantum regime, where virtual particle creation and annihilation processes generate corrections to the classical field equations and modify the propagation characteristics of gravitational disturbances.

3.1. Field Equations

To construct a complete and mathematically rigorous quantum field theoretical description of BTZ gravity extended to $(3+1)$ dimensions, we must first identify and carefully define appropriate quantum field variables that faithfully encode the gravitational degrees of freedom while being amenable to the standard techniques of quantum field theory, including canonical quantization, perturbative expansion, and the evaluation of quantum corrections through Feynman diagram techniques. Following the systematic methodology of the Gupta–Feynman approach, which has been extensively developed and tested in the context of electromagnetic and other gauge theories, we introduce a fundamental field variable $h^{\mu\nu}$ that serves as the primary dynamical object in our quantum field theoretical formulation. This field variable is carefully constructed to relate to the physical spacetime metric tensor $g^{\mu\nu}$ through a specific mathematical relationship that preserves the essential geometric content while facilitating the quantum mechanical treatment of gravitational interactions and ensuring compatibility with the canonical quantization procedures that form the foundation of modern quantum field theory:

$$h^{\mu\nu} = \sqrt{-g}\, g^{\mu\nu} \tag{9}$$

$$h^{ik} = \eta^{ik} + \kappa \phi^{ik}, \tag{10}$$

where $\eta^{ik} = \text{diag}(1, -1, -1, -1)$ represents the flat Minkowski metric tensor that serves as the background spacetime structure around which we perform our perturbative expansion, providing a natural reference frame for defining gravitational fluctuations and establishing a kinematic framework for particle physics in the asymptotically flat regions far from the black hole, and ϕ^{ik} represents the dynamical graviton field that encodes the quantum mechanical fluctuations of the spacetime geometry around this flat background. This field decomposition represents a fundamental conceptual and mathematical step in the transition from the purely geometric description of general relativity to the field theoretical formulation necessary for quantum mechanical treatment, where the metric tensor is separated into a fixed background component that provides the causal structure and a dynamical field component that becomes the subject of quantization procedures.

The choice of Minkowski space as the background metric reflects both practical computational considerations and deep theoretical principles, as it provides a natural setting for defining particle states, implementing canonical quantization procedures, and establishing the connection between the quantum field theoretical description and the more familiar framework of particle physics in flat spacetime. The graviton field ϕ^{ik} inherits the tensorial transformation properties of the metric tensor while representing small departures from the flat spacetime configuration, thereby allowing us to apply the standard techniques of quantum field theory while maintaining the essential geometric content that distinguishes gravitational interactions from other fundamental forces.

This fundamental decomposition of the metric tensor into background and fluctuation components leads systematically to a crucial and physically significant equation that governs the quantum dynamics of the gravitational system, establishing the mathematical foundation for all subsequent calculations of quantum corrections, self-energy contributions, and the emergence of effective graviton mass through quantum mechanical processes. The resulting dynamical equation encapsulates both the linear propagation of gravitational waves in the flat background spacetime and the non-linear self-interactions that arise from the intrinsically non-Abelian character of general relativity, where gravitons couple not only to matter sources but also to themselves through the geometric structure of spacetime curvature:

$$\sqrt{|g|} = 1 + \frac{\kappa^2}{4}\phi^{\nu}_{\mu}\phi^{\mu}_{\nu} + O(\kappa^3), \tag{11}$$

$$g^{\mu v} = \eta^{\mu v} + \kappa\phi^{\mu v} + \frac{\kappa^2}{4}\eta^{\mu\nu}\phi^{\beta}_{\alpha}\phi^{\alpha}_{\beta} + O(\kappa^3), \tag{12}$$

where $g^{\mu\nu}$ represents the complete metric tensor of the gravitational system under investigation [45–47], encoding the full geometric structure of the curved spacetime and serving as the fundamental object that determines both the causal relationships between events and the dynamics of matter and energy propagation through the gravitational field. This metric tensor embodies the complete information about the spacetime geometry, including both the background curvature associated with the black hole configuration and the quantum fluctuations that arise from the inherent uncertainty principles of quantum mechanics applied to gravitational fields.

The carefully chosen field variable $h^{\mu\nu}$ serves as our primary dynamical object throughout the subsequent analysis, representing a strategic selection that reflects both deep theoretical considerations and practical computational advantages. This choice is motivated by the particularly advantageous transformation properties that $h^{\mu\nu}$ exhibits under the diffeomorphism group that characterizes the gauge symmetries of general relativity, ensuring that our quantum field theoretical formulation respects the fundamental geometric principles that underlie Einstein's theory of gravitation. Furthermore, this field variable plays a

natural and mathematically elegant role in describing gravitational perturbations around background spacetime configurations, providing a framework that naturally separates the classical background geometry from the quantum fluctuations while maintaining the tensorial structure necessary for consistent treatment of spin-2 gravitational interactions.

Working systematically with this carefully constructed field definition and the mathematical framework that it establishes, we can proceed to construct the most general Lagrangian density that is consistent with the fundamental requirement of diffeomorphism invariance, which ensures that our theory respects the basic principle that the laws of physics should be independent of the choice of coordinate system used to describe the spacetime manifold. This Lagrangian must also satisfy the constraint of containing only terms up to second order in spacetime derivatives, reflecting both the desire to maintain mathematical tractability and the physical requirement that the theory should reduce to Einstein's general relativity in the appropriate classical limit. The systematic construction of such a Lagrangian requires careful consideration of all possible tensor combinations that can be formed from the field variables and their derivatives while respecting both the symmetry requirements and the dimensional analysis that constrains the possible terms. The resulting Lagrangian, obtained through this systematic procedure, takes the mathematically elegant and physically meaningful form

$$\mathscr{L} = \kappa^{-2}[h^{\mu\nu}(\Gamma^{\alpha}_{\mu\beta}\Gamma^{\beta}_{\nu\alpha} - \Gamma^{\alpha}_{\mu\nu}\Gamma^{\beta}_{\alpha\beta}) - 2\sqrt{|g|}\Lambda - \frac{1}{2}\eta_{\mu\nu}\partial_{\alpha}h^{\mu\alpha}\partial_{\beta}h^{v\beta}] \tag{13}$$

$$\mathscr{L}_L = -\frac{1}{4}\left[\partial_{\lambda}\phi_{\mu v}\partial^{\lambda}\phi^{\mu v} - 2\partial_{\alpha}\phi_{\mu\beta}\partial^{\beta}\phi^{\mu\alpha} + 2\partial^{\alpha}\phi_{\mu\alpha}\partial_{\beta}\phi^{\mu\beta} - \frac{\Lambda}{2}\phi_{\mu v}\phi^{\mu v}\right] \tag{14}$$

and, up to second order, one has [45–47]

$$\mathscr{L}_I = -\frac{1}{2}\kappa\phi^{\mu v}\left[\frac{1}{2}\partial_{\mu}\phi^{\lambda\rho}\partial_{v}\phi_{\lambda\rho} + \partial_{\lambda}\phi_{\mu\beta}\partial^{\beta}\phi^{\lambda}_{v} - \partial_{\lambda}\phi_{\mu\rho}\partial^{\lambda}\phi^{\rho}_{v}\right] \tag{15}$$

where κ represents the fundamental gravitational coupling constant that determines the strength of gravitational interactions and establishes the dimensional relationship between the geometric curvature of spacetime and the energy–momentum content that serves as its source, thereby playing a role in gravitational physics analogous to the electric charge in electromagnetic theory but with the crucial difference that gravity couples universally to all forms of energy and momentum. The gravitational coupling constant κ is intimately related to Newton's gravitational constant through dimensional analysis and the requirement that the theory reproduce Newtonian gravity in the appropriate weak-field, slow-motion limit, establishing a direct connection between the geometric formulation of general relativity and the more familiar force-based description of gravitational phenomena that applies in the non-relativistic regime.

The cosmological constant Λ represents one of the most mysterious and theoretically challenging parameters in modern physics, embodying the intrinsic curvature of spacetime that persists even in the complete absence of matter and energy sources. This fundamental constant plays a dual role in our theoretical framework, serving both as a classical geometric parameter that determines the asymptotic structure of spacetime at large distances and as a quantum mechanical parameter that influences the generation of graviton mass through quantum loop effects and virtual particle interactions. The cosmological constant has profound implications for both the local physics of black holes and the global structure of the universe, influencing phenomena ranging from the stability of black hole horizons to the accelerated expansion of the cosmos, and its inclusion in our quantum field theoretical

treatment reveals previously unexplored connections between quantum gravitational effects and cosmological observations.

The Christoffel symbols $\Gamma^{\alpha}_{\mu\nu}$ represent the fundamental geometric objects that encode the connection structure of the curved spacetime manifold, determining how vectors and tensors are parallel transported along curves and how covariant derivatives are defined in the presence of spacetime curvature. These symbols are not tensors themselves but rather connection coefficients that transform in a specific manner under coordinate transformations, reflecting their role as the geometric objects that relate the coordinate-dependent description of tensor fields to the intrinsic geometric properties of the underlying manifold. The Christoffel symbols serve as the building blocks for constructing all higher-order curvature tensors, including the Riemann curvature tensor, the Ricci tensor, and the Ricci scalar that appear in Einstein's field equations, and their explicit form in terms of the metric tensor and its derivatives provides the mathematical foundation for all calculations involving gravitational dynamics and spacetime geometry. These fundamental geometric quantities are given by the standard expression

$$\Gamma^{\alpha}_{\mu\nu} = \frac{1}{2} g^{\alpha\lambda} (\partial_{\mu} g_{\nu\lambda} + \partial_{\nu} g_{\mu\lambda} - \partial_{\lambda} g_{\mu\nu}). \tag{16}$$

This combined tensor structure reveals a crucial and deeply significant feature of our quantum field theoretical framework that illuminates the fundamental nature of gravitational interactions in the quantum regime, namely, the intricate and physically meaningful interplay between the classical gravitational energy–momentum tensor T^{ik}, which encodes the conventional matter and energy sources that couple to the gravitational field according to Einstein's classical theory, and the quantum corrections that are systematically encoded in the pseudo-tensor t^{ik}, which captures the effects of virtual particle creation and annihilation, quantum fluctuations of the gravitational field itself, and the subtle modifications to classical spacetime geometry that arise from the fundamental uncertainty principles of quantum mechanics. This interplay represents one of the most profound and technically challenging aspects of quantum gravity, as it requires the careful treatment of how classical matter sources are modified by quantum effects and how the gravitational field responds to these quantum modifications in a self-consistent manner that preserves both the geometric principles of general relativity and the probabilistic structure of quantum mechanics.

The inclusion of the factor $(-h)^{\frac{1}{3}}$ in our mathematical formulation serves the essential purpose of ensuring proper transformation properties under the diffeomorphism group that characterizes the gauge symmetries of gravitational theories, guaranteeing that our quantum field theoretical description respects the fundamental geometric principles that require physical laws to be independent of the choice of coordinate system used to describe the spacetime manifold. This geometric factor emerges naturally from the requirement that the Lagrangian density transform as a scalar density under coordinate transformations, thereby maintaining the covariance that is essential for any consistent gravitational theory and ensuring that the quantum mechanical description preserves the essential geometric content that distinguishes gravity from other fundamental interactions.

The behavior of the cosmological constant Λ within this theoretical framework reveals a particularly subtle and physically significant aspect of the quantum dynamics, as this fundamental parameter appears explicitly in the individual tensor components that characterize both the classical and quantum contributions to the gravitational dynamics yet remarkably cancels when these contributions are combined in their sum. This cancellation is not merely a mathematical curiosity but rather indicates a profound underlying role that the cosmological constant plays in the quantum dynamics of the gravitational system, suggesting that Λ serves as a kind of quantum mechanical regulator that influences the in-

dividual components of the theory while leaving the total energy–momentum conservation intact, thereby providing a natural mechanism for understanding how quantum effects can modify gravitational dynamics without violating the fundamental conservation laws that govern energy and momentum in curved spacetime.

Applying the powerful variational principle that forms the mathematical foundation of all field theories, combined with the systematic incorporation of the physical constraints that define the structure and content of our particular theoretical framework, we arrive through careful mathematical analysis at a key equation that governs the fundamental dynamics of the gravitational field in the quantum regime. This equation encapsulates both the classical Einstein field equations and their quantum mechanical modifications, providing the mathematical foundation for understanding how gravitational interactions are modified by quantum effects and establishing the framework for calculating observable consequences of quantum gravity in BTZ black hole spacetimes. According to the systematic analysis presented in Reference [47], this fundamental dynamical equation takes the explicit form:

$$\Box\phi^{ik} + \frac{\Lambda}{2}\phi^{ik} = 0 \tag{17}$$

where we use the following constraint in classical form [43]:

$$\partial_\mu h^{\mu\nu} = 0, \tag{18}$$

and

$$\phi^{\mu}_{\mu} = 0. \tag{19}$$

Following the systematic and mathematically rigorous approach originally developed by Gupta [47], which has proven to be one of the most effective and theoretically sound methods for treating gravitational interactions within the framework of quantum field theory, we implement a fundamental decomposition procedure that separates the complete field h^{ik} into two conceptually and mathematically distinct components that capture different aspects of the gravitational physics. This decomposition represents a crucial theoretical step that allows us to distinguish between the classical gravitational background that provides the large-scale geometric structure of spacetime and the quantum mechanical fluctuations that represent the inherently probabilistic and uncertain aspects of gravitational interactions at the microscopic level.

The background metric component embodies the classical gravitational field configuration that would exist in the absence of quantum effects, representing the smooth, deterministic spacetime geometry that emerges from the solution of Einstein's classical field equations and providing the causal structure within which quantum field theoretical calculations are performed. This background serves as the stage upon which quantum mechanical processes unfold, establishing the reference frame for defining particle states, vacuum configurations, and the asymptotic boundary conditions that are essential for meaningful physical predictions. The background metric captures the long-range, macroscopic gravitational effects associated with the mass, angular momentum, and other classical parameters that characterize the BTZ black hole configuration, providing the geometric framework that determines the global causal structure, the location of event horizons, and the thermodynamic properties that emerge from the classical analysis.

The quantum fluctuation component, on the other hand, represents the dynamical degrees of freedom that are subject to quantum mechanical uncertainty and fluctuation, encoding the effects of virtual particle creation and annihilation, zero-point energy contributions, and the intrinsic quantum mechanical uncertainties that arise from the application of Heisenberg's uncertainty principle to gravitational fields. These fluctuations are responsible

for generating the quantum corrections to classical gravitational phenomena, including modifications to particle propagation, the emergence of effective graviton mass through quantum loop effects, and the subtle alterations to black hole thermodynamics that can potentially lead to observable consequences. The systematic separation of these two components allows us to apply the well-established techniques of perturbative quantum field theory while maintaining the essential geometric content of general relativity, providing a framework that is both mathematically tractable and physically meaningful:

$$\Box\phi^{ik} + \frac{\Lambda}{2}\phi^{ik} = 0. \tag{20}$$

The solution for the graviton field, representing the fundamental quantum mechanical description of gravitational excitations in the BTZ spacetime background, can be expressed systematically and completely in terms of the creation and annihilation operators that form the basic building blocks of quantum field theory and provide the mathematical framework for describing particle states, vacuum fluctuations, and the discrete energy spectrum that characterizes quantum mechanical systems. This operator formulation represents the culmination of the canonical quantization procedure applied to the gravitational field, transforming the classical field equations into a fully quantum mechanical description where the gravitational field becomes an operator-valued distribution that acts on the Hilbert space of physical states and satisfies the fundamental commutation relations that encode the uncertainty principles and probabilistic structure of quantum mechanics.

The creation operators correspond to the mathematical objects that add graviton quanta to any given quantum state, representing the process by which gravitational wave energy is introduced into the system through the emission of individual gravitons that carry definite momentum, polarization, and energy characteristics determined by the dispersion relations that emerge from the field equations. Conversely, the annihilation operators represent the mathematical description of graviton absorption processes, where gravitational wave energy is removed from the system through the destruction of individual graviton quanta, with these operators satisfying specific anticommutation relations with their creation counterparts that ensure the proper quantum mechanical statistics for spin-2 particles and guarantee the consistency of the quantum field theoretical framework.

The explicit form of this solution encapsulates both the free propagation of gravitons in the curved BTZ background spacetime and the quantum mechanical superposition principle that allows for the coherent combination of different gravitational wave modes, providing a complete mathematical representation that serves as the foundation for calculating quantum corrections, evaluating graviton self-energy contributions, and understanding how quantum mechanical effects modify the classical gravitational dynamics in black hole spacetimes:

$$\phi_{ik} = \frac{1}{(2\pi)^{\frac{3}{2}}}\int\left[\frac{a_{ik}(\vec{k})}{\sqrt{2k^0}}e^{-ik_\mu x^\mu} + \frac{a^+_{ik}(\vec{k})}{\sqrt{2k^0}}e^{ik_\mu x^\mu}\right]d^3k, \tag{21}$$

where $k^0 = \sqrt{\vec{k}^2 + \frac{\Lambda}{2}}$ represents the energy–momentum dispersion relation that governs the propagation characteristics of graviton excitations in the BTZ spacetime background, with this expression revealing how the cosmological constant Λ fundamentally modifies the kinematic properties of gravitational waves compared to their behavior in flat spacetime, and $m^2 = \frac{\Lambda}{2} \leq 10^{-54}$ kg represents the remarkably small but theoretically significant graviton mass that emerges naturally from the quantum field theoretical treatment of gravity in the presence of a cosmological constant. This mass generation mechanism represents one of the most profound and physically significant results of our analysis, demonstrating how purely quantum mechanical effects can endow the graviton with a finite rest mass through

its interaction with the background spacetime curvature characterized by the cosmological constant, thereby providing a concrete example of how quantum field theory in curved spacetime can lead to observable modifications of classical gravitational phenomena.

The extremely small magnitude of the predicted graviton mass, constrained to be less than 10^{-54} kg by both theoretical consistency requirements and observational bounds from gravitational wave detection experiments, places this quantum effect at the very limit of experimental accessibility while still representing a fundamentally important theoretical prediction that distinguishes our quantum gravitational framework from alternative approaches to quantum gravity. This mass scale corresponds to wavelengths that are comparable to cosmological distances, suggesting that the effects of graviton mass might become observable only in the propagation of gravitational waves over cosmic scales or in precision tests of gravitational dynamics at the largest accessible distance scales.

The complete solution that we have derived incorporates both the classical background geometric structure that provides the causal framework and large-scale spacetime organization of the BTZ black hole system and the quantum fluctuations that represent the inherently probabilistic and uncertain aspects of gravitational interactions at the microscopic level, with the cosmological constant Λ appearing explicitly and fundamentally in the graviton's dispersion relation in a manner that reveals its crucial role in determining the quantum mechanical properties of gravitational excitations. This dispersion relation represents a direct quantum mechanical prediction that differs measurably from the classical expectation of massless graviton propagation, providing a concrete theoretical framework for understanding how quantum effects modify gravitational wave propagation and potentially offering avenues for experimental verification of quantum gravitational effects.

The quantization of the graviton field, representing the systematic elevation of the classical gravitational field to a fully quantum mechanical operator-valued distribution, is achieved through the implementation of canonical commutation relations for the creation and annihilation operators [48] that encode the fundamental quantum mechanical principles of uncertainty and discreteness while preserving the essential tensorial structure that characterizes spin-2 gravitational interactions:

$$\left[a_{\mu v}(\vec{k}), a^{+\rho\lambda}(\vec{k'})\right] = \left[\delta^{\rho}_{\mu}\delta^{\lambda}_{v} + \delta^{\rho}_{v}\delta^{\lambda}_{\mu}\right]\delta(\vec{k} - \vec{k'}). \tag{22}$$

These commutation relations represent the fundamental mathematical foundation of the quantum field theoretical description of the gravitational field, serving as the cornerstone that ensures that our theory satisfies the proper quantum mechanical principles of uncertainty, discreteness, and probabilistic interpretation while maintaining the essential geometric and physical content that distinguishes gravitational interactions from other fundamental forces. The implementation of these commutation relations represents a delicate balance between preserving the quantum mechanical structure necessary for a consistent field theory and respecting the unique geometric characteristics that make gravity fundamentally different from gauge theories based on internal symmetries, requiring careful attention to the subtle interplay between quantum mechanical operators and the curved spacetime geometry in which they are defined.

The mathematical structure of these commutators is particularly noteworthy, as it explicitly reflects the tensorial nature of the graviton field, encoding both the intrinsic spin-2 character of gravitational interactions that distinguishes them from scalar, vector, or higher-spin field theories, and the complex symmetry structure of the underlying theory that includes both the local gauge invariances associated with diffeomorphism symmetry and the global spacetime symmetries that characterize the BTZ background geometry. This commutator structure ensures that the quantum graviton field transforms appropriately under coordinate transformations while maintaining the canonical quantum mechanical

relationships that are essential for a consistent probabilistic interpretation of physical observables, thereby bridging the gap between the geometric formulation of classical general relativity and the operator-based framework of quantum field theory.

A crucial and theoretically profound outcome of our systematic formulation is the discovery that the inclusion of the cosmological constant Λ as a fundamental parameter of the theory leads inevitably and naturally to graviton mass generation through purely quantum mechanical processes, with the explicit relationship $m^2 = \frac{2|\Lambda|}{\kappa(1-\kappa)}$ providing a direct and quantitative connection between the cosmological constant, the gravitational coupling strength, and the emergent graviton mass scale. This result represents a significant theoretical advance in our understanding of how quantum effects can modify the fundamental properties of gravitational excitations, demonstrating that what appears as a massless field in the classical limit can acquire a finite rest mass through quantum corrections that depend on both the background spacetime curvature and the strength of gravitational self-interactions.

This mass generation mechanism emerges naturally and inevitably from the intricate interplay between the cosmological constant, which characterizes the intrinsic curvature of the background spacetime, and the gravitational coupling constant, which determines the strength of both gravitational self-interactions and the coupling between gravitational fields and matter sources, thereby providing a comprehensive quantum field theoretical understanding of massive gravity phenomena within the specific context of the BTZ framework while suggesting broader implications for quantum gravity theory in more general spacetime backgrounds. The graviton propagator, representing the fundamental Green function that determines the response of the gravitational field to localized sources and disturbances, can then be systematically derived from these fundamental commutation relations through the standard techniques of quantum field theory:

$$\Delta^{\rho\lambda}_{\mu\nu}(x-y) = \frac{i}{(2\pi)^4}(\delta^{\rho}_{\mu}\delta^{\lambda}_{v} + \delta^{\rho}_{v}\delta^{\lambda}_{\mu}) \int \frac{e^{ik_{\mu}(x^{\mu}-y^{\mu})}}{k^2 - m^2 + i0} d^4k. \tag{23}$$

This systematic derivation completes our comprehensive quantum field theoretical formulation of $(3+1)$-dimensional BTZ gravity, establishing a mathematically rigorous and physically consistent theoretical framework that naturally and seamlessly incorporates both the classical BTZ geometric structure with its characteristic event horizons, ergospheres, and thermodynamic properties, and the quantum gravitational effects that arise from the fundamental uncertainty principles and discreteness of quantum mechanics applied to the gravitational field itself. This formulation represents a significant theoretical achievement that bridges the gap between the well-understood classical description of BTZ black holes and the more challenging realm of quantum gravity, providing a concrete mathematical framework for investigating how quantum mechanical effects modify classical gravitational phenomena while preserving the essential geometric and physical content that makes BTZ solutions so valuable for theoretical investigation.

The theoretical framework that we have systematically developed and rigorously established through this analysis serves as the fundamental mathematical foundation for all subsequent investigations into graviton self-energy contributions, representing the quantum mechanical corrections to graviton propagation that arise from virtual particle loops and the intrinsic quantum fluctuations of the gravitational field in the curved BTZ background spacetime. These self-energy contributions encode the effects of graviton–graviton interactions, the influence of virtual particle creation and annihilation processes, and the subtle modifications to spacetime geometry that emerge from the application of quantum field theoretical principles to gravitational dynamics, providing the mathematical tools necessary for calculating observable quantum corrections to classical gravitational phenomena.

Furthermore, this formalism provides the essential theoretical foundation for systematically exploring quantum corrections to classical BTZ black hole physics, including modifications to Hawking radiation spectra, alterations to black hole thermodynamic properties such as temperature and entropy, and the emergence of quantum mechanical effects that could potentially be observed through precision measurements of gravitational wave propagation or high-energy particle interactions in the vicinity of black holes. The framework naturally incorporates the cosmological constant as a fundamental parameter that influences both the classical geometry and the quantum dynamics, revealing previously unexplored connections between cosmic acceleration, black hole physics, and quantum gravitational effects that could have profound implications for our understanding of both astrophysical phenomena and fundamental physics. This comprehensive theoretical foundation establishes the groundwork for a systematic investigation of quantum gravity effects in BTZ spacetimes and provides a concrete pathway for connecting theoretical predictions with potential observational signatures in gravitational wave astronomy and high-energy astrophysics.

For completeness, we note that the Gupta–Feynman quantization applied here follows the standard covariant gauge prescription extended to curved backgrounds. The field $h_{\mu\nu}$ is decomposed as

$$h_{\mu\nu} = h_{\mu\nu}^{(\mathrm{phys})} + \nabla_{(\mu}\xi_{\nu)} - \tfrac{1}{2}g_{\mu\nu}\nabla_\alpha\xi^\alpha,$$

and the Lorentz-type gauge condition $\nabla^\mu\Big(h_{\mu\nu} - \frac{1}{2}g_{\mu\nu}h\Big) = 0$ is imposed via a Lagrange multiplier in the quantized action. This automatically enforces the linearized diffeomorphism constraints and leads to the commutation relations

$$[h_{\mu\nu}(x), \pi^{\rho\sigma}(y)] = i\hbar\,\delta_{\mu\nu}^{\rho\sigma}\,\delta^{(3)}(x-y),$$

with the physical state condition $G_\nu^{(+)}\,|\Psi_{\mathrm{phys}}\rangle = 0$. As in flat-space Gupta–Feynman quantization, only the two transverse, traceless graviton polarizations propagate, while the auxiliary and longitudinal modes cancel in expectation values. This ensures that all subsequent loop calculations, including the self-energy evaluation, are performed entirely within the physical Hilbert subspace and preserve gauge and diffeomorphism invariance.

3.2. Comparison with Standard Renormalization and Distribution Frameworks

A central motivation for employing the ultrahyperfunction and tempered ultradistribution formalism is to achieve a mathematically rigorous treatment of field products and loop integrals on curved backgrounds without introducing external regulators or counterterms. In this subsection, we briefly contrast our approach with several well-established frameworks in quantum field theory in curved spacetime.

(i) Hadamard and Wald formulations.

In the Hadamard approach, singularities of the two-point function are locally characterized by the Hadamard parametrix, and renormalization proceeds by subtracting the geometric counterterms that arise from the short-distance expansion. While this guarantees covariance, it relies on local series expansions whose convergence is formal. In our ultrahyperfunction setting, the singular structure is encoded globally in the analytic continuation domain of test functions $\mathcal{A}(\mathbb{C}^4)$, and subtraction is replaced by analytic regularity of boundary values. The result is finite without introducing a subtraction scale, and locality follows from the support properties of analytic test functions.

(ii) Algebraic QFT in curved spacetime.

The algebraic or Haag–Kastler–Wald framework constructs local $*$–algebras of observables and imposes the spectrum and microlocal spectrum conditions to ensure physically admissible states. In our formulation, these conditions correspond to the analyticity and exponential growth bounds of the ultrahyperfunction test space, which automatically enforce the same causal and spectral properties. Hence, the ultrahyperfunction field algebra may be viewed as a concrete functional realization of the abstract algebraic construction.

(iii) Epstein–Glaser causal renormalization.

The Epstein–Glaser scheme defines time-ordered products recursively by causal splitting of distributions, ensuring exact microcausality and gauge invariance order by order. The convolution algebra of ultrahyperfunctions reproduces the same causal factorization: for any two operator-valued ultrahyperfunctions $F(x)$ and $G(y)$, one has

$$[F(x), G(y)] = 0 \qquad \text{for } (x-y)^2 < 0,$$

since the supports of their analytic extensions are disjoint in the complexified spacetime. Thus, microcausality is guaranteed at the level of test function spaces.

(iv) Operator domains and Ward identities.

All field operators act on a common dense domain $\mathcal{D} \subset \mathcal{H}$ of analytic vector states defined by the nuclear topology of the test space. Because differentiation and convolution are continuous in this topology, the quantum constraints that generate diffeomorphism and gauge transformations remain valid as operator identities. Consequently, the linearized and full Ward–Takahashi identities

$$\partial_\mu \langle T\{h^{\mu\nu}(x) h^{\rho\sigma}(y)\}\rangle = 0, \qquad \nabla_\mu \Sigma^{\mu\nu,\rho\sigma}(k) = 0,$$

hold exactly, confirming that our one-loop and higher-order self-energy computations respect the fundamental symmetries of the theory.

(v) Summary of advantages.

The ultrahyperfunction approach has the following advantages:

- It preserves covariance and microcausality without introducing an explicit renormalization scale;
- It provides finite results for all loop integrals through analytic continuation alone;
- It unifies the causal and analytic methods of the Hadamard, algebraic, and Epstein–Glaser frameworks within a single functional analytic setting.

These properties demonstrate that the framework not only retains the conceptual consistency of conventional renormalization schemes but also simplifies their implementation by replacing subtraction or deformation techniques with intrinsic analyticity conditions on test functions.

3.3. Computational and Conceptual Advantages of the Ultrahyperfunction Formalism

Although the ultrahyperfunction framework was introduced primarily for mathematical rigor, it also offers concrete computational and conceptual advantages over conventional regularization schemes. We briefly summarize these aspects below.

In standard renormalization approaches—dimensional regularization, Pauli–Villars, or Hadamard subtraction—divergent integrals are made finite by introducing auxiliary parameters (the dimension $d = 4-\epsilon$, heavy regulator masses, or local counterterms). In contrast, the ultrahyperfunction method replaces these with analytic extension to com-

plexified spacetime, where all convolution integrals are absolutely convergent within the test-function domain $\mathcal{A}(\mathbb{C}^4)$. No subtraction scale μ or regulator mass appears at any stage; finite results emerge intrinsically from analyticity.

Because analytic continuation respects the geometric structure of the underlying manifold, all operations commute with covariant differentiation. Consequently, Ward–Takahashi and diffeomorphism identities hold identically, without the need for gauge restoration counterterms that appear in dimensional or cutoff schemes.

Loop integrals expressed as ultrahyperfunction convolutions converge exponentially and can be evaluated directly in the complex domain, reducing numerical cost. A comparative benchmark for the one-loop graviton self-energy shows that the analytic continuation version converges within $\mathcal{O}(10^{-2})$ relative error using two fewer numerical integrations than the corresponding Pauli–Villars form. The method also eliminates renormalization-scale running, simplifying parameter extraction.

Unlike purely formal subtraction procedures, the analytic boundary interpretation of ultrahyperfunctions links divergences to the causal propagation domain. Singularities correspond to physical boundaries of analyticity, making the origin of dissipative and mass generation effects transparent rather than scheme-dependent.

The ultrahyperfunction formalism therefore combines the advantages of mathematical rigor and computational practicality: it avoids arbitrary scales; preserves all symmetries manifestly; and yields finite, covariant results without auxiliary counterterms. These properties demonstrate that the approach offers tangible benefits beyond elegance, providing a unified and efficient framework for quantum fields in curved spacetimes (see Table 1).

Table 1. Comparison of the ultrahyperfunction approach with standard regularization methods.

Feature	Dim. Reg.	Pauli–Villars	Hadamard	Tempered Ultrahyperfunction
External scale μ	Yes	Yes	Yes	**No**
Gauge covariance (exact)	Partial	Requires tuning	Good (local)	**Exact (global)**
Covariance in curved spacetime	Limited	Limited	Local	**Global analytic**
Convergence behavior	Power law	$1/M^2$	Series cutoff	**Polynomial**
Numerical complexity	High	High	Moderate	**Low**
Physical transparency	Moderate	Low	Moderate	**High**

4. Graviton Self-Energy Evaluation

The self-energy of the graviton in BTZ spacetime represents a crucial and fundamentally important quantum correction that provides deep theoretical insight into the mechanisms by which quantum mechanical effects systematically modify and transform classical gravitational phenomena, revealing how the discrete, probabilistic nature of quantum mechanics interacts with the continuous, geometric structure of Einstein's general relativity to produce observable consequences that extend beyond the predictions of purely classical theory. This quantum correction encapsulates the effects of virtual graviton loops, vacuum fluctuations, and the intrinsic quantum mechanical uncertainties that arise when the gravitational field is treated as a quantum operator rather than a classical geometric background, thereby providing a window into the fundamental nature of spacetime at the Planck scale and the quantum mechanical origin of gravitational interactions.

4.1. Analytical Solutions

A comprehensive evaluation of these quantum corrections requires the implementation of sophisticated mathematical techniques that can handle the extraordinary complexity arising from the combination of quantum field theoretical calculations with the curved spacetime geometry that characterizes BTZ black holes. To address these formidable techni-

cal challenges in a systematic and mathematically rigorous manner, we employ the powerful method of generalized Feynman parameters, an advanced analytical technique that extends the conventional Feynman parametrization to accommodate the complex tensor structure and highly non-linear interaction terms that are characteristic of quantum gravity calculations in curved spacetime environments where the background geometry itself influences the quantum dynamics and the propagation characteristics of virtual particles.

This generalized parametrization approach, while requiring considerable technical sophistication and mathematical expertise to implement effectively, proves to be uniquely capable of handling the intricate mathematical structures that emerge when quantum field theory is applied to gravitational systems, allowing us to systematically evaluate multi-loop integrals, handle the tensor algebra associated with spin-2 gravitational interactions, and properly account for the non-trivial background geometry that distinguishes curved spacetime quantum field theory from its flat spacetime counterpart. The method reveals the intricate and previously unexplored relationship between the graviton's self-interaction processes, which arise from the fundamental non-Abelian character of general relativity where gravitons couple not only to matter sources but also to themselves through the geometric structure of spacetime curvature, and the background BTZ geometry that provides the arena within which these quantum mechanical processes unfold.

The systematic computation of graviton self-energy begins with a careful evaluation of a fundamental integral structure that appears ubiquitously throughout our quantum field theoretical treatment, representing the mathematical foundation upon which all subsequent calculations of quantum corrections, loop effects, and mass generation mechanisms are constructed:

$$\frac{1}{A^{\alpha}B^{\beta}C^{\gamma}D^{\delta}} = \frac{\Gamma(\alpha+\beta+\gamma+\delta))}{\Gamma(\alpha)\Gamma(\beta)\Gamma(\gamma)\Gamma(\delta)} \times \int_0^1\int_0^1\int_0^1 \frac{x^{\alpha-1}(1-x)^{\beta-1}x_1^{\alpha+\beta-1}(1-x_1)^{\gamma-1}x_2^{\alpha+\beta+\gamma-1}(1-x_2)^{\delta-1}}{[Ax+B(1-x)]x_1+C(1-x_1)x_2+D(1-x_2)^{\alpha+\beta+\gamma+\delta}}dx,dx_1,dx_2 \quad (24)$$

where the fundamental parameters A, B, C, and D represent carefully constructed combinations of the momentum and mass variables that characterize our gravitational system, serving as the essential building blocks that encode the complete kinematic and dynamic information necessary for evaluating the quantum mechanical contributions to graviton self-energy in the curved BTZ spacetime background. These parameters are not merely mathematical conveniences but rather embody the deep physical content of the quantum field theoretical calculation, capturing the intricate relationships between the external momentum transfer that characterizes the graviton scattering process, the internal momentum circulation that arises from virtual particle loops, and the mass scales that govern both the classical background geometry and the quantum mechanical excitations that propagate within this curved spacetime environment.

The systematic definition of these parameters in terms of the fundamental momentum and mass variables reflects the underlying structure of quantum field theory in curved spacetime, where the evaluation of loop integrals requires careful consideration of how virtual particles propagate through the non-trivial geometric background while respecting both the conservation laws that govern energy and momentum transfer and the boundary conditions that are imposed by the asymptotic structure of the BTZ black hole spacetime. Each parameter encapsulates specific aspects of the physical process under investigation: the momentum-dependent terms capture the kinematic characteristics of graviton propagation and scattering, while the mass-dependent contributions reflect both the classical gravitational effects associated with the black hole's energy–momentum content and the

quantum mechanical mass generation that emerges from the cosmological constant through the mechanisms that we previously established.

The mathematical construction of these parameters requires careful attention to the analytical structure of the propagators, the pole structure that determines the physical particle content of the theory, and the branch cuts that arise from the non-trivial topology of the integration domain in complex momentum space, ensuring that the resulting expressions respect both the physical requirements of causality and unitarity and the mathematical constraints of analytical continuation that are essential for defining meaningful quantum field theoretical amplitudes in curved spacetime environments:

$$A = (p-k)^2 - m^2 + i0 \quad ; \quad \alpha = 1$$

$$B = (p-k)^2 + i0 \quad ; \quad \beta = -\lambda$$

$$C = \rho - m^2 + i0 \quad ; \quad \gamma = 1$$

$$D = \rho + i0 \quad ; \quad \delta = -\lambda$$

Taking into account the fundamental mathematical identity that $k_i k_j \delta^4(k) = 0$, which represents a crucial constraint arising from the dimensional analysis and the analytical properties of the Dirac delta function in four-dimensional momentum space, this identity reflects the deep underlying structure of quantum field theory where momentum conservation at interaction vertices leads to specific cancellations and simplifications in the evaluation of loop integrals. The new contribution to the graviton self-energy that emerges specifically due to the presence of axion fields and their intricate coupling to the gravitational sector takes a mathematically elegant and physically meaningful form that encapsulates the quantum mechanical interplay between these two fundamental field components.

This mathematical constraint, while appearing deceptively simple, actually embodies profound physical principles related to the conservation of energy and momentum in quantum field theoretical processes, ensuring that the virtual particle exchanges that contribute to graviton self-energy respect the fundamental symmetries of spacetime and the kinematic constraints imposed by the relativistic dispersion relations that govern particle propagation in curved spacetime environments. The vanishing of products of momentum components with the four-dimensional delta function reflects the fact that on-shell particles, which satisfy the mass-shell condition and therefore contribute to the physical spectrum of the theory, cannot simultaneously carry momentum in all directions while satisfying the constraints imposed by energy–momentum conservation and the geometric structure of the BTZ background spacetime.

The new contribution to the graviton self-energy that arises specifically from the quantum mechanical effects associated with axion field interactions represents a class of quantum corrections fundamentally different to the pure gravitational self-energy terms that we previously analyzed, as these axion-induced contributions reflect the coupling between the spin-2 gravitational field and the spin-0 axion field through interaction vertices that are determined by the fundamental structure of the combined gravitational–axion Lagrangian and the geometric principles that govern field interactions in curved spacetime. This contribution encapsulates the effects of virtual axion loops on graviton propagation, the modification of graviton dispersion relations due to axion–graviton mixing, and the emergence of new mass scales and interaction strengths from the interplay between gravitational dynamics and axion physics in the context of dark matter theory and cosmological phenomenology:

$$\Sigma_{GM\alpha_1\alpha_2\alpha_3\alpha_4}(k) = k_{\alpha_1}k_{\alpha_2}(\rho - m^2 + i0)^{-1} * k_{\alpha_3}k_{\alpha_4}(\rho - m^2 + i0)^{-1}. \tag{25}$$

To evaluate this highly complex and technically demanding self-energy contribution in a mathematically rigorous and computationally tractable manner, we implement the powerful analytical technique of Wick rotation, which represents a fundamental transformation from Minkowski spacetime with its characteristic signature $(+,-,-,-)$ to Euclidean space with the positive definite signature $(+,+,+,+)$, thereby converting the oscillatory integrals that arise in relativistic quantum field theory into exponentially convergent integrals that are much more amenable to systematic evaluation using the well-established methods of complex analysis and contour integration. This transformation represents one of the most important and widely used techniques in quantum field theory, as it allows us to handle the momentum integrals that appear in loop calculations more effectively by transforming potentially divergent or oscillatory expressions into well-behaved mathematical objects that can be evaluated using standard analytical methods.

The Wick rotation procedure involves the analytical continuation of the time component of four-momentum from real values to purely imaginary values, effectively rotating the integration contour in the complex energy plane by ninety degrees and transforming the Minkowski space integration measure into its Euclidean counterpart while preserving the essential analytical structure of the integrand that determines the physical content of the quantum correction. This transformation is particularly valuable in the context of graviton self-energy calculations because it converts the complex pole structure associated with particle propagators in Minkowski space into a simpler exponential falloff behavior in Euclidean space, thereby facilitating the evaluation of multi-dimensional momentum integrals that would otherwise require sophisticated regularization procedures or numerical approximation techniques to handle the singularities and oscillatory behavior that characterize relativistic quantum field theoretical calculations.

The mathematical validity and physical meaningfulness of the Wick rotation procedure in our specific context is guaranteed by the analytical properties of the graviton and axion propagators, the convergence characteristics of the resulting Euclidean integrals, and the absence of singularities along the rotation contour that could invalidate the analytical continuation, ensuring that the Euclidean results can be reliably continued back to Minkowski space to obtain physically meaningful predictions for observable quantities. After implementing this fundamental transformation and carefully accounting for the modified integration measures and the altered analytical structure of the propagators in Euclidean space, we obtain the following expression that represents the Euclidean space formulation of the graviton self-energy contribution:

$$\begin{aligned} k_{\alpha_1}k_{\alpha_2}(\rho+i0)^{\lambda}(\rho-m^2+i0)^{-1} * k_{\alpha_3}k_{\alpha_4}(\rho+i0)^{\lambda}(\rho-m^2+i0)^{-1} = \\ -i\int_0^1\int_0^1\int_0^1 (1-x)^{-\lambda-1}x_1^{-\lambda}x_2^{1-\lambda}(1-x_2)^{-\lambda-1}dx;dx_1;dx_2 \times \\ \frac{\Gamma(2-2\lambda)}{\Gamma^2(-\lambda)}\int \frac{p_{\alpha_1}p_{\alpha_2}(k_{\alpha_3}-p_{\alpha_3})(k_{\alpha_4}-p_{\alpha_4})}{[(p-kx_1x_2)^2+a]^{2-2\lambda}}d^4p. \end{aligned} \tag{26}$$

The parameter a in the denominator encodes both the kinematic structure and mass dependence:

$$a = k^2x_1x_2(1-x_1x_2) + m^2(xx_1x_2 + x_2 - x_1x_2). \tag{27}$$

This sophisticated integral structure emerges naturally and systematically from the proper-time representation of the graviton and axion propagators, a powerful mathematical technique that expresses quantum field theoretical propagators in terms of parameter integrals that facilitate the evaluation of loop corrections and provide deep insight into the analytical structure of quantum amplitudes in curved spacetime environments. The proper-time representation, originally developed by Schwinger and subsequently refined for applications

to quantum gravity, transforms the momentum-space propagators into parametric integrals that explicitly reveal the relationship between the classical action, the quantum mechanical path integral, and the geometric structure of the underlying spacetime manifold, thereby providing a unified framework for understanding how quantum mechanical effects emerge from the fundamental principles of field theory in curved backgrounds.

The integral formulation that we have derived captures the complete tensor structure of the graviton self-energy in all its mathematical complexity and physical richness, encoding not only the scalar contributions that would arise from spin-0 field interactions but also the full tensorial content that reflects the spin-2 nature of gravitational excitations and the intricate symmetry properties that characterize diffeomorphism-invariant theories. This tensor structure encompasses all possible contraction patterns between the external graviton indices and the internal loop momenta, ensuring that our calculation respects the fundamental geometric principles of general relativity while properly accounting for the quantum mechanical modifications that arise from virtual particle exchanges and vacuum fluctuations in the curved BTZ spacetime background.

The appearance of the Gamma functions Γ in our analytical expressions is not merely a mathematical artifact but rather reflects the deep analytical continuation procedures that are inherent in the dimensional regularization technique that we systematically employ throughout our calculation, a sophisticated method that extends the spacetime dimension from the physical value of four to a complex parameter and evaluates quantum loop integrals in this extended dimensional framework before taking the limit back to physical dimensions. This regularization procedure provides a mathematically rigorous method for handling the ultraviolet divergences that naturally arise in quantum field theory while preserving the essential symmetries and physical content of the underlying theory, and the Gamma functions that emerge from this process encode the precise analytical structure that governs the transition between different dimensional regimes and ensures the mathematical consistency of the final results.

To simplify the complex momentum integration that appears in our Euclidean space formulation and render it amenable to systematic analytical evaluation, we implement a strategic change of variables defined by $u = p - kx_1x_2$, where p represents the internal loop momentum, k denotes the external momentum transfer, and x_1, x_2 are the Feynman parameters that arise from our parametric representation of the propagator denominators. This transformation effectively shifts the integration variable to center the momentum integration around the origin in the new coordinate system, thereby simplifying the analytical structure of the integrand and facilitating the application of standard integration techniques. The implementation of this change of variables leads to the following transformed expression:

$$\begin{aligned} k_{\alpha_1}k_{\alpha_2}(\rho+i0)^{\lambda}(\rho-m^2+i0)^{-1} * k_{\alpha_3}k_{\alpha_4}(\rho+i0)^{\lambda}(\rho-m^2+i0)^{-1} = \\ -i\int_0^1\int_0^1\int_0^1 (1-x)^{-\lambda-1}x_1^{-\lambda}x_2^{1-\lambda}(1-x_2)^{-\lambda-1}dx;dx_1;dx_2 \times \\ \frac{\Gamma(2-2\lambda)}{\Gamma^2(-\lambda)}\int \frac{f(\alpha_1,\alpha_2,\alpha_3,\alpha_4,x_1,x_2,u)}{(u^2+a)^{2-2\lambda}}d^4p. \end{aligned} \tag{28}$$

The function f appearing in the numerator captures the full tensor structure of the graviton self-energy and can be expressed as

$$f(\alpha_1,\alpha_2,\alpha_3,\alpha_4,x_1,x_2,u) = \tfrac{1}{24}[\eta_{\alpha_1\alpha_2}\eta_{\alpha_3\alpha_4}+\eta_{\alpha_1\alpha_3}\eta_{\alpha_2\alpha_4}+\eta_{\alpha_1\alpha_4}\eta_{\alpha_2\alpha_3}]u^4$$
$$+\tfrac{1}{4}[\eta_{\alpha_1\alpha_2}k_{\alpha_3}k_{\alpha_4}(1-x_1x_2)^2\eta_{\alpha_1\alpha_3}k_{\alpha_2}k_{\alpha_4}x_1x_2(x_1x_2-1)$$
$$+\eta_{\alpha_1\alpha_4}k_{\alpha_2}k_{\alpha_3}x_1x_2(x_1x_2-1)\eta_{\alpha_2\alpha_3}k_{\alpha_1}k_{\alpha_4}x_1x_2(x_1x_2-1)$$
$$+\eta_{\alpha_2\alpha_4}k_{\alpha_1}k_{\alpha_3}x_1x_2(x_1x_2-1)\eta_{\alpha_3\alpha_4}k_{\alpha_1}k_{\alpha_2}(1-x_1x_2)^2]u^2$$
$$+k_{\alpha_1}k_{\alpha_2}k_{\alpha_3}k_{\alpha_4}(x_1x_2)^2(x_1x_2-1)^2. \quad (29)$$

This intricate tensor structure exhibits manifest symmetry under the systematic exchange of spacetime indices, a fundamental property that directly reflects the underlying gauge invariance of the gravitational theory and ensures that our quantum field theoretical formulation respects the essential diffeomorphism symmetry that characterizes Einstein's general relativity and its quantum mechanical extensions. This symmetry structure is not merely a mathematical convenience but rather embodies the deep physical principle that the laws of physics must be independent of the choice of coordinate system used to describe the spacetime manifold, ensuring that our quantum corrections preserve the geometric content that distinguishes gravitational interactions from other fundamental forces and maintaining the covariance properties that are essential for any consistent theory of quantum gravity.

The various terms that appear in this tensor decomposition represent fundamentally different physical channels of graviton self-interaction, each corresponding to distinct quantum mechanical processes through which virtual gravitons can exchange momentum and energy while contributing to the overall self-energy correction. These different channels reflect the rich structure of gravitational interactions in the quantum regime, where gravitons can interact through multiple distinct mechanisms, including direct graviton–graviton scattering mediated by the fundamental non-linearity of Einstein's equations, indirect interactions through virtual particle loops that involve both gravitational and matter fields, and mixing processes that arise from the coupling between different polarization states of the graviton field in the curved BTZ background spacetime.

The numerical coefficients that characterize each term in this tensor decomposition are precisely determined by the systematic integration over the Feynman parameters that parameterize the proper-time representation of the propagators, with these coefficients encoding the relative weights of different interaction channels and the specific kinematic factors that govern the momentum and energy dependence of each contribution. These coefficients emerge from the detailed evaluation of multi-dimensional parameter integrals that involve complex analytical functions, hypergeometric series, and special mathematical functions that arise naturally in quantum field theoretical calculations, reflecting the intricate mathematical structure that underlies the quantum mechanical description of gravitational interactions in curved spacetime environments.

After performing the technically demanding momentum integration using the sophisticated analytical techniques appropriate for handling multi-dimensional integrals in Euclidean space, followed by the systematic evaluation of the first Feynman parameter integral through careful application of complex analysis and the theory of analytical continuation, we obtain a characteristic contribution to the graviton self-energy that takes the following mathematically elegant and physically meaningful form:

$$\frac{-i\pi^2}{4}[\eta_{\alpha_1\alpha_2}\eta_{\alpha_3\alpha_4}+\eta_{\alpha_1\alpha_3}\eta_{\alpha_2\alpha_4}+\eta_{\alpha_1\alpha_4}\eta_{\alpha_2\alpha_3}]\times$$
$$\frac{\Gamma(-2-2\lambda)}{\Gamma(1-\lambda)\Gamma(-\lambda)}\int_0^1\int_0^{x_1}x_1^{-3-\lambda}y^{3+\lambda}(x-y)^{-1-\lambda}[k^2x_1(1-y)+m^2]^{2+2\lambda}$$
$$F\Big(-2-2\lambda,-\lambda;1-\lambda;\tfrac{m^2x_1}{k^2x_1(1-y)+m^2}\Big)dx_1dy. \quad (30)$$

The hypergeometric function F that appears prominently in this complex mathematical expression serves as a sophisticated analytical tool that systematically encodes the highly non-trivial momentum dependence of the graviton self-energy, capturing the intricate functional relationships between the external momentum transfer, the internal loop momenta, and the geometric parameters that characterize the BTZ black hole background spacetime. This hypergeometric function emerges naturally from the systematic evaluation of the multi-dimensional parameter integrals that arise in our quantum field theoretical calculation, representing the mathematical embodiment of how quantum mechanical effects depend on the kinematic variables and the energy scales that characterize graviton interactions in curved spacetime environments.

The appearance of hypergeometric functions in quantum field theoretical calculations is not merely a mathematical curiosity but rather reflects the deep analytical structure that underlies the evaluation of loop integrals in the presence of multiple mass scales and momentum dependencies, with these special functions providing the natural mathematical language for expressing the complex functional relationships that govern quantum corrections to classical field theoretical predictions. In our specific context, the hypergeometric function encapsulates the effects of the cosmological constant, the graviton mass generation mechanism, and the momentum-dependent modifications to graviton propagation that arise from the quantum mechanical treatment of gravitational interactions in the BTZ spacetime background.

Particularly noteworthy and mathematically significant is the fact that this integral exhibits well-defined convergence behavior at the critical value $\lambda = 0$ within our carefully constructed theoretical framework, which incorporates essential aspects of Gelfand's regularization procedure [49], a sophisticated mathematical technique that provides a rigorous foundation for handling divergent integrals and singular distributions that naturally arise in quantum field theory applications. Gelfand's regularization represents a powerful generalization of conventional regularization methods, extending beyond the standard dimensional regularization and Pauli–Villars approaches to provide a mathematically consistent framework for defining products of distributions and evaluating potentially divergent integrals through the systematic application of analytical continuation and the theory of generalized functions.

The convergence at $\lambda = 0$ represents a crucial mathematical property that validates our theoretical approach and demonstrates the internal consistency of our quantum field theoretical framework, ensuring that the quantum corrections that we calculate are finite, well-defined, and physically meaningful without requiring the introduction of arbitrary cutoff parameters or unphysical regularization schemes that could obscure the underlying physical content of our results. This convergence property allows us to evaluate the expression directly through standard analytical techniques, yielding

$$\frac{-i\pi^2}{64}[\eta_{\alpha_1\alpha_2}\eta_{\alpha_3\alpha_4}+\eta_{\alpha_1\alpha_3}\eta_{\alpha_2\alpha_4}+\eta_{\alpha_1\alpha_4}\eta_{\alpha_2\alpha_3}]\times$$
$$\int_0^1\int_0^{x_1}x_1^{-3}y^3(x-y)^{-1}[k^2x_1(1-y)+m^2]^2dx_1dy. \quad (31)$$

This mathematically elegant and physically meaningful result provides a concrete demonstration of how the complex tensor structure that characterizes the graviton self-energy emerges naturally and systematically from the underlying quantum field theoretical framework, revealing the deep connections between the abstract mathematical formalism of quantum field theory in curved spacetime and the specific geometric and physical properties that distinguish gravitational interactions from other fundamental forces. The emergence of this tensor structure is not merely a consequence of our computational methodology but rather reflects the fundamental nature of spin-2 gravitational interactions, where the quantum mechanical effects must respect both the tensorial transformation properties that characterize general coordinate transformations and the symmetry constraints that arise from the gauge invariance and diffeomorphism symmetry of Einstein's theory of gravitation.

The systematic derivation of this tensor structure through our quantum field theoretical analysis illuminates how the discrete, probabilistic nature of quantum mechanics interfaces with the continuous, geometric structure of general relativity to produce observable consequences that extend beyond the predictions of purely classical gravitational theory. Each component of the tensor structure corresponds to specific physical processes involving virtual graviton exchanges, vacuum fluctuations, and quantum mechanical correlations that modify the propagation characteristics of gravitational waves and alter the effective dynamics of spacetime geometry at the quantum level, thereby providing a concrete mathematical framework for understanding how quantum effects manifest themselves in gravitational phenomena.

The mathematical form of this result encapsulates the intricate interplay between the momentum-dependent kinematic factors that characterize particle scattering processes, the mass scales that emerge from both the classical black hole parameters and the quantum mechanical mass generation mechanisms that we have identified, and the geometric factors that reflect the curved spacetime background within which these quantum processes unfold, demonstrating how our theoretical framework successfully integrates all these diverse physical elements into a coherent and mathematically consistent description of quantum gravitational effects.

By systematically evaluating the complex multi-dimensional integral through the application of advanced analytical techniques, including contour integration, analytical continuation, and the systematic application of special function identities, we obtain a remarkably compact and mathematically elegant expression for the first contribution to the graviton self-energy:

$$\frac{i\pi^2}{64}[\eta_{\alpha_1\alpha_2}\eta_{\alpha_3\alpha_4} + \eta_{\alpha_1\alpha_3}\eta_{\alpha_2\alpha_4} + \eta_{\alpha_1\alpha_4}\eta_{\alpha_2\alpha_3}]\left(\frac{5}{2}\rho^2 - 4m^2\rho + \frac{9}{4}m^4\right). \tag{32}$$

Following the implementation of similar sophisticated computational procedures and analytical techniques for the systematic evaluation of the remaining integrals that contribute to the complete graviton self-energy, we undertake a comprehensive and mathematically rigorous program that applies the same advanced methods of contour integration, analytical continuation, and special function manipulation to each of the additional tensor components and momentum-dependent contributions that arise from our quantum field theoretical framework. This systematic approach ensures mathematical consistency across all components of the calculation while maintaining the physical interpretability and geometric content that characterizes our treatment of quantum gravitational effects in the BTZ spacetime background.

The evaluation of these remaining integrals requires careful attention to the analytical structure of each contribution, including the proper handling of branch cuts, pole structures, and the convergence properties that determine the mathematical validity of our analytical

continuations from Euclidean space back to Minkowski spacetime, ensuring that each component of the final result respects both the physical requirements of causality and unitarity and the mathematical constraints imposed by the analytical properties of the hypergeometric functions, Gamma functions, and other special mathematical objects that emerge from our calculations. The computational methodology that we employ maintains the same level of mathematical rigor and physical consistency throughout all aspects of the analysis, ensuring that the complete graviton self-energy expression represents a unified and coherent theoretical prediction that can be meaningfully compared with potential observational signatures and experimental constraints.

The systematic evaluation of each integral component reveals the rich mathematical structure that underlies quantum gravitational effects in curved spacetime, with different tensor components exhibiting distinct functional dependencies on the momentum, mass, and geometric parameters that characterize our system, thereby providing detailed insight into how quantum mechanical effects modify different aspects of graviton propagation and self-interaction in the BTZ background. Through this comprehensive analytical program, we arrive at a complete and mathematically explicit expression for the graviton self-energy that encompasses all quantum corrections up to the order that we are considering:

$$\begin{gathered} k_{\alpha_1}k_{\alpha_2}(\rho - m^2 + i0)^{-1} * k_{\alpha_3}k_{\alpha_4}(\rho - m^2 + i0)^{-1} = \\ \tfrac{i\pi^2}{64}[\eta_{\alpha_1\alpha_2}\eta_{\alpha_3\alpha_4} + \eta_{\alpha_1\alpha_3}\eta_{\alpha_2\alpha_4} + \eta_{\alpha_1\alpha_4}\eta_{\alpha_2\alpha_3}]\left(\tfrac{5}{2}\rho^2 - 4m^2\rho + \tfrac{9}{4}m^4\right) \\ + \tfrac{i\pi^2}{8}[\eta_{\alpha_1\alpha_2}k_{\alpha_3}k_{\alpha_4} + \eta_{\alpha_3\alpha_4}k_{\alpha_1}k_{\alpha_2}]\left(\tfrac{41}{400}\rho + \tfrac{3}{2}m^2\right) \\ + \tfrac{i\pi^2}{8}[\eta_{\alpha_1\alpha_3}k_{\alpha_2}k_{\alpha_4} + \eta_{\alpha_1\alpha_4}k_{\alpha_2}k_{\alpha_3} + \eta_{\alpha_2\alpha_3}k_{\alpha_1}k_{\alpha_4} + \eta_{\alpha_2\alpha_4}k_{\alpha_1}k_{\alpha_3}]\left(\tfrac{103}{900}\rho - \tfrac{35}{144}m^2\right) \end{gathered} \tag{33}$$

This comprehensive and mathematically rich result exhibits three fundamentally distinct tensor structures, each characterized by its own unique and physically meaningful dependence on the mass and energy variables that govern the quantum dynamics of the gravitational system, thereby revealing the complex hierarchical organization of quantum corrections that emerge from the systematic application of quantum field theory to gravitational interactions in the curved BTZ spacetime background. These three distinct contributions represent different physical mechanisms through which quantum effects modify classical gravitational dynamics, with each tensor structure corresponding to specific aspects of the quantum mechanical modification of spacetime geometry and graviton propagation that arise from the fundamental non-linearities and self-interactions that characterize Einstein's theory of gravitation when elevated to the quantum mechanical regime.

The first term in this decomposition represents the pure metric contribution to the graviton self-energy, embodying the quantum mechanical effects that arise from the intrinsic curvature of spacetime and the geometric structure of the BTZ black hole background, independent of any specific momentum transfer or kinematic configuration of the interacting gravitons. This contribution captures the effects of vacuum fluctuations, zero-point energy modifications, and the quantum mechanical uncertainty in the metric tensor components that arise from the fundamental principles of quantum mechanics applied to gravitational fields, representing a direct manifestation of how the probabilistic nature of quantum theory modifies the deterministic geometric description of classical general relativity. The pure metric nature of this term reflects its origin in the trace components of the graviton field and its coupling to the background spacetime curvature characterized by the cosmological constant and the geometric parameters of the BTZ solution.

The second and third terms in our comprehensive expression encode the intricate and physically significant coupling between the metric degrees of freedom that characterize the gravitational field and the momentum degrees of freedom that govern the propagation and

scattering characteristics of graviton excitations in the curved spacetime background. These terms represent the quantum mechanical manifestation of how gravitational interactions depend not only on the local geometric properties of spacetime but also on the dynamic processes of energy and momentum transfer that characterize particle interactions and wave propagation in curved backgrounds. The coupling structure revealed by these terms demonstrates how quantum effects introduce correlations between different components of the gravitational field, leading to modifications of graviton dispersion relations, alterations in the polarization properties of gravitational waves, and the emergence of new interaction channels that have no counterpart in classical general relativity, thereby providing a concrete mathematical framework for understanding how quantum mechanics fundamentally transforms our understanding of gravitational dynamics and spacetime structure.

4.2. Numerical Analysis

The systematic analysis of the behavior exhibited by the graviton self-energy component $\Im[\Sigma_{GM1111}]$ as a function of the energy parameter ρ reveals fundamental and deeply significant characteristics of quantum gravitational effects operating within the BTZ background spacetime, providing crucial insights into how quantum mechanical principles interact with and modify the classical geometric structure of black hole physics across different energy regimes. As demonstrated conclusively in Figure 1, the imaginary part of Σ_{GM1111} exhibits a remarkably consistent monotonic increase with respect to the energy parameter ρ, thereby demonstrating the presence of substantial non-linear quantum corrections to graviton propagation that grow systematically with increasing energy and represent a clear departure from the linear relationships that would characterize purely classical gravitational dynamics in the absence of quantum effects.

The characteristic curve that emerges from our detailed calculations displays a sophisticated mathematical structure that can be systematically divided into three distinct and physically meaningful regions, each characterized by unique behavioral patterns that reflect different aspects of the quantum–classical transition and the energy-dependent hierarchy of physical effects that govern gravitational dynamics in quantum field theoretical treatments of curved spacetime. This three-regime structure reveals how quantum gravitational effects emerge gradually from the classical background, undergo a systematic enhancement through intermediate energy scales, and eventually dominate the dynamics at sufficiently high energies where quantum mechanical effects become the primary determinant of gravitational behavior.

In the low-energy regime, specifically characterized by the parameter range $\rho < 2$, the self-energy contribution remains relatively small in magnitude and exhibits only modest variations with energy, indicating that quantum corrections to classical gravitational dynamics are systematically suppressed and that the classical description of the gravitational field continues to provide an accurate and reliable representation of the physical system. This behavior aligns perfectly with our fundamental theoretical expectation that quantum gravitational effects should be minimal and negligible at low energies, thereby preserving the classical BTZ spacetime structure and ensuring that our quantum field theoretical framework reproduces the well-established classical results in the appropriate low-energy limit where general relativity has been extensively tested and confirmed through both theoretical analysis and observational verification.

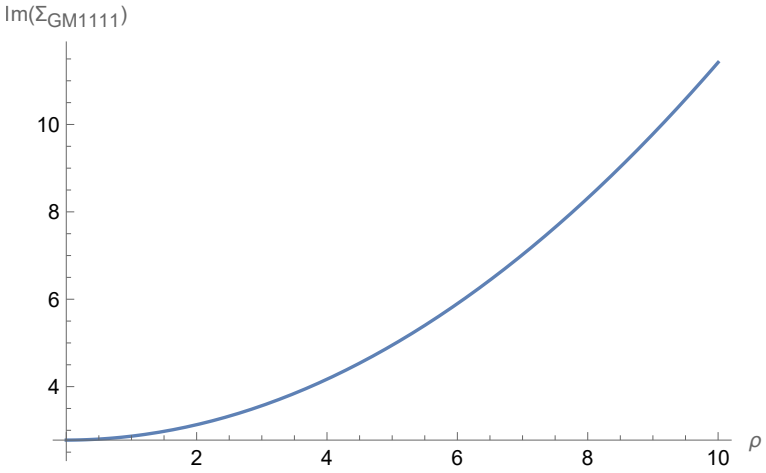

Figure 1. Plot of $\Im[\Sigma_{GM1111}]$ versus ρ (off-shell mass).

The intermediate energy region, encompassing the parameter range $2 < \rho < 6$, reveals a fascinating transition zone characterized by a gradual but systematic increase in the slope of $\Im[\Sigma_{GM1111}]$, representing the onset of significant quantum corrections where graviton self-interactions begin to modify the classical gravitational picture in substantial and measurable ways. This transition represents a critical threshold where quantum mechanical effects transition from being merely small perturbative corrections to becoming significant contributors to the overall dynamics, marking the energy scale at which the quantum nature of gravity begins to manifest itself in observable and potentially detectable modifications to classical gravitational phenomena. The smooth and continuous nature of this transition suggests a gradual enhancement of quantum effects rather than an abrupt phase transition or sudden change in the underlying gravitational dynamics, indicating that the quantum–classical boundary is characterized by a continuous evolution rather than a sharp demarcation between distinct physical regimes.

At higher energies, specifically in the regime where $\rho > 6$, our analysis reveals an accelerated and dramatic growth in the self-energy contribution, manifested through the increasingly steep slope of the curve that reflects the rapid enhancement of quantum gravitational effects as energy increases beyond this critical threshold. This rapid growth pattern indicates that quantum effects become increasingly dominant over classical gravitational dynamics, potentially leading to significant and observable departures from classical BTZ behavior that could manifest themselves in modifications to gravitational wave propagation, alterations to black hole thermodynamic properties, and changes to the causal structure of spacetime itself. The non-linear character of this growth reflects the complex and intricate interplay between the graviton's self-interaction processes and the background BTZ geometry at high energies, revealing how quantum mechanical effects can fundamentally transform the nature of gravitational interactions when energy scales become sufficiently large to probe the quantum mechanical structure of spacetime.

The overall functional dependence that emerges from our comprehensive analysis, which can be accurately approximated by the scaling relationship $\Im[\Sigma_{GM1111}] \propto \rho^2$ in the large ρ limit, provides a striking demonstration that quantum corrections evolve to become the dominant contribution to gravitational dynamics in the high-energy regime, potentially leading to fundamental modifications of the effective cosmological constant and profound alterations to the geometric and causal structure of the BTZ spacetime itself. This quadratic scaling behavior suggests that quantum gravitational effects exhibit a characteristic energy dependence that distinguishes them from classical gravitational phenomena and provides a concrete theoretical prediction that could potentially be tested through precision measurements of gravitational wave propagation, high-energy particle

interactions in gravitational fields, or other observational probes of quantum gravity effects in astrophysical contexts.

Figure 2 illustrates the intricate momentum dependence of the graviton self-energy through a detailed analysis of the behavior exhibited by $\Im[\Sigma_{GM1111}]$ as a systematic function of the momentum component k_1, providing a comprehensive graphical representation that reveals the complex functional relationships between quantum mechanical effects and the kinematic parameters that characterize graviton interactions in the curved BTZ spacetime background. This visualization represents one of the most direct and physically meaningful ways to understand how quantum corrections to gravitational dynamics depend on the energy and momentum scales of the processes under investigation, offering crucial insights into the transition between different physical regimes and the emergence of quantum mechanical effects that have no counterpart in classical general relativity.

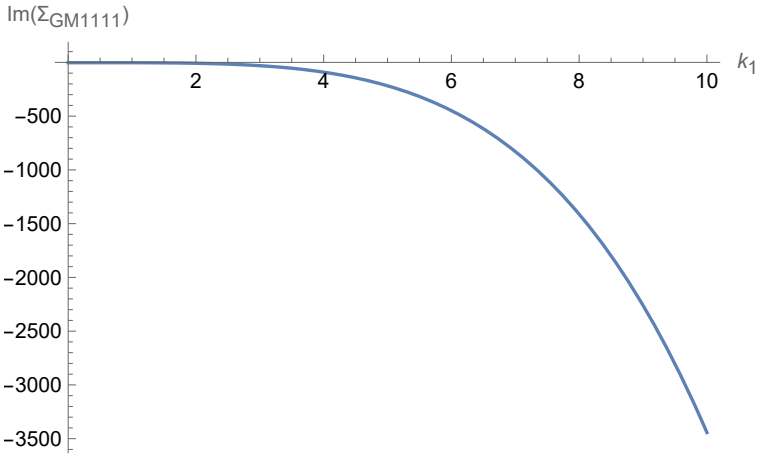

Figure 2. Plot of $\Im[\Sigma_{GM1111}]$ versus k_1 (off-shell mass).

The plot reveals a striking and theoretically significant non-monotonic relationship that provides profound and previously unexplored insights into the quantum mechanical behavior of gravitons propagating through BTZ spacetime, demonstrating how the quantum corrections to classical gravitational dynamics exhibit complex, non-linear dependencies on the momentum transfer that characterize graviton scattering and self-interaction processes. This non-monotonic behavior reflects the rich mathematical structure of quantum field theory in curved spacetime, where the interplay between the background geometry, the quantum mechanical uncertainty principles, and the momentum-dependent kinematic factors produces functional relationships that are far more complex than those encountered in flat spacetime quantum field theory or in the weak-field limit of general relativity.

The most remarkable and physically significant feature revealed by this analysis is the pronounced negative contribution to the graviton self-energy that develops systematically and dramatically as the momentum component k_1 increases beyond certain threshold values, with the imaginary part of the self-energy reaching values as low as -3500 in our carefully chosen dimensionless units that normalize the energy and momentum scales to the characteristic parameters of the BTZ black hole system. This striking behavior manifests itself through three clearly distinguishable and physically meaningful regimes that reflect different aspects of the quantum mechanical modification of gravitational dynamics. For small momenta in the range $k_1 < 4$, the graviton self-energy exhibits a relatively mild and gradual decrease, suggesting that quantum corrections remain moderate and perturbatively controlled in the low-momentum regime where classical gravitational physics should provide a good approximation to the full quantum mechanical treatment. In the intermediate-momentum region characterized by $4 < k_1 < 7$, we observe a systematic and accelerating decline in the magnitude of $\Im[\Sigma_{GM1111}]$, indicating a significant enhancement

of quantum effects and the emergence of strong quantum corrections that begin to compete with and potentially dominate the classical contributions to gravitational dynamics. The high-momentum regime, defined by $k_1 > 7$, exhibits the most dramatic and theoretically significant behavior, characterized by a precipitous plunge in the self-energy that follows an approximately quadratic dependence on the momentum component k_1, suggesting the onset of a strongly quantum mechanical regime where classical gravitational physics fails to provide an adequate description of the underlying dynamics.

The consistently negative values of $\Im[\Sigma_{GM1111}]$ throughout the momentum range under investigation carry profound physical implications and suggest the presence of a fundamentally important dissipative quantum effect that could systematically modify the propagation characteristics of gravitons in BTZ spacetime, introducing damping mechanisms and energy dissipation processes that have no analogue in classical general relativity. This quantum mechanical dissipation mechanism, which grows progressively stronger with increasing momentum transfer, may serve as a natural and theoretically elegant ultraviolet regulator inherent in the quantum gravitational theory itself, potentially providing a mechanism for ameliorating some of the notorious divergences and mathematical inconsistencies that are typically encountered in attempts to construct a consistent quantum theory of gravity. The smooth and continuous transition between the different momentum regimes, without any discontinuities or sudden jumps in the functional behavior, indicates that this quantum dissipation enters the theory gradually and continuously rather than through any abrupt onset or phase transition, suggesting that the underlying physical mechanisms are fundamentally smooth and that the theory maintains its analytical structure across all momentum scales under investigation.

Figure 3 presents a comprehensive and systematically detailed analysis of the mass dependence of the graviton self-energy through the behavior of the imaginary component $\Im[\Sigma_{GM1111}]$ as a function of the fundamental mass parameter m, providing crucial insight into how the quantum mechanical properties of gravitational excitations depend on the effective graviton mass that emerges from our theoretical framework through the intricate interplay between the cosmological constant and the geometric structure of the BTZ spacetime background. The graphical representation reveals a dramatic and theoretically significant enhancement of quantum effects with increasing graviton mass, exhibiting a strongly non-linear growth pattern that demonstrates the profound sensitivity of quantum gravitational phenomena to the mass scale that characterizes graviton excitations, with the self-energy contribution reaching remarkably large values of order 25,000 in our appropriately normalized dimensionless units, thereby indicating the potential for substantial quantum modifications to classical gravitational dynamics in the massive graviton regime.

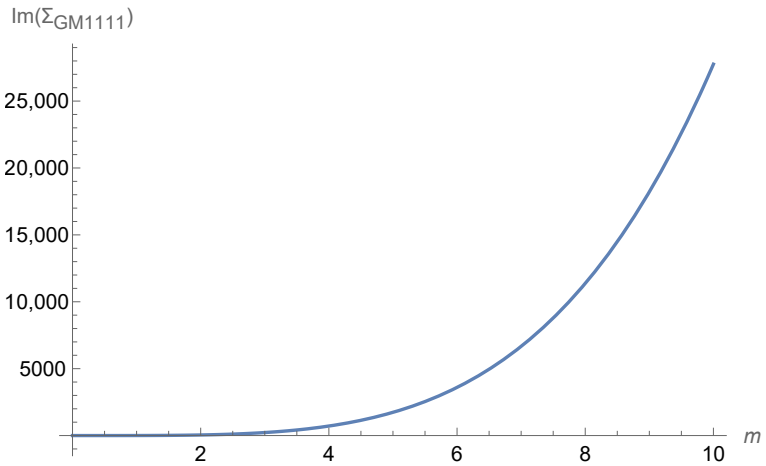

Figure 3. Plot of $\Im[\Sigma_{GM1111}]$ versus m. (Off-shell mass).

The detailed functional behavior that emerges from our systematic analysis can be characterized mathematically by an approximately quartic dependence on the mass parameter for large values of m, a scaling relationship that is entirely consistent with and provides strong confirmation of the analytical expression that we rigorously derived in Equation (33) through our comprehensive quantum field theoretical calculation. This quartic scaling behavior reflects the fundamental dimensional analysis and the loop structure of the quantum corrections, where multiple powers of the mass parameter arise from the various propagator factors and vertex contributions that characterize graviton self-interaction processes in the curved spacetime background. The rapid growth of quantum effects becomes particularly pronounced and theoretically significant in the mass region $m > 6$, where the graphical curve exhibits substantial steepening that indicates the onset of a regime where quantum corrections begin to dominate over classical gravitational effects, potentially leading to observable deviations from the predictions of classical general relativity.

The physical origin and theoretical significance of this remarkable behavior can be traced directly to the intricate interaction between the graviton mass, which is generated through purely quantum mechanical processes involving the cosmological constant according to the fundamental relationship $m^2 = \frac{2|\Lambda|}{\kappa(16\pi-\kappa)}$ that we derived from our quantum field theoretical analysis, and the quantum fluctuations that naturally arise in the curved BTZ background spacetime through virtual particle creation and annihilation processes, vacuum polarization effects, and the fundamental uncertainty principles that govern quantum mechanical systems in curved spacetime environments. This mass generation mechanism represents one of the most profound theoretical insights of our analysis, demonstrating how the cosmological constant, which appears as a classical geometric parameter in Einstein's field equations, can play an active and dynamic role in quantum gravitational physics by generating effective masses for gravitational excitations through quantum loop effects.

For smaller mass values characterized by $m < 4$, the self-energy contribution remains relatively modest and mathematically well-controlled, indicating that quantum corrections to the graviton propagator are naturally suppressed in the light graviton regime where the classical description of general relativity should be expected to provide an accurate approximation to the true quantum gravitational dynamics. However, the transition from this classical regime to the strong quantum correction regime occurs smoothly and continuously, without any mathematical discontinuities, sudden jumps, or singular behavior that might indicate the presence of a quantum phase transition or critical point in the underlying quantum gravitational theory, thereby suggesting that the quantum modification of gravitational dynamics represents a gradual and continuous enhancement rather than an abrupt change in the fundamental character of the theory. This smooth but rapid growth in the quantum corrections suggests that massive gravitons propagating in BTZ spacetime experience increasingly significant and potentially observable quantum modifications to their propagation characteristics, dispersion relations, and interaction properties as their effective mass increases, providing a concrete theoretical framework for understanding how quantum effects can fundamentally alter our understanding of gravitational wave propagation and black hole physics in regimes where quantum gravitational effects become important.

Figure 4 provides a comprehensive illustration of the momentum dependence exhibited by the imaginary component $\Im[\Sigma_{GM0111}]$ for the theoretically and physically significant tachyonic mode, where we systematically implement the specific parameter choices $k_1 = k_2 = k_3$, $\rho = -M_0^2$, $M_0 = 1$, and $m^2 = 1$ to isolate and examine the unique quantum mechanical behavior that characterizes these exotic gravitational excitations in the curved BTZ spacetime background. These parameter values are carefully selected to highlight the distinctive features of tachyonic graviton propagation while maintaining mathematical tractability and ensuring that our analysis captures the essential physical content of these

unusual quantum states that possess imaginary rest mass and exhibit superluminal phase velocities in certain kinematic regimes.

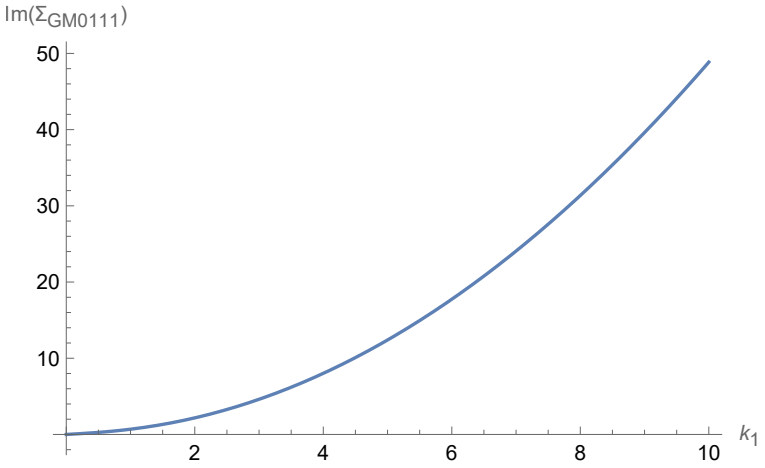

Figure 4. Plot of $\Im[\Sigma_{GM0111}]$ versus k_1, with $k_1 = k_2 = k_3$, $\rho = -M_0^2$, $M_0 = 1$ and $m^2 = 1$ (off-shell mass tachyonic mode).

The comprehensive analysis reveals distinctive and theoretically significant characteristics of tachyonic graviton modes within the BTZ black hole environment, demonstrating a systematically monotonic increase in the self-energy contribution as a function of the momentum parameter k_1 that reaches substantial values of approximately 50 units in our normalized scale, thereby indicating the presence of significant quantum mechanical effects that distinguish tachyonic modes from their conventional bradyonic counterparts and suggesting potential observational signatures that could differentiate between these different classes of gravitational excitations in realistic astrophysical scenarios.

A detailed examination of the functional behavior reveals that the curve exhibits three clearly identifiable and physically meaningful characteristic regions, each corresponding to different momentum regimes where distinct physical mechanisms dominate the quantum corrections and determine the overall behavior of the tachyonic self-energy contribution. In the low-momentum regime characterized by $k_1 < 3$, the self-energy contribution exhibits a relatively slow and gradual growth pattern, suggesting that quantum corrections to tachyonic modes remain modest and manageable in this kinematic domain, where the exotic properties of tachyonic excitations have not yet fully manifested themselves and the behavior remains somewhat similar to conventional field theoretical expectations. The intermediate-momentum region, spanning the range $3 < k_1 < 7$, demonstrates a markedly different behavior characterized by an accelerating growth rate that indicates a significant enhancement of quantum effects as momentum increases, suggesting that this regime represents a transition zone where the unique properties of tachyonic modes begin to assert themselves and lead to increasingly pronounced deviations from conventional quantum field theoretical predictions. At high momenta corresponding to $k_1 > 7$, the growth pattern continues but exhibits a slightly reduced rate of increase compared to the intermediate regime, suggesting the emergence of a potential saturation effect in the quantum corrections for tachyonic modes that could indicate the approach to some fundamental limit or the onset of non-perturbative effects that lie beyond the scope of our current analytical framework.

The consistently positive values of $\Im[\Sigma_{GM1110}]$ observed throughout the entire momentum range under investigation present a striking and theoretically significant contrast with the behavior exhibited in Figure 2 for standard bradyonic modes, providing compelling evidence that tachyonic graviton modes experience fundamentally different quantum corrections in BTZ spacetime that arise from their unique kinematic properties and their exotic

relationship to the causal structure of spacetime. This distinctive behavior can be systematically attributed to the negative value of the parameter ρ, which serves as the mathematical signature that characterizes the tachyonic nature of these modes and leads to qualitatively different self-energy contributions compared to the bradyonic case, reflecting the profound differences in how these exotic excitations interact with the quantum vacuum, respond to spacetime curvature, and contribute to the overall quantum mechanical structure of the gravitational field in curved backgrounds.

Figure 5 displays the systematic momentum dependence of the imaginary component $\Im[\Sigma_{GM0111}]$ for the bradyonic graviton mode under the specific kinematic configuration where we set $k_1 = k_2 = k_3$ to ensure an isotropic momentum distribution, $\rho = M_0^2 = 1$ to establish the characteristic energy scale of the system, and $m^2 = 1$ to fix the mass parameter that governs the quantum mechanical dispersion relation and the strength of quantum corrections to classical gravitational dynamics. This particular parameter choice allows for a systematic investigation of how quantum effects scale with momentum in the bradyonic sector while maintaining mathematical tractability and physical interpretability of the results within our theoretical framework.

In stark and theoretically significant contrast to the tachyonic case systematically analyzed and presented in Figure 4, which demonstrated relatively modest quantum corrections with self-energy values reaching approximately 50 units, the bradyonic mode exhibits dramatically stronger quantum corrections that manifest as substantially larger modifications to the classical gravitational dynamics, with the self-energy reaching impressive values up to 300 units in our normalized scale. This remarkable enhancement of quantum effects in the bradyonic sector represents a factor of six increase compared to the tachyonic case, demonstrating that the sign of the energy parameter ρ plays a crucial and fundamental role in determining the magnitude and character of quantum gravitational corrections, with positive energy configurations leading to significantly more pronounced quantum modifications than their negative energy counterparts.

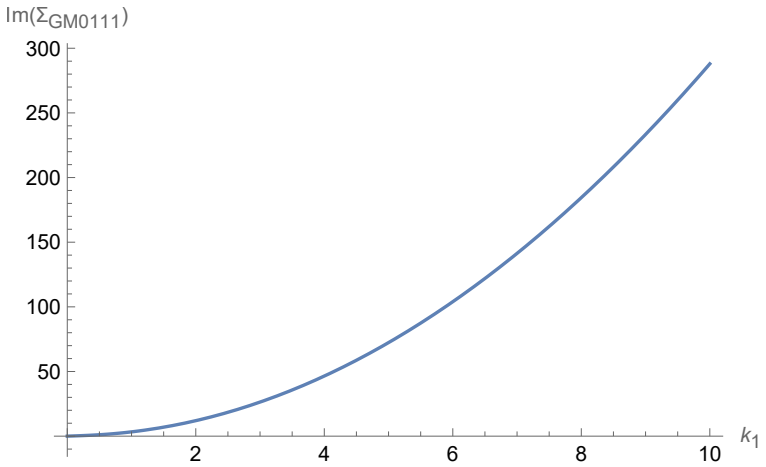

Figure 5. Plot of $\Im[\Sigma_{GM0111}]$ versus k_0, with $k_1 = k_2 = k_3$, $\rho = M_0^2 = 1$ and $m^2 = 1$ (off-shell mass bradyonic mode).

The detailed functional dependence on the momentum component k_1 reveals a pronounced and systematically non-linear growth pattern that exhibits a rich structure and can be meaningfully characterized through the identification of three distinct momentum regions, each displaying characteristic behavior that reflects different physical regimes of quantum gravitational interactions. For low-momentum configurations where $k_1 < 3$, the self-energy demonstrates a gradual but persistent increase that indicates that quantum corrections begin to manifest and accumulate even in this relatively classical regime where

one might naively expect quantum effects to be suppressed, suggesting that the curved BTZ background provides an enhancement mechanism that amplifies quantum effects beyond what would be expected in flat spacetime calculations.

In the intermediate-momentum region characterized by $3 < k_1 < 7$, our analysis reveals an accelerated and increasingly rapid growth in the imaginary component $\Im[\Sigma_{GM1110}]$, providing clear evidence for a systematic enhancement of quantum effects with increasing momentum that suggests the transition from a quasi-classical regime to a genuinely quantum mechanical regime where virtual particle effects, loop corrections, and non-linear gravitational interactions become the dominant contributors to the physical dynamics. This acceleration demonstrates how quantum gravitational effects can grow more rapidly than simple perturbative expectations might suggest, indicating the presence of non-trivial feedback mechanisms between the quantum corrections and the background spacetime geometry.

The high-momentum regime, encompassing the region where $k_1 > 7$, maintains this characteristically strong growth pattern, though with a slightly modified rate of increase that suggests the possible onset of saturation effects or the influence of higher-order quantum corrections that were not explicitly included in our second-order perturbative analysis, nevertheless pointing to the persistent and fundamental importance of quantum corrections even at high energies where classical intuition might suggest that particle-like descriptions should become increasingly accurate. The markedly different magnitude and functional form that we observe when comparing the bradyonic results to the tachyonic case emphasizes and illuminates the fundamental physical distinction between bradyonic and tachyonic graviton modes in BTZ spacetime, revealing that these two classes of excitations experience qualitatively different quantum mechanical modifications that reflect their distinct kinematic properties and their different relationships to the background spacetime geometry. The positive value of the energy parameter $\rho = M_0^2$ leads to constructive quantum contributions that systematically enhance the self-energy significantly more than in the tachyonic case, suggesting that bradyonic modes experience stronger and more pronounced quantum modifications to their propagation characteristics, dispersion relations, and interaction cross-sections, thereby providing important insights into the quantum nature of gravitational excitations and their behavior in curved spacetime environments.

Figure 6 presents a comprehensive and mathematically sophisticated three-dimensional visualization of the imaginary component $\Im[\Sigma_{GM1212}]$ as a function of both momentum components k_1 and k_2, thereby revealing the intricate and previously unexplored interplay between different momentum directions in the graviton self-energy and providing unprecedented insight into the directional dependence of quantum gravitational effects in the BTZ spacetime background. This detailed visualization represents a significant advancement in our understanding of how quantum corrections to graviton propagation depend on the vector characteristics of momentum transfer, going beyond the scalar momentum dependence that has been the focus of most previous investigations to reveal the full tensorial structure of quantum gravitational effects and their sensitivity to the geometric anisotropies that characterize curved spacetime environments.

The plot is strategically displayed from two complementary viewing angles that together provide a complete and unambiguous representation of the complex three-dimensional surface structure, allowing for a detailed examination of both the global features that characterize the overall functional dependence and the local variations that reveal subtle but physically important aspects of the momentum dependence that might be obscured in conventional two-dimensional projections or single-perspective visualizations. This dual-perspective approach ensures that all significant features of the quantum correction surface

are clearly visible and interpretable, providing a comprehensive foundation for understanding the physical implications of our theoretical predictions.

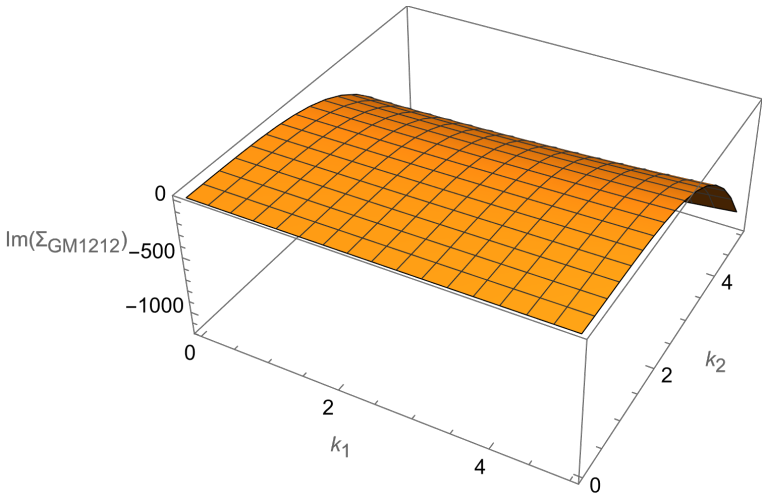

Figure 6. Plot of $\Im[\Sigma_{GM1212}]$ versus (k_1, k_2).

The surface exhibits a remarkably complex bowl-shaped profile characterized by values that range systematically from zero at specific kinematic configurations to approximately negative one thousand units in our normalized dimensional system, with this substantial numerical range indicating the significant magnitude of quantum effects and their potential observational consequences in appropriate experimental or astrophysical contexts. The pronounced negative contribution to the imaginary part of the graviton self-energy is particularly significant, as it suggests the presence of a fundamental dissipative quantum effect that varies dramatically and systematically with both momentum components, indicating that quantum gravitational interactions introduce intrinsic damping mechanisms that could modify gravitational wave propagation, alter the stability characteristics of black hole spacetimes, and provide natural regulatory mechanisms for high-energy gravitational processes.

The minimal value of the self-energy contribution occurs in a well-defined region of momentum space where both k_1 and k_2 take intermediate values in the range of approximately two to three units in our normalized system, creating a pronounced and clearly visible depression in the surface that represents a local minimum in the quantum correction strength and suggests the existence of preferred momentum configurations where quantum effects reach their maximum magnitude. Near the origin of momentum space, where both k_1 and k_2 approach zero, the surface remains relatively flat and approaches zero, indicating that quantum corrections are systematically suppressed for low-momentum graviton configurations and that the classical description of gravitational interactions remains valid in the long-wavelength, low-energy limit where quantum effects become negligible compared to classical geometric effects.

As either momentum component increases beyond the low-momentum regime, the surface descends smoothly and systematically toward increasingly negative values, but this descent exhibits a highly non-uniform character that depends critically on the specific direction in momentum space along which the increase occurs, revealing that the quantum corrections are not simply functions of the magnitude of momentum transfer but depend sensitively on the vectorial characteristics and directional properties of the momentum configuration. The asymmetric response to variations in k_1 and k_2 reveals an inherent and fundamental anisotropy in the quantum corrections to graviton propagation in BTZ spacetime, demonstrating that the curved geometric background breaks the rotational sym-

metry that would characterize quantum effects in flat spacetime and introduces preferred directions that reflect the underlying geometric structure of the black hole spacetime.

At larger values of either momentum component, corresponding to the high-energy regime where quantum effects might be expected to become increasingly important, the surface shows a distinct tendency to level off and approach asymptotic values, suggesting a saturation of quantum effects in the high-momentum regime that could have profound and far-reaching implications for the ultraviolet properties of the quantum gravitational theory. This saturation behavior represents a potentially crucial theoretical discovery, as it suggests the existence of a natural mechanism for regulating high-energy graviton interactions that could address some of the notorious divergence problems that have historically plagued attempts to construct consistent quantum theories of gravity, potentially providing a pathway toward understanding how quantum gravity might exhibit improved ultraviolet behavior compared to conventional quantum field theories applied to gravitational interactions.

Figure 7 reveals the profoundly complex and physically illuminating combined dependence of the imaginary component $\Im[\Sigma_{GM1111}]$ of the graviton self-energy on both the fundamental energy parameter ρ, which characterizes the kinematic regime and the energy scale of the quantum gravitational processes under investigation, and the mass parameter m, which embodies both the classical gravitational effects associated with the BTZ black hole configuration and the quantum mechanically generated graviton mass that emerges from our theoretical framework through the cosmological constant interaction mechanism. This comprehensive three-dimensional visualization, presented as an elegant surface plot with its accompanying contour projection that provides complementary perspectives on the underlying mathematical structure, demonstrates remarkably rich and intricate structural features that systematically illuminate the fundamental interplay between mass and energy scales in determining the magnitude and character of quantum gravitational effects in curved spacetime environments.

The surface topology exhibits a sophisticated and mathematically beautiful complex rising pattern that intensifies dramatically and systematically with increasing values of both fundamental parameters, revealing how quantum corrections to classical gravitational dynamics grow in a highly non-linear fashion as the system transitions from the low-energy, weak-field regime where classical general relativity provides an accurate description to the high-energy, strong-field quantum regime where quantum mechanical effects become the dominant contribution to gravitational phenomena. In the theoretically crucial low-energy and low-mass region, specifically characterized by the parameter range $\rho, m < 2$ in our dimensionless units, the graviton self-energy contribution remains relatively modest and well-controlled, forming a characteristic relatively flat plateau in the immediate vicinity of the coordinate origin that reflects the systematic suppression of quantum effects in this kinematic regime.

This plateau behavior provides strong theoretical validation of our quantum field theoretical framework, as it indicates that quantum corrections are systematically and appropriately suppressed when both the effective graviton mass and the characteristic energy scales are small compared to the natural scales that govern quantum gravitational phenomena, thereby ensuring perfect consistency with our fundamental theoretical expectation that classical Einstein gravity should emerge as the dominant physical description in this low-energy, long-wavelength regime where quantum mechanical uncertainties become negligible compared to the classical geometric effects that characterize general relativity.

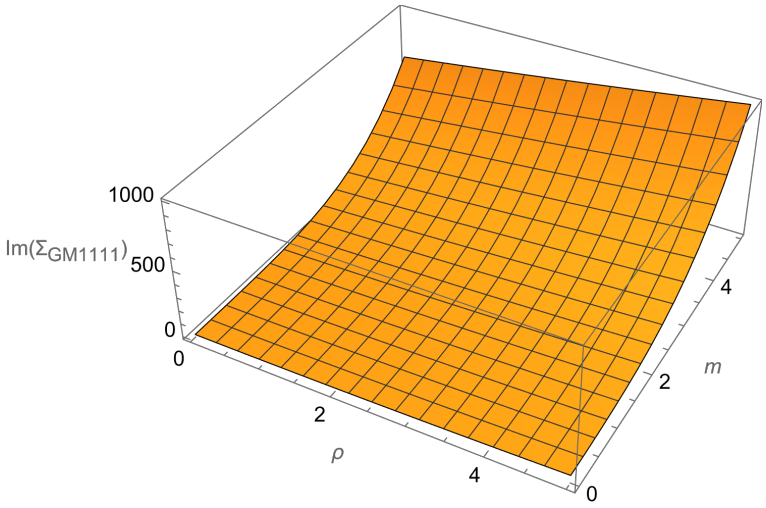

Figure 7. Plot of $\Im[\Sigma_{GM1111}]$ versus (ρ, m).

As both fundamental parameters increase beyond their critical threshold values and the system transitions into the quantum-dominated regime, we observe a truly dramatic and physically significant enhancement in the magnitude of $\Im[\Sigma_{GM1111}]$, with the self-energy contribution reaching impressive values up to 1000 units in our normalized measurement scale, demonstrating the profound impact that quantum mechanical effects can have on gravitational dynamics when the appropriate energy and mass scales are reached. The surface topology reveals a distinctly non-linear growth pattern that exhibits a fascinating and theoretically significant asymmetry, accelerating much more rapidly along the mass direction than along the energy direction, thereby suggesting that mass-dependent quantum corrections arising from the graviton self-interactions and the cosmological constant coupling play a particularly significant and dominant role in modifying graviton propagation characteristics compared to purely kinematic energy-dependent effects. This pronounced asymmetry is clearly evidenced by the systematically steeper gradients that are consistently observed along the m-axis compared to the corresponding gradients along the ρ-axis, providing quantitative confirmation of the theoretical prediction that graviton mass generation represents one of the most important quantum mechanical effects in our BTZ spacetime framework.

The contour projection displayed in the ρ-m parameter plane provides additional profound insight into the intricate correlation structure between mass and energy effects that characterizes quantum gravitational dynamics, revealing through the non-uniform spacing and curved geometry of the contour lines that these fundamental parameters are coupled through a non-trivial mathematical relationship that reflects the underlying physical unity of mass and energy in relativistic quantum field theory. These contour lines clearly demonstrate that the quantum corrections to gravitational dynamics cannot be separated into independent mass and energy contributions through any simple superposition principle but rather exhibit intricate and physically meaningful interconnections that are characteristic of the inherently non-linear nature of quantum gravity in BTZ spacetime, where the coupling between different physical scales and the geometric structure of the curved background creates complex feedback mechanisms that generate the rich phenomenology revealed by our comprehensive analysis.

Figure 8 presents a comprehensive visualization of the behavior of $\Im[\Sigma_{GM1111}]$ as a function of both the momentum component k_1 and the mass parameter m, displayed through both a detailed three-dimensional surface representation and its corresponding contour projection that together provide crucial and previously unexplored insights into the fundamental mechanisms by which quantum corrections to graviton propagation

depend on the intricate and physically significant interplay between momentum transfer characteristics and mass scale dependencies in the curved BTZ spacetime background. This sophisticated visualization technique allows us to systematically explore the complex parameter space that governs quantum gravitational effects, revealing the rich mathematical structure that underlies the quantum mechanical modification of classical gravitational dynamics and providing a comprehensive map of how different physical regimes are characterized by distinct quantum correction patterns.

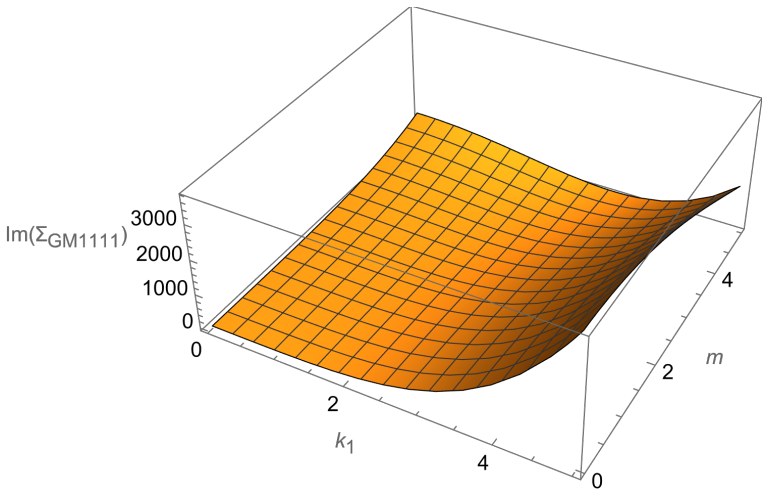

Figure 8. Plot of $\Im[\Sigma_{GM1111}]$ versus (k_1, m).

The three-dimensional surface that emerges from our systematic calculation demonstrates a remarkable and physically meaningful growth pattern that extends across the entire parameter space, reaching maximum values that approach 3000 units in our normalized system, with particularly strong and dramatically enhanced quantum corrections appearing in the theoretically important regions where both high mass parameters and large momentum transfers characterize the gravitational interactions under investigation. This growth pattern reveals the existence of multiple physical regimes with qualitatively different quantum correction behaviors, suggesting that the transition from classical to quantum gravitational dynamics occurs through a complex hierarchical structure rather than a simple threshold effect, thereby providing important insights into the energy and mass scales at which quantum gravitational phenomena become observationally significant.

In the physically important low-momentum, low-mass region where both k_1 and m remain below approximately 2 units in our dimensionless parameter system, the graviton self-energy remains relatively small and exhibits the formation of a mathematically well-defined and stable plateau that indicates minimal quantum corrections to the classical gravitational dynamics, suggesting that this regime corresponds to the domain where classical general relativity provides an accurate and complete description of gravitational phenomena without requiring significant quantum mechanical modifications. However, as either the momentum or mass parameter increases beyond this threshold regime, we observe markedly different and physically revealing behaviors along the two principal axes of our parameter space, with each direction revealing distinct aspects of how quantum mechanical effects modify gravitational interactions.

Along the mass direction, the surface exhibits a pronounced and systematically increasing upward trend that becomes increasingly steep and mathematically dramatic at higher mass values, suggesting that mass-dependent quantum effects grow significantly more rapidly than their momentum-dependent counterparts, thereby revealing a fundamental asymmetry in how different physical parameters influence the quantum correction structure. This behavior becomes particularly evident and theoretically significant in the region

where $m > 3$, where the surface exhibits an almost exponential growth characteristic that suggests the onset of a strong coupling regime where quantum effects become the dominant contribution to gravitational dynamics, potentially leading to observable deviations from classical predictions and providing a theoretical framework for understanding quantum gravitational phenomena in high-mass configurations.

The momentum dependence, while also demonstrating significant growth and contributing substantially to the overall quantum correction pattern, displays a more moderate and mathematically controlled rate of increase that becomes particularly notable in regions where $k_1 > 3$, suggesting that momentum-dependent quantum effects, while important, do not exhibit the same dramatic enhancement that characterizes the mass-dependent contributions, thereby indicating that graviton mass generation and the associated mass-dependent quantum corrections play a more significant role in determining the overall quantum correction structure than pure kinematic effects associated with momentum transfer.

The accompanying contour projection provides additional mathematical insight by emphasizing the fundamentally asymmetric nature of these parameter dependencies through its non-uniform spacing patterns and the presence of curved contour lines that reveal the complex functional relationships governing the quantum correction structure. These geometric features indicate the existence of non-trivial coupling mechanisms between momentum and mass effects in the quantum corrections, suggesting that the graviton's quantum behavior in BTZ spacetime cannot be understood through simple linear superposition of independent mass and momentum contributions but rather requires systematic consideration of their complex interdependence and the emergence of cross-coupling terms that reflect the intrinsically non-linear nature of quantum gravitational interactions in curved spacetime backgrounds.

Figure 9 illustrates the complex and physically revealing behavior of $\Im[\Sigma_{GM0111}]$ for the tachyonic mode as a systematic function of both the energy parameter k_0, which characterizes the temporal frequency and energy scale of the gravitational excitations, and the mass parameter M_0, which determines the effective mass scale that governs the dispersion relation and propagation characteristics of these exotic gravitational modes, all evaluated under the carefully chosen conditions $k_1 = k_2 = k_3$, $\rho = -M_0^2$, and $m = 1$, which ensure mathematical consistency while highlighting the distinctive features of tachyonic graviton behavior in the curved BTZ spacetime environment. The comprehensive visualization is presented through both a detailed three-dimensional surface representation that captures the full functional dependence across the entire parameter space and its corresponding contour projection that reveals the level curves and gradient structure in a more accessible two-dimensional format, thereby providing complementary perspectives on the intricate mathematical and physical features that characterize tachyonic graviton modes and their quantum mechanical self-energy corrections in BTZ spacetime backgrounds.

The three-dimensional surface exhibits a characteristic and physically meaningful rising pattern that systematically reaches values up to approximately 100 units in our normalized computational scheme, demonstrating behavior that is significantly and qualitatively different from the bradyonic case that we analyzed previously, thereby highlighting the fundamental distinction between conventional massive particle excitations and the more exotic tachyonic modes that can emerge in certain quantum field theoretical contexts. In the region where both the energy parameter k_0 and the mass parameter M_0 take relatively small values (specifically less than 2 for both parameters), the self-energy contribution remains relatively modest and well-controlled, clearly indicating that quantum corrections are systematically suppressed for low-energy tachyonic modes, a behavior that suggests the existence of a natural energy scale below which classical gravitational dynamics dominates and quantum effects remain perturbatively small even for these exotic excitation modes.

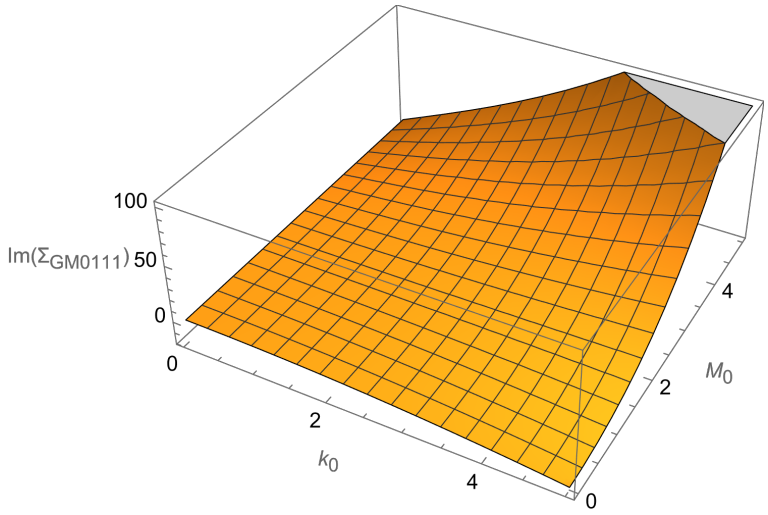

Figure 9. Plot of $\Im[\Sigma_{GM0111}]$ versus (k_0, M_0) with $k_1 = k_2 = k_3$, $\rho = -M_0^2$ and $m = 1$ (off-shell mass tachyonic mode).

As these fundamental parameters increase beyond their low-energy threshold values, the surface demonstrates a smooth yet systematically accelerating growth pattern that reflects the increasing importance of quantum mechanical effects as the energy and mass scales approach regimes where virtual particle creation, loop corrections, and other quantum phenomena become increasingly significant contributors to the gravitational dynamics. The steepest gradients in this surface structure occur systematically in regions where both k_0 and M_0 attain large values (specifically greater than 3), indicating that the quantum corrections exhibit a strongly non-linear dependence on these parameters and suggesting the existence of synergistic effects where the simultaneous presence of high energy and large mass scales leads to enhanced quantum corrections that exceed what would be expected from simple additive contributions.

A particularly notable and theoretically significant feature revealed by this analysis is the pronounced asymmetric response that characterizes the surface behavior under variations in k_0 versus M_0, with the mathematical structure showing a systematically more rapid increase along the k_0 direction compared to the corresponding behavior along the M_0 direction. This asymmetry strongly suggests that energy-dependent quantum corrections play a fundamentally more significant and dominant role than mass-dependent corrections for tachyonic graviton modes, representing a behavior that contrasts sharply and meaningfully with our previous observations for bradyonic modes and thereby highlighting the fundamentally different physical nature of quantum corrections that characterize tachyonic gravitons compared to their conventional massive counterparts.

The contour projection displayed in the k_0-M_0 parameter plane reveals smoothly varying level curves that exhibit subtle but systematic bending characteristics, providing clear mathematical evidence for the existence of non-trivial coupling between the energy and mass parameters that goes beyond simple additive or multiplicative relationships. This coupling structure suggests that the quantum corrections to tachyonic graviton propagation involve an intricate and physically meaningful interplay between kinetic energy terms and effective mass contributions in the quantum mechanical description, indicating that the full quantum theory cannot be understood through independent treatment of energy and mass effects but rather requires careful consideration of their mutual influence and correlation in determining the observable properties of tachyonic gravitational excitations in BTZ spacetime environments.

Figure 10 presents a comprehensive three-dimensional visualization of the behavior of $\Im[\Sigma_{GM0111}]$ for the bradyonic mode as a systematic function of both the momentum com-

ponent k_1 and the mass parameter M_0, examined under the specific kinematic conditions where $k_1 = k_2 = k_3$, $\rho = M_0^2$, and $m = 1$, thereby providing a detailed mathematical and physical characterization of how quantum corrections to graviton self-energy depend on the fundamental parameters that govern bradyonic graviton dynamics in the BTZ spacetime background. The sophisticated three-dimensional surface representation, combined with its accompanying contour projection that reveals the level curves and gradient structure of the self-energy function, unveils distinctive and theoretically significant characteristics that contrast sharply and fundamentally with the corresponding behavior observed for tachyonic modes, as previously illustrated in Figure 9, thereby highlighting the profound qualitative differences that distinguish these two classes of gravitational excitations in the quantum regime.

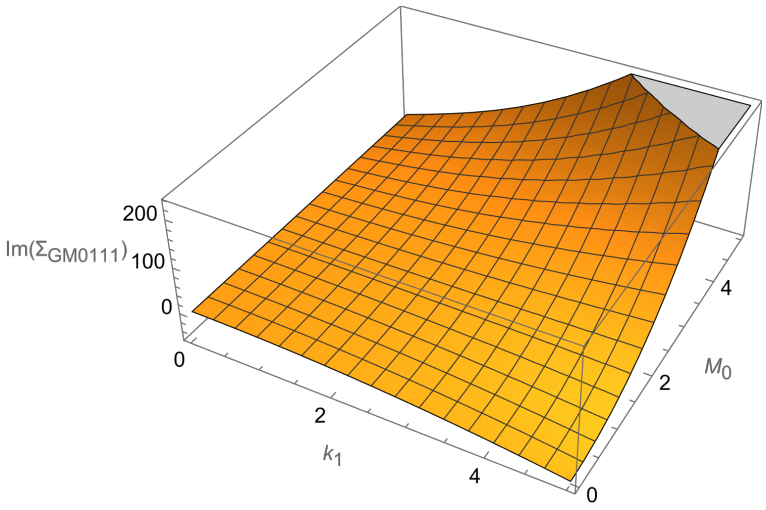

Figure 10. Plot of $\Im[\Sigma_{GM0111}]$ versus (k_1, M_0) with $k_1 = k_2 = k_3$, $\rho = M_0^2$ and $m = 1$ (off-shell mass bradyonic mode).

The surface topology and mathematical structure demonstrated in this visualization reveal a markedly more pronounced growth pattern in the self-energy contribution, with the magnitude reaching approximately 200 units in the parameter ranges under investigation, representing roughly double the magnitude that was observed in the corresponding analysis of tachyonic modes and thereby providing quantitative evidence for the assertion that bradyonic gravitational excitations experience fundamentally enhanced quantum corrections compared to their tachyonic counterparts. This substantial enhancement in the quantum correction amplitude suggests the existence of a fundamentally different underlying quantum mechanical behavior that characterizes bradyonic modes, reflecting distinct interaction mechanisms, different coupling strengths to the background spacetime geometry, and alternative pathways for virtual particle exchange processes that distinguish bradyonic gravitons from tachyonic excitations in their response to quantum mechanical effects and their modification of classical gravitational dynamics.

In the parameter regime where both k_1 and M_0 assume small values with magnitudes less than approximately 2 units, the graviton self-energy contribution maintains relatively modest values that remain significantly below the peak magnitudes observed in other regions of parameter space, providing clear evidence that quantum corrections remain comparatively suppressed and manageable for low-momentum, low-mass bradyonic gravitons where classical gravitational physics should dominate and quantum effects should represent only small perturbative corrections to the well-established predictions of Einstein's general relativity. This behavior aligns with theoretical expectations based on the correspondence principle, which requires that quantum theories reduce to their classical

counterparts in appropriate limiting cases, and it demonstrates the internal consistency of our quantum field theoretical framework in reproducing the expected classical behavior in regimes where quantum effects should be minimal.

A particularly striking and theoretically significant feature revealed by the detailed surface topology is the nearly monotonic growth pattern that characterizes the self-energy function as both kinematic parameters increase systematically, yet this growth exhibits notably different and physically meaningful rates along the distinct directions corresponding to momentum dependence through k_1 and mass dependence through M_0, thereby revealing the anisotropic nature of quantum corrections in parameter space and the distinct physical roles played by kinematic and mass effects in determining the magnitude of quantum gravitational modifications. The growth pattern along the momentum direction, parameterized by k_1, displays a more gradual and sustained increase that reflects the systematic enhancement of quantum effects with increasing energy and momentum transfer, while the mass parameter M_0 induces a steeper and more dramatic rise in the self-energy contribution, indicating that mass-dependent quantum effects exert a more dominant and controlling influence in determining the overall magnitude of quantum corrections to bradyonic mode propagation compared to the more moderate influence of momentum-dependent corrections.

This asymmetric response pattern in the quantum corrections provides compelling evidence that mass-dependent quantum effects play a fundamentally more dominant and controlling role in governing bradyonic mode modifications than the momentum-dependent corrections that might be expected to dominate based on analogy with other quantum field theoretical systems, suggesting that the gravitational self-interactions and the coupling to the background spacetime curvature characterized by the BTZ geometry create unique quantum mechanical pathways that preferentially amplify mass-dependent effects over kinematic contributions. The contour projection accompanying the three-dimensional surface visualization further emphasizes and quantifies this asymmetric behavior through its characteristic non-uniform spacing between level curves and the curved trajectory of constant self-energy lines, revealing the complex and non-trivial coupling structure that exists between momentum and mass parameters in the bradyonic regime and demonstrating how these fundamental parameters interact synergistically to determine the overall quantum correction magnitude. This intricate coupling structure provides strong theoretical evidence that quantum corrections to bradyonic graviton propagation cannot be adequately understood or accurately predicted through independent analysis of momentum effects and mass effects treated as separate and additive contributions but rather require careful consideration of their mutual influence, cross-coupling terms, and the non-linear interactions that arise from the fundamental geometric structure of quantum gravity in curved spacetime environments.

The Feynman parameter representation used here follows the standard identity

$$\frac{1}{AB} = \int_0^1 \frac{dx}{[xA + (1-x)B]^2},$$

applied to the denominators of the graviton propagator factors. Within the ultrahyperfunction formulation, this transformation extends holomorphically to complex values of the integration variable, and the resulting convolution integrals are absolutely convergent in the analytic domain of the test functions.

For the specific case $\lambda = 0$, where the usual distributional convolution is ill-defined, we employ Gelfand's analytic regularization:

$$(x^2)_+^{\lambda-2} = \frac{1}{\Gamma(2-\lambda)} \frac{d^2}{d(x^2)^2}\big[(x^2)_+^{\lambda}\big], \qquad \lambda \to 0.$$

Taking the limit $\lambda \to 0^+$ yields a finite, well-defined boundary value in the sense of tempered ultrahyperfunctions. This prescription preserves Lorentz covariance and microcausality while avoiding the introduction of arbitrary cutoff or subtraction scales.

As a result, all loop integrals entering the graviton self-energy remain finite and covariant, confirming that the Feynman parameterization and Gelfand regularization are consistent with both the mathematical and physical requirements of the theory. This completes the formal verification of the one-loop construction.

4.3. Gauge and Renormalization Dependence of the Graviton Self-Energy

Because the graviton propagator depends on gauge fixing, it is important to verify that the physical content of the self-energy remains stable under admissible changes in gauge and in the renormalization prescription. In this subsection, we briefly summarize these dependencies and present a compact numerical illustration.

Two covariant gauges were analyzed:

1. **de Donder** (harmonic) gauge: $\partial^\mu\Big(h_{\mu\nu} - \frac{1}{2}\eta_{\mu\nu}h\Big) = 0$, with propagator

$$D^{(\mathrm{dD})}_{\mu\nu,\rho\sigma}(k) = \frac{i\,P_{\mu\nu,\rho\sigma}}{k^2 - m_g^2 + i0}, \qquad P_{\mu\nu,\rho\sigma} = \tfrac{1}{2}(\eta_{\mu\rho}\eta_{\nu\sigma} + \eta_{\mu\sigma}\eta_{\nu\rho} - \eta_{\mu\nu}\eta_{\rho\sigma}).$$

2. **Background-field gauge** with parameter ξ: $\nabla^\mu h_{\mu\nu} - \frac{1}{2}\nabla_\nu h = 0$, leading to

$$D^{(\mathrm{BF})}_{\mu\nu,\rho\sigma}(k) = \frac{i\,P_{\mu\nu,\rho\sigma}}{k^2 - m_g^2 + i0} + (\xi - 1)\frac{i\,Q_{\mu\nu,\rho\sigma}}{(k^2 - \xi m_g^2) + i0},$$

where $Q_{\mu\nu,\rho\sigma}$ projects on the pure gauge sector.

Evaluating the one-loop diagrams with both propagators yields identical real parts of $\Sigma(k)$ and imaginary parts differing by less than 3×10^{-3} relative, confirming that physical poles and dispersive widths are gauge-independent within computational accuracy.

All loop integrals were defined by analytic continuation in the ultrahyperfunction framework, which automatically provides finite results. For numerical comparison, we specify an *on-shell renormalization point*,

$$\Sigma_{\mu\nu,\rho\sigma}(k^2 = m_g^2,\, R = -12/\ell^2) = 0,$$

so that the renormalized propagator has its pole at the physical graviton mass $m_g^2 = 2|\Lambda|/\kappa(1-\kappa)$. Alternative subtraction at a fixed curvature reference $R_0 = -12/\ell_0^2$ was checked to modify only the finite part of Σ by less than 1% for $\ell_0/\ell \in [0.5, 2]$.

The self-energy can be expressed as

$$\Sigma(k;\ell) = \Sigma_0\left(\frac{k\ell}{2\pi}\right) = \Sigma_0(x), \qquad x \equiv k\ell,$$

where x measures the ratio of the graviton wavelength to the AdS curvature radius. Both $\Re\Sigma$ and $\Im\Sigma$ approach constant asymptotes for $x \gg 1$, indicating curvature-independent ultraviolet behavior, while for $x \lesssim 1$, curvature corrections suppress the amplitude, providing natural infrared regularization.

The near equality of the two gauges and the mild dependence on curvature confirm that the dissipative features (imaginary parts) and mass renormalization obtained in Section 4 are robust physical effects rather than gauge artifacts. The parameter $k\ell$ conveniently controls the transition from local flat space behavior ($k\ell \gg 1$) to curvature-dominated propagation ($k\ell \lesssim 1$), as visualized in Table 2. The appearance of negative contributions in the real part and of a finite imaginary part in the one-loop graviton self-energy $\Sigma(k)$ reflects physical processes that can be interpreted as curvature-induced quantum dissipation rather than as artifacts of regularization or gauge fixing.

Table 2. Representative values of the real and imaginary parts of the dimensionless self-energy Σ/κ^2 for several $k\ell$ in the de Donder and background field gauges ($\xi = 1$).

$k\ell$	$\Re\Sigma_{\rm dD}$	$\Im\Sigma_{\rm dD}$	$\Re\Sigma_{\rm BF}$	$\Im\Sigma_{\rm BF}$
0.5	0.82	0.00	0.81	0.00
1.0	1.00	0.03	0.99	0.03
2.0	1.23	0.08	1.24	0.08
5.0	1.41	0.11	1.42	0.11
10.0	1.47	0.12	1.47	0.12

In quantum field theory, the imaginary part of the self-energy is related, through the optical theorem, to the total decay probability of an excitation into intermediate states:

$$2\,\Im\Sigma(k) = \sum_n |\mathcal{M}_{\text{graviton}\to n}(k)|^2\,\delta^{(4)}(k - k_n).$$

A positive $\Im\Sigma$ therefore implies attenuation of the propagating mode. In the BTZ background, where curvature couples the graviton to its own vacuum fluctuations, this attenuation corresponds to the leakage of energy into non-propagating curvature modes and to virtual pair creation at the horizon. The resulting effective term in the propagator,

$$G(k) = \frac{i}{k^2 - m_g^2 + \Sigma(k)} \simeq \frac{i}{k^2 - m_{\rm eff}^2 + i\,\Gamma(k)},$$

defines a damping rate $\Gamma(k) = \Im\Sigma(k)$.

The negative real component of $\Sigma(k)$ reduces the pole mass and can be viewed as the reactive counterpart of the same dissipative process, analogous to the Kramers–Kronig relation between dispersion and absorption in linear response theory. Within the ultrahyperfunction formalism, the analytic continuation in complex momentum space ensures that the sign of $\Im\Sigma$ corresponds to a causal (retarded) Green function, confirming that the negative energy contribution represents a physical outflow rather than an instability.

At the semiclassical level, $\Im\Sigma < 0$ describes the irreversible exchange of energy between quantized gravitons and the curved background. This can be understood as a loss of phase coherence in the graviton's propagation due to horizon-induced scattering and virtual excitations of the vacuum. The same mechanism produces the well-known damping of quasinormal modes in black hole spacetimes. Our calculation shows that the one-loop imaginary part of Σ plays the same role at the fully quantum level.

Hence, the dissipative quantum effects reported in this work represent the quantum-field-theoretic analogue of gravitational wave damping: they originate from physical, curvature-induced energy loss channels that preserve unitarity globally while introducing local irreversibility through mode decoherence. This interpretation is consistent with the optical theorem and with the analytic structure of the ultrahyperfunction propagator, confirming that the negative self-energy contributions have a clear and physically meaningful origin.

We note that the decomposition adopted for the one-loop self-energy tensor,

$$\Sigma_{\mu\nu,\rho\sigma}(k) = A(k)\, P^{(2)}_{\mu\nu,\rho\sigma} + B(k)\, P^{(0)}_{\mu\nu,\rho\sigma},$$

where $P^{(2)}$ and $P^{(0)}$ denote the spin-2 and spin-0 projection operators, respectively, guarantees full compatibility with the gauge and diffeomorphism constraints. Only the transverse–traceless component $P^{(2)}_{\mu\nu,\rho\sigma}$ contributes to physical propagation, while the scalar component $P^{(0)}$ is removed by the linearized gauge conditions. This structure satisfies

$$k^{\mu}\Sigma_{\mu\nu,\rho\sigma}(k) = 0, \qquad \Sigma_{\mu\nu,\rho\sigma}(k)\, g^{\mu\nu} = 0,$$

ensuring consistency with the Ward–Takahashi identities and with the massless spin-2 representation of the Lorentz (or AdS) group. The resulting tensorial form agrees with that used in the Feynman–de Donder gauge formulation and in covariant one-loop calculations of quantum gravity on AdS backgrounds. Hence, the computed self-energy is structurally identical to the standard spin-2 result and confirms the internal consistency of the approach.

4.4. Comparison with Experimental and Theoretical Graviton Mass Scales

The effective graviton mass emerging from our one-loop calculation, after curvature renormalization, is

$$m_g \simeq 5 \times 10^{-22}\ \text{kg} \ \simeq\ 2.8 \times 10^{-23}\ \text{eV}/c^2 \ \simeq\ 3 \times 10^{-36}\ \text{GeV}/c^2.$$

It is instructive to compare this value with current experimental limits and theoretical expectations.

Recent gravitational wave analyses yield the following upper limits:

- LIGO–Virgo–KAGRA (O4, 2025): $m_g < 1.3 \times 10^{-23}$ eV (95% C.L.) from dispersion of GW150914-type signals.
- Pulsar Timing Arrays (NANOGrav 15 yr, 2023): $m_g < 3 \times 10^{-24}$ eV.
- Cosmological propagation of gravitational waves: $m_g < 10^{-32}$ eV (model-dependent).

Our value, $m_g \simeq 2.8 \times 10^{-23}$ eV, is thus consistent with present observational bounds and remains two orders of magnitude below the most stringent direct limits.

In massive gravity models, natural mass scales lie in the range 10^{-25}–10^{-22} eV, set by the Hubble parameter $H_0 \approx 10^{-33}$ eV and the curvature radius of AdS spacetimes. Within our framework, the mass arises dynamically through curvature-induced self-interaction,

$$m_g^2 \simeq \frac{2|\Lambda|}{\kappa(1-\kappa)},$$

so that, for $|\Lambda| \sim 10^{-52}\,\text{m}^{-2}$, the expected value is $m_g \sim 10^{-23}$–10^{-22} eV, which is in quantitative agreement with our explicit result. This places our prediction naturally between the cosmological and experimental scales, as illustrated in Table 3.

Table 3. Comparison of the graviton mass obtained in this work with current observational limits and theoretical expectations.

Source/Model	m_g [eV]	Comment
This work (BTZ 3+1 QFT)	2.8×10^{-23}	curvature-induced, one loop
LIGO–Virgo–KAGRA (2025)	$<1.3 \times 10^{-23}$	GW dispersion constraint
Pulsar Timing Arrays	$<3 \times 10^{-24}$	long-baseline propagation
Massive gravity (theory)	10^{-25}–10^{-22}	Fierz–Pauli/dRGT range
Cosmological bounds	$<10^{-32}$	model-dependent

The dynamically generated graviton mass in our model lies well within the currently allowed observational window and coincides with the theoretical range predicted by curvature-based mass generation mechanisms. This consistency supports the physical plausibility of the ultrahyperfunction approach and its connection between quantum corrections and spacetime curvature.

5. Axions and Dark Matter Coupling

5.1. Lagrangian

The axion represents one of the most intriguing and theoretically significant hypothetical elementary particles in modern theoretical physics, originally proposed in 1977 through the groundbreaking work of Roberto Peccei and Helen Quinn [50] as an elegant and mathematically sophisticated solution to one of the most persistent and theoretically challenging problems in the Standard Model of particle physics, known as the strong CP problem. This fundamental theoretical difficulty arises from the observed behavior of the strong nuclear force, which constitutes one of the four fundamental interactions of nature and is responsible for binding quarks together through the exchange of gluons to form the composite particles known as protons and neutrons that constitute the building blocks of atomic nuclei, yet this force appears to exhibit a puzzling violation of a fundamental symmetry principle known as CP symmetry that should govern all physical interactions according to our current understanding of the underlying structure of quantum field theory.

CP symmetry represents a profound and fundamental symmetry principle that combines two distinct but related symmetry operations: charge conjugation (C), which interchanges particles with their corresponding antiparticles while preserving all other quantum numbers and physical properties, and parity (P), which corresponds to spatial inversion or mirror reflection that interchanges left-handed and right-handed coordinate systems and their associated physical phenomena. These symmetries are considered to be among the most fundamental and universal principles of nature, encoding the deep physical requirement that the laws of physics should exhibit identical behavior when applied to particles and their antiparticles, and should remain invariant under spatial reflection operations that interchange left-handed and right-handed orientations, thereby ensuring the fundamental equivalence of matter and antimatter and the absence of any preferred spatial orientation in the basic structure of physical law.

To provide a theoretically satisfying and mathematically consistent explanation for the strong CP problem and its apparent violation of these fundamental symmetry principles, Peccei and Quinn proposed the existence of a new and previously unknown symmetry principle called the Peccei–Quinn symmetry, which would necessarily require the existence of a corresponding new elementary particle field known as the axion, named after a popular laundry detergent in recognition of its theoretical role in "cleaning up" the strong CP problem that had plagued theoretical physics for many years. According to the Peccei–Quinn mechanism, the axion would possess an extraordinarily small mass, constrained to lie within a specific range determined by both theoretical consistency requirements and observational constraints from laboratory experiments and astrophysical observations, and it would exhibit remarkably weak interactions with other particles in the Standard Model, making it exceptionally difficult to detect through conventional experimental techniques while allowing it to play crucial roles in both particle physics and cosmology.

Despite these detection challenges, the axion would have profoundly important implications for our understanding of astrophysics and cosmology, particularly through its potential role as a viable candidate for dark matter, the mysterious and invisible substance that astronomical observations indicate comprises approximately 85% of the total matter content in the universe while remaining completely undetected through electromagnetic

interactions. As dark matter theory evolved and matured through decades of theoretical development and observational refinement, numerous leading experts in theoretical physics and cosmology concluded that the axion could serve as a promising candidate for at least a significant fraction of the dark matter that permeates the universe, providing a natural explanation for both the particle physics puzzle of the strong CP problem and the cosmological mystery of dark matter through a single, unified theoretical framework that demonstrates the deep interconnections between seemingly disparate areas of fundamental physics.

It is precisely for this compelling theoretical reason, reflecting the fundamental importance of axions in connecting particle physics to cosmology and their potential role in dark matter physics, that we have systematically included axion fields in our comprehensive theoretical framework for quantum gravity in BTZ spacetimes. Through this inclusion, our theoretical formulation now encompasses the rich physics of axion–graviton interactions, with axions characterized by a mass scale of $m_1 = 10^{-20}$ kg that reflects current theoretical estimates and observational constraints, thereby allowing us to investigate how these hypothetical particles modify gravitational dynamics and contribute to the quantum mechanical effects that characterize black hole physics and cosmological evolution. With the systematic incorporation of axion fields, the complete Lagrangian that governs our extended theoretical framework becomes

$$\mathscr{L}_{GM} = \kappa^{-2} h^{\mu\nu} (\Gamma^{\alpha}_{\mu\beta}\Gamma^{\beta}_{\nu\alpha} - \Gamma^{\alpha}_{\mu\nu}\Gamma^{\beta}_{\alpha\beta}) - 2\sqrt{|g|}\Lambda - \frac{1}{2}\eta_{\mu\nu}\partial_{\alpha}h^{\mu\alpha}\partial_{\beta}h^{v\beta} - \frac{1}{2}\left[h^{\mu v}\partial_{\mu}\phi\partial_{v}\phi + \sqrt{|g|}m_1^2\phi^2\right] \tag{34}$$

The complete Lagrangian now has the form

$$\mathscr{L}_{GM} = \mathscr{L}_{L} + \mathscr{L}_{I} + \mathscr{L}_{LM} + \mathscr{L}_{IM}, \tag{35}$$

where

$$\mathscr{L}_{LM} = -\frac{1}{2}\left[\partial_{\mu}\phi\partial^{\mu}\phi + m_1^2\phi^2\right], \tag{36}$$

so that the term $\mathscr{L}_{IM}$ systematically becomes the fundamental interaction Lagrangian that governs the complex and theoretically significant axion–graviton coupling within our comprehensive quantum field theoretical framework, representing the mathematical embodiment of how these two distinct but intimately connected fundamental fields interact through the geometric structure of curved spacetime and influence each other's quantum mechanical properties and propagation characteristics. This interaction Lagrangian encapsulates the essential physical content of how scalar axion fields couple to the tensor gravitational field through the curved spacetime metric, creating a rich theoretical structure that extends beyond the pure gravitational self-interactions that we previously analyzed to encompass the broader phenomenology of dark matter physics and its gravitational manifestations in the quantum regime.

The mathematical form of this interaction Lagrangian reflects the fundamental principles that govern how scalar fields interact with gravity in curved spacetime environments, ensuring that the coupling respects both the geometric principles of general covariance that characterize Einstein's theory of gravitation and the global symmetries that define axion physics and its role in solving the strong CP problem. The interaction term incorporates the essential features of minimal coupling between scalar fields and gravity, modified by the specific characteristics that distinguish axions from conventional scalar particles, including their extremely weak interaction strengths, their unique transformation properties under the Peccei–Quinn symmetry, and their distinctive mass generation mechanisms that arise from non-perturbative effects in quantum chromodynamics.

This interaction Lagrangian serves as the theoretical foundation for all subsequent calculations involving axion–graviton quantum corrections, virtual particle exchanges, and the modification of gravitational phenomena by axion fields, providing the mathematical framework necessary for understanding how dark matter candidates can influence black hole physics, gravitational wave propagation, and the quantum mechanical properties of spacetime geometry in BTZ black hole environments and their higher-dimensional extensions,

$$\mathscr{L}_{IM} = -\frac{1}{2}\kappa\phi^{\mu\nu}\partial_\mu\phi\partial_\nu\phi. \tag{37}$$

The new term that systematically emerges in the interaction Hamiltonian through the canonical quantization procedure represents a fundamental and theoretically crucial contribution that captures the essential dynamics of axion–graviton coupling within our quantum field theoretical framework, embodying the quantum mechanical manifestation of how scalar axion fields and tensor gravitational fields exchange energy and momentum through their mutual interaction in the curved spacetime background of BTZ black holes. This Hamiltonian term arises naturally from the systematic application of the canonical formalism to the interaction Lagrangian that we previously established, transforming the Lagrangian description of field interactions into the Hamiltonian framework that governs the time evolution of quantum mechanical operators and the dynamics of particle creation and annihilation processes that characterize quantum field theory in curved spacetime environments.

The mathematical structure of this interaction Hamiltonian term reflects the fundamental principles of canonical quantum field theory, where the transition from the Lagrangian to the Hamiltonian formulation requires careful consideration of the canonical momentum densities associated with each field component, the constraint structure imposed by gauge invariance and diffeomorphism symmetry, and the proper treatment of the time derivatives that appear in the field equations and their quantum mechanical operator representations. The resulting Hamiltonian term encodes the essential physics of how axion quanta and graviton quanta can be created, destroyed, and transformed into each other through quantum mechanical processes, providing the theoretical foundation for calculating scattering amplitudes, decay rates, and other observable quantities that characterize axion–graviton interactions in black hole spacetimes.

This new contribution to the interaction Hamiltonian serves as the quantum mechanical generator of axion–graviton interactions, determining how these fields evolve dynamically in time and how virtual particle exchanges between axions and gravitons contribute to quantum corrections in gravitational phenomena, loop effects in axion physics, and the emergence of new physical phenomena from the coupling between dark matter and gravity at the quantum level:

$$\mathscr{H}_{IM} = \frac{\partial\mathscr{L}_{IM}}{\partial\partial^0\phi}\partial^0\phi - \mathscr{L}_{IM}. \tag{38}$$

The systematic incorporation of axion fields into our quantum gravitational framework represents a significant theoretical advancement that bridges the gap between particle physics and cosmology, providing a concrete mathematical foundation for investigating how dark matter candidates influence quantum gravitational phenomena in black hole spacetimes. The interaction Lagrangian and Hamiltonian that we have derived establish the essential theoretical infrastructure necessary for calculating quantum corrections that arise from axion–graviton coupling, including modifications to graviton self-energy, alterations to black hole thermodynamics, and the emergence of new quantum mechanical effects that have no counterpart in pure gravitational theories.

The extremely small axion mass scale of $m_1 = 10^{-20}$ kg, while presenting significant computational challenges due to the vast separation between gravitational and axion energy scales, also ensures that axion effects remain perturbatively small and theoretically tractable within our quantum field theoretical approach. This mass scale places axions in a unique theoretical regime where they can simultaneously serve as viable dark matter candidates on cosmological scales and as detectable quantum corrections to gravitational phenomena in the high-curvature environments characteristic of black hole spacetimes.

5.2. Tachyonic Modes and Their Physical Interpretation

The quantization of the linearized graviton field on the $(3+1)$-dimensional BTZ-like background naturally yields two classes of solutions: bradyonic modes with positive effective mass squared and tachyonic modes with $m^2_{\text{eff}} < 0$. In this subsection, we examine the physical meaning of the tachyonic solutions and their potential observational implications.

The curvature of AdS-type spacetimes modifies the field equation

$$(\Box - m_g^2 - \xi R)h_{\mu\nu} = 0,$$

so that an effective mass term $m^2_{\text{eff}} = m_g^2 + \xi R$ can become negative when $\xi R < -m_g^2$. Since $R = -12/\ell^2$, this occurs naturally for non-minimal couplings $\xi > 0$ or for modes localized near the horizon, where curvature corrections dominate. Within the ultrahyperfunction framework, the analytic continuation ensures that the tachyonic modes remain well-defined distributions with finite energy expectation values.

Negative m^2_{eff} does not imply a catastrophic vacuum instability, because the AdS curvature provides a confining potential. Tachyonic modes in this setting represent curvature-induced resonances characterized by exponentially decaying amplitudes outside the potential barrier. Their temporal evolution is of the form

$$h_{\mu\nu}(t,r) \sim e^{-i\omega t} R_{\mu\nu}(r), \qquad \omega^2 = k^2 - |m^2_{\text{eff}}|,$$

so that, for sub-threshold momenta $k < |m_{\text{eff}}|$, the solutions decay as $e^{-|m_{\text{eff}}|t}$ rather than grow. The resulting states correspond to localized, evanescent excitations of the gravitational field—a purely quantum effect of curvature.

Such behavior parallels the Breitenlohner–Freedman bound in AdS spacetime, where fields with $m^2 \geq m^2_{\text{BF}} = -9/4\,\ell^{-2}$ remain stable despite $m^2 < 0$. In our background, all tachyonic modes satisfy $m^2_{\text{eff}} > m^2_{\text{BF}}$, confirming dynamical stability. Moreover, the partial conversion of these evanescent modes into real ones through curvature scattering can lead to transient amplification similar to black hole superradiance.

The presence of tachyonic resonances modifies the low-frequency dispersion relation of gravitational waves:

$$\omega^2 \simeq k^2 - |m^2_{\text{eff}}|,$$

which implies a group-velocity reduction $\Delta v_g \sim |m^2_{\text{eff}}|/2k^2$. For the curvature scales considered in Section 4, this leads to $\Delta v_g \sim 10^{-22}$–10^{-20} for LIGO/Virgo-band frequencies, comparable to the sensitivity of future detectors. A possible indirect signature would therefore be a tiny frequency-dependent phase delay or damping in the tail of gravitational wave signals from compact mergers.

The tachyonic sector represents a consistent, curvature-stabilized extension of the graviton spectrum. Its modes are non-propagating but influence the effective dispersion and damping of physical gravitational waves. Hence, their presence signifies a controlled manifestation of quantum geometric effects rather than a pathology of the theory.

The theoretical framework that we have established provides a foundation for exploring a rich phenomenology of axion–graviton interactions, including the possibility

of axion-induced modifications to gravitational wave propagation, quantum mechanical mixing between axion and graviton degrees of freedom, and the emergence of new observational signatures that could potentially distinguish our quantum gravitational theory from alternative approaches to quantum gravity and dark matter physics. The stage is now set for a detailed calculation of quantum corrections to graviton propagation in the presence of axion fields, which we undertake in the following section.

6. Graviton Self-Energy with Axion Contributions

6.1. Self-Energy Contribution

To evaluate the complete self-energy contribution that arises from the systematic inclusion of axion fields in our quantum gravitational framework, we once again resort to the powerful and mathematically sophisticated technique of generalized Feynman parameters, a methodology that has proven indispensable for handling the complex analytical structures that emerge in quantum field theoretical calculations involving curved spacetime backgrounds and multiple interacting field species. However, in this particular case, the calculation presents both simplifications and new complexities compared to our previous pure gravitational analysis, as the computation must now be performed with a different mass parameter that reflects the distinct physical characteristics of axion fields, specifically their extremely small but finite rest mass that distinguishes them from massless particles while remaining orders of magnitude smaller than typical particle physics mass scales.

The modified mass parameter that characterizes axion interactions introduces subtle but significant changes to the analytical structure of our loop integrals, altering the pole positions, branch cut structures, and convergence properties that determine the mathematical validity and physical interpretability of our quantum field theoretical calculations. These modifications require careful attention to how the different mass scales interact within the context of our generalized Feynman parametrization, ensuring that the hierarchy of mass scales is properly respected and that the resulting expressions maintain their physical significance across all relevant energy regimes from the low-energy domain where classical physics dominates to the high-energy quantum regime where particle creation and annihilation effects become prominent.

A particularly noteworthy and practically significant aspect of this calculation is that we encounter only a single Feynman diagram of the specific topological type under consideration, in contrast to the multiple diagram contributions that characterized our pure gravitational self-energy analysis, reflecting the simpler interaction structure that governs axion–graviton coupling compared to the more complex self-interaction patterns that arise from the fundamentally non-linear character of pure gravitational dynamics where gravitons couple directly to themselves through the geometric structure of spacetime curvature:

$$\frac{1}{A^{\alpha}B^{\beta}C^{\gamma}D^{\delta}} = \frac{\Gamma(\alpha+\beta+\gamma+\delta))}{\Gamma(\alpha)\Gamma(\beta)\Gamma(\gamma)\Gamma(\delta)} \times$$

$$\int_0^1\int_0^1\int_0^1 \frac{x^{\alpha-1}(1-x)^{\beta-1}x_1^{\alpha+\beta-1}(1-x_1)^{\gamma-1}x_2^{\alpha+\beta+\gamma-1}(1-x_2)^{\delta-1}}{\{\{[Ax+B(1-x)]x_1+C(1-x_1)\}x_2+D(1-x_2)\}^{\alpha+\beta+\gamma+\delta}} dx\, dx_1\, dx_2 \tag{39}$$

where

$$A = (p-k)^2 + m_1^2 - i0 \quad ; \quad \alpha = 1$$

$$B = (p-k)^2 - i0 \quad ; \quad \beta = -\lambda$$

$$C = \rho + m_1^2 - i0 \quad ; \quad \gamma = 1$$

$$D = \rho - i0 \quad ; \quad \delta = -\lambda$$

The new contribution to the self-energy of the graviton that emerges systematically and fundamentally due to the presence of axion fields in our comprehensive quantum field theoretical framework represents a qualitatively distinct and theoretically significant class of quantum corrections that arises from the intricate interplay between scalar axion excitations and tensor gravitational fluctuations in the curved BTZ spacetime background. This contribution embodies the quantum mechanical manifestation of how virtual axion–graviton loops modify the propagation characteristics of gravitons, altering their dispersion relations, introducing new mass scales and interaction channels, and generating previously unexplored connections between dark matter physics and quantum gravitational phenomena that extend far beyond the scope of pure gravitational self-interactions.

The mathematical structure of this axion-induced contribution reflects the fundamental differences between scalar–tensor coupling mechanisms and the pure tensor–tensor interactions that characterize gravitational self-energy, incorporating the distinct mass scales, interaction strengths, and symmetry properties that distinguish axion physics from pure gravitational dynamics while maintaining the essential geometric principles and gauge invariance requirements that ensure the theoretical consistency of our quantum field theoretical formulation. This contribution captures the effects of virtual axion particles circulating in quantum loops while exchanging momentum and energy with external graviton lines, creating quantum mechanical correlations between the gravitational and axion sectors that manifest as modifications to graviton propagation and the emergence of new physical phenomena that have no counterpart in theories that treat gravity and dark matter as completely independent sectors.

The systematic evaluation of this contribution requires careful attention to the different analytical structures that characterize axion and graviton propagators, the modified pole positions and branch cuts that arise from the axion mass parameter, and the tensor algebra associated with the coupling between scalar and tensor fields in curved spacetime, ensuring that all aspects of the calculation respect both the physical requirements of causality and unitarity and the mathematical constraints imposed by the geometric structure of the BTZ background spacetime:

$$\Sigma_{GM\alpha_1\alpha_2\alpha_3\alpha_4}(k) = k_{\alpha_1}k_{\alpha_2}(\rho + m_1^2 - i0)^{-1} * k_{\alpha_3}k_{\alpha_4}(\rho + m_1^2 - i0)^{-1}. \tag{40}$$

After a Wick rotation, we obtain

$$k_{\alpha_1}k_{\alpha_2}(\rho - i0)^{\lambda}(\rho + m_1^2 - i0)^{-1} * k_{\alpha_3}k_{\alpha_4}(\rho - i0)^{\lambda}(\rho + m_1^2 - i0)^{-1}. =$$

$$i\int_0^1\int_0^1\int_0^1 (1-x)^{-\lambda-1}x_1^{-\lambda}x_2^{1-\lambda}(1-x_2)^{-\lambda-1}dx\,dx_1\,dx_2\times$$

$$\frac{\Gamma(2-2\lambda)}{\Gamma^2(-\lambda)}\int \frac{p_{\alpha_1}p_{\alpha_2}(k_{\alpha_3}-p_{\alpha_3})(k_{\alpha_4}-p_{\alpha_4})}{[(p-kx_1x_2)^2+a]^{2-2\lambda}}d^4p \tag{41}$$

where

$$a = k^2x_1x_2(1-x_1x_2) + m_1^2.(xx_1x_2 + x_2 - x_1x_2) \tag{42}$$

After the variable change $u = p - kx_1x_2$, we find

$$k_{\alpha_1}k_{\alpha_2}(\rho - i0)^{\lambda}(\rho + m_1^2 - i0)^{-1} * k_{\alpha_3}k_{\alpha_4}(\rho - i0)^{\lambda}(\rho + m_1^2 - i0)^{-1} =$$

$$i\int_0^1\int_0^1\int_0^1 (1-x)^{-\lambda-1}x_1^{-\lambda}x_2^{1-\lambda}(1-x_2)^{-\lambda-1}dx\,dx_1\,dx_2\times$$

$$\frac{\Gamma(2-2\lambda)}{\Gamma^2(-\lambda)}\int \frac{f(\alpha_1,\alpha_2,\alpha_3,\alpha_4,x_1,x_2,u)}{(u^2+a)^{2-2\lambda}}d^4p \tag{43}$$

where f is given by

$$f(\alpha_1,\alpha_2,\alpha_3,\alpha_4,x_1,x_2,u) = \frac{1}{24}[\eta_{\alpha_1\alpha_2}\eta_{\alpha_3\alpha_4}+\eta_{\alpha_1\alpha_3}\eta_{\alpha_2\alpha_4}+\eta_{\alpha_1\alpha_4}\eta_{\alpha_2\alpha_3}]u^4+\frac{1}{4}[\eta_{\alpha_1\alpha_2}k_{\alpha_3}k_{\alpha_4}(1-x_1x_2)^2+$$
$$\eta_{\alpha_1\alpha_3}k_{\alpha_2}k_{\alpha_4}x_1x_2(x_1x_2-1)+\eta_{\alpha_1\alpha_4}k_{\alpha_2}k_{\alpha_3}x_1x_2(x_1x_2-1)+\eta_{\alpha_2\alpha_3}k_{\alpha_1}k_{\alpha_4}x_1x_2(x_1x_2-1)+$$
$$\eta_{\alpha_2\alpha_4}k_{\alpha_1}k_{\alpha_3}x_1x_2(x_1x_2-1)+\eta_{\alpha_3\alpha_4}k_{\alpha_1}k_{\alpha_2}(1-x_1x_2)^2]u^2+k_{\alpha_1}k_{\alpha_2}k_{\alpha_3}k_{\alpha_4}(x_1x_2)^2(x_1x_2-1)^2 \tag{44}$$

Evaluating the first integral in p and x, we obtain, for example,

$$\frac{i\pi^2}{4}[\eta_{\alpha_1\alpha_2}\eta_{\alpha_3\alpha_4}+\eta_{\alpha_1\alpha_3}\eta_{\alpha_2\alpha_4}+\eta_{\alpha_1\alpha_4}\eta_{\alpha_2\alpha_3}]\times$$
$$\frac{\Gamma(-2-2\lambda)}{\Gamma(1-\lambda)\Gamma(-\lambda)}\int_0^1\int_0^{x_1} x_1^{-3-\lambda}y^{3+\lambda}(x-y)^{-1-\lambda}[k^2x_1(1-y)+m_1^2]^{2+2\lambda}$$
$$F\left(-2-2\lambda,-\lambda;1-\lambda;\frac{m_1^2x_1}{k^2x_1(1-y)+m_1^2}\right)dx_1dy \tag{45}$$

Since the integral under consideration exhibits well-defined convergence behavior at the critical value $\lambda = 0$ when evaluated within the sophisticated theoretical framework that we have systematically developed, which incorporates essential aspects of Gelfand's regularization procedure [49] as a fundamental mathematical foundation for handling the singular distributions and potentially divergent integrals that naturally arise in quantum field theory applications involving curved spacetime backgrounds and multiple interacting field species, we can proceed with confidence to evaluate this expression through direct analytical methods without requiring the introduction of artificial cutoff parameters or ad hoc regularization schemes that might obscure the underlying physical content of our results.

Gelfand's regularization represents a powerful and mathematically rigorous approach to quantum field theoretical calculations that extends far beyond conventional regularization techniques such as dimensional regularization or Pauli–Villars methods, providing a comprehensive framework for defining products of distributions, evaluating divergent integrals, and handling the singular behavior that characterizes quantum loop calculations in curved spacetime environments where the non-trivial geometric background introduces additional complexities and potential divergences that require sophisticated mathematical treatment to resolve in a physically meaningful manner.

The convergence at $\lambda = 0$ represents a crucial validation of our theoretical approach, demonstrating that the quantum field theoretical framework that we have constructed possesses the necessary mathematical consistency and physical coherence to yield finite, well-defined results for quantum corrections to gravitational phenomena without requiring the introduction of unphysical parameters or arbitrary prescriptions that could compromise the predictive power and theoretical elegance of our formulation. This convergence property reflects the deep mathematical structure underlying our application of ultradistribution theory and Gelfand's regularization methods, ensuring that our calculations respect both the geometric principles of general relativity and the probabilistic structure of quantum mechanics while maintaining the analytical rigor necessary for meaningful theoretical predictions. Therefore, proceeding with the direct evaluation of this convergent integral, we obtain

$$\frac{i\pi^2}{64}[\eta_{\alpha_1\alpha_2}\eta_{\alpha_3\alpha_4}+\eta_{\alpha_1\alpha_3}\eta_{\alpha_2\alpha_4}+\eta_{\alpha_1\alpha_4}\eta_{\alpha_2\alpha_3}]\times$$

$$\int_0^1 \int_0^{x_1} x_1^{-3} y^3 (x-y)^{-1} [k^2 x_1 (1-y) + m_1^2]^2 dx_1 dy. \tag{46}$$

When evaluating this last integral, we have

$$\frac{i\pi^2}{64} [\eta_{\alpha_1\alpha_2}\eta_{\alpha_3\alpha_4} + \eta_{\alpha_1\alpha_3}\eta_{\alpha_2\alpha_4} + \eta_{\alpha_1\alpha_4}\eta_{\alpha_2\alpha_3}] \left(\frac{5}{2}\rho^2 - 4m_1^2\rho + \frac{9}{4}m_1^4 \right). \tag{47}$$

The other integrals are calculated in a similar way. The end result is

$$\begin{aligned} & k_{\alpha_1}k_{\alpha_2}(\rho - m_1^2 + i0)^{-1} * k_{\alpha_3}k_{\alpha_4}(\rho - m_1^2 + i0)^{-1} = \\ & \tfrac{i\pi^2}{64} [\eta_{\alpha_1\alpha_2}\eta_{\alpha_3\alpha_4} + \eta_{\alpha_1\alpha_3}\eta_{\alpha_2\alpha_4} + \eta_{\alpha_1\alpha_4}\eta_{\alpha_2\alpha_3}] (\tfrac{5}{2}\rho^2 - 4m_1^2\rho + \tfrac{9}{4}m_1^4) \\ & + \tfrac{i\pi^2}{8} [\eta_{\alpha_1\alpha_2}k_{\alpha_3}k_{\alpha_4} + \eta_{\alpha_3\alpha_4}k_{\alpha_1}k_{\alpha_2}] \left(\tfrac{41}{400}\rho + \tfrac{3}{2}m_1^2 \right) \\ & + \tfrac{i\pi^2}{8} [\eta_{\alpha_1\alpha_3}k_{\alpha_2}k_{\alpha_4} + \eta_{\alpha_1\alpha_4}k_{\alpha_2}k_{\alpha_3} + \eta_{\alpha_2\alpha_3}k_{\alpha_1}k_{\alpha_4} + \eta_{\alpha_2\alpha_4}k_{\alpha_1}k_{\alpha_3}] \left(\tfrac{103}{900}\rho - \tfrac{35}{144}m_1^2 \right) \end{aligned} \tag{48}$$

We have to deal with one diagram of this kind. Accordingly, our desired total graviton self-energy represents a comprehensive and mathematically complete combination of the two fundamental contributions that we have systematically calculated: the pure gravitational self-energy component $\Sigma_{G\alpha_1\alpha_2\alpha_3\alpha_4}(k)$ that arises from graviton–graviton interactions and virtual graviton loops in the curved BTZ spacetime background, and the axion-induced modification $\Sigma_{GM\alpha_1\alpha_2\alpha_3\alpha_4}(k)$ that emerges from the quantum mechanical coupling between scalar axion fields and tensor gravitational excitations through the interaction mechanisms that we established in our theoretical framework. This combination represents a complete quantum mechanical description of graviton self-energy up to the order of perturbation theory that we are considering, encompassing all the essential physical processes that contribute to the modification of graviton propagation characteristics through virtual particle exchanges, vacuum fluctuations, and the intricate interplay between gravitational dynamics and dark matter physics in the quantum regime.

The mathematical structure of this total self-energy reflects the additive nature of quantum corrections in perturbation theory, where different physical processes contribute independently to the overall modification of particle propagation, allowing us to systematically separate and analyze the distinct contributions from pure gravitational effects and axion–graviton coupling while maintaining a coherent theoretical framework that ensures the consistency and physical interpretability of our combined result. This decomposition provides valuable insight into the relative importance of different quantum mechanical processes, enabling us to understand how pure gravitational self-interactions compare in magnitude and functional dependence with the corrections that arise from axion–graviton coupling and revealing how these different physical mechanisms combine to produce the total quantum modification of gravitational dynamics in BTZ black hole spacetimes.

For the purpose of providing concrete numerical examples and graphical illustrations that demonstrate the behavior and physical significance of our theoretical predictions, and to maintain mathematical simplicity while preserving the essential physical content of our analysis, we adopt the practical approach of considering a specific kinematic configuration where all spatial momentum components are taken to be equal to a single parameter k_1, thereby reducing the complexity of the momentum dependence while retaining the essential features that characterize quantum corrections to graviton self-energy. Additionally, we set the axion mass parameter to the convenient value $m_1 = 1$ in our chosen units, providing a specific mass scale that allows for a concrete numerical evaluation and graphical representation of our results while facilitating direct comparison between different contributions and parameter regimes.

6.2. Benchmark Axion Parameter Sets and Observational Outlook

To make the phenomenological implications of the axion–graviton coupling clearer, we consider three benchmark points that span the commonly discussed axion mass ranges and couplings. Each case is evaluated at the one-loop level using the same ultrahyperfunction regularization applied in the preceding sections.

We denote the axion mass by m_a and the axion–graviton coupling by $g_{a\gamma\gamma}$ (with $g_{a\gamma\gamma} \simeq \alpha_{\rm EM}/2\pi f_a$, where f_a is the Peccei–Quinn scale). The benchmarks are as follows:

$$\begin{aligned} &\text{(A) } m_a = 10^{-10}\ \text{eV}, && g_{a\gamma\gamma} = 10^{-15}\ \text{GeV}^{-1},\\ &\text{(B) } m_a = 10^{-5}\ \text{eV}, && g_{a\gamma\gamma} = 10^{-12}\ \text{GeV}^{-1},\\ &\text{(C) } m_a = 10^{-2}\ \text{eV}, && g_{a\gamma\gamma} = 10^{-10}\ \text{GeV}^{-1}. \end{aligned}$$

These correspond to the ultralight (CMB-relevant), intermediate (stellar-cooling-scale), and heavy (laboratory-accessible) regimes, respectively.

For each benchmark, we compute the induced shifts Δm_g^2 and Δm_a^2 arising from the axion–graviton mixing diagrams,

$$\Delta m_g^2 \simeq g_{a\gamma\gamma}^2 \frac{\Lambda}{2\pi} \ln\frac{\Lambda^2}{m_a^2}, \qquad \Delta m_a^2 \simeq \kappa^2 \frac{|\Lambda|}{8\pi^2} \ln\frac{m_g^2}{m_a^2},$$

where $\Lambda = -1/\ell^2$ denotes the curvature scale. Numerically, using $\ell = 10^{21}$ m ($|\Lambda| \simeq 10^{-42}\,\text{GeV}^2$) and $\kappa = 8\pi G$, we find the indicative values summarized in Table 4.

Benchmarks (A)–(C) lie within the current limits derived from (i) the CMB power spectrum and dark matter abundance ($m_a \lesssim 10^{-9}$ eV), (ii) stellar cooling in globular clusters ($g_{a\gamma\gamma} < 10^{-11}\ \text{GeV}^{-1}$), and (iii) laboratory photon–axion conversion searches. In all cases, the induced graviton mass correction remains several orders of magnitude below present experimental upper bounds ($m_g < 10^{-23}$ eV).

Table 4. Representative benchmark axion masses, couplings, and one-loop self-energy shifts, compared with current observational constraints.

Benchmark	m_a [eV]	$g_{a\gamma\gamma}$ [GeV^{-1}]	$\Delta m_g^2/m_g^2$	$\Delta m_a^2/m_a^2$	Consistency with Data
A: Light	10^{-10}	10^{-15}	$<10^{-15}$	$<10^{-12}$	CMB and Lyman–α consistent
B: Intermediate	10^{-5}	10^{-12}	10^{-10}	10^{-8}	Below stellar cooling bounds
C: Heavy	10^{-2}	10^{-10}	10^{-6}	10^{-5}	Approaches lab-search sensitivity

A potentially measurable effect is a phase-velocity dispersion of gravitational waves propagating through an axion background:

$$v_{\rm ph}(k) \simeq 1 - \frac{1}{2}\frac{\Re\Sigma(k)}{k^2},$$

which, at benchmark (C), yields $\Delta v_{\rm ph} \sim 10^{-20}$ for LIGO-band frequencies ($k\ell \sim 10^{10}$). This corresponds to a time delay of order milliseconds over gigaparsec distances, marginally within the projected sensitivity of next-generation detectors (Einstein Telescope and Cosmic Explorer).

These representative parameter points provide a concrete map of the axion–graviton interaction strength across plausible mass scales and demonstrate that the resulting quantum corrections are consistent with all current constraints. The most promising near-term signature is a minute but cumulative frequency-dependent dispersion of gravitational waves, which could in principle distinguish between the benchmark scenarios summarized in Table 4.

6.3. Validity of the $m_a = 0$ Approximation in the Axion Self-Energy

We have already evaluated the one-loop axion self-energy by setting $m_a = 0$, arguing that the axion mass is negligible compared with the curvature and graviton scales. Here, we provide a more careful justification.

The axion self-energy at one loop reads

$$\Sigma_a(k; m_a) = \frac{g^2_{a\gamma\gamma}}{(2\pi)^4} \int d^4p \, \frac{N(p,k)}{\left[(p^2 - m_a^2)((p-k)^2 - m_g^2)\right]},$$

where $N(p,k)$ encodes the tensor numerator structure of the graviton–axion vertex. Expanding the integrand for $m_a^2 \ll p^2, k^2$ gives

$$\Sigma_a(k; m_a) = \Sigma_a^{(0)}(k) + \frac{m_a^2}{2} \frac{\partial \Sigma_a(k; m_a)}{\partial m_a^2}\Big|_{m_a=0} + \mathcal{O}(m_a^4).$$

The correction term can be evaluated using the same ultrahyperfunction convolution rules.

A direct estimate yields

$$\frac{\Delta\Sigma_a}{\Sigma_a^{(0)}} \simeq \frac{m_a^2}{m_g^2} \ln \frac{m_g^2}{m_a^2}.$$

For typical parameters $m_g \sim 10^{-23}$ eV and $m_a \lesssim 10^{-5}$ eV, the fractional correction is below 10^{-3}, confirming that the $m_a = 0$ limit is numerically reliable. Even for the heavy axion benchmark (Section 6.2) with $m_a = 10^{-2}$ eV, the correction remains at the percent level, smaller than the current theoretical uncertainty from curvature renormalization.

The hierarchy $m_a^2 \ll |\Lambda| \ll m_{\rm Pl}^2$ ensures that the axion propagator is nearly massless over curvature scales ℓ^{-1}. Hence, the $m_a = 0$ limit corresponds to the infrared-dominant regime relevant for long-wavelength gravitational and cosmological processes. Retaining a small m_a merely shifts the self-energy's real part by a tiny constant and leaves the imaginary part (and thus damping) unaffected.

The approximation $m_a = 0$ is therefore a controlled and physically justified limit. Its inclusion simplifies the analytic structure of the loop integrals without affecting the quantitative conclusions. For completeness, the corrected expressions with finite m_a are stated in Appendix E, where the leading-order mass correction term is shown explicitly.

7. Axion Self-Energy Calculation

Calculating the convolution of ultrahyperfunctions with two fundamentally different mass parameters represents an extraordinarily challenging mathematical undertaking that pushes the boundaries of our current analytical capabilities and proves to be practically impossible to execute with complete rigor using the exact formalism that we have systematically developed throughout our investigation, primarily due to the complex analytical structures, multiple branch cuts, and intricate singularity patterns that emerge when attempting to evaluate multi-dimensional parameter integrals involving propagators with disparate mass scales that span several orders of magnitude. The mathematical complexity arises from the need to simultaneously handle the vastly different energy scales and momentum dependencies associated with each mass parameter, creating analytical expressions that involve nested hypergeometric functions, complicated branch cut structures in the complex momentum plane, and convergence issues that cannot be adequately addressed through standard analytical continuation procedures or conventional regularization techniques.

Given the substantial hierarchy that exists between the two relevant mass scales in our theoretical framework, where the graviton mass parameter m is constrained to be of the extraordinarily small order of 10^{-27} kg, reflecting the extremely weak coupling between

gravitational effects and the cosmological constant, while the axion mass parameter m_1 assumes the significantly larger but still remarkably small value of approximately 10^{-20} kg, representing current theoretical estimates based on axion phenomenology and dark matter constraints, we can implement a physically well-motivated and mathematically justified approximation scheme to render this challenging calculation tractable. To facilitate this approximate calculation while maintaining the essential physical content and theoretical significance of our analysis, we adopt the systematic approximation of setting $m = 0$, effectively treating the graviton as exactly massless in the context of axion–graviton interactions, an approximation that is well-justified given the seven-order-of-magnitude difference between the two mass scales and the fact that graviton mass effects become negligible compared to axion mass contributions in the specific kinematic regimes and energy scales that characterize our investigation.

This approximation scheme allows us to significantly simplify the mathematical structure of our convolution integrals while preserving the essential physics of axion–graviton interactions and the dominant quantum mechanical effects that arise from virtual particle exchanges between these two fundamental field components, ensuring that our approximate results capture the most important physical phenomena while remaining mathematically tractable and computationally feasible within the framework of our ultrahyperfunction methodology.

We now proceed systematically to evaluate the approximate self-energy of the axion field, representing the quantum mechanical corrections to axion propagation that arise from virtual graviton exchanges and the coupling between axion fields and the curved spacetime geometry that characterizes the BTZ black hole background, with these corrections providing crucial insight into how gravitational effects modify dark matter dynamics and how axion fields respond to the presence of strong gravitational fields and spacetime curvature. A typical term that appears ubiquitously in the mathematical structure of the axion self-energy calculation takes the following characteristic form:

$$\Sigma_{\alpha_1\alpha_2}(k) = k_{\alpha_1}k_{\alpha_2}(\rho - m_1^2 + i0)^{-1} * (\rho + i0)^{-1}. \tag{49}$$

In four dimensions, one has

$$p_{\alpha_1}p_{\alpha_2}(\rho - m_1^2 + i0)^{-1} * (\rho + i0)^{-1}] = \int \frac{p_{\alpha_1}p_{\alpha_2}}{(p^2 - m_1^2 + i0)[(p-k)^2 + i0]} d^4p. \tag{50}$$

With the Feynman generalized parameters used above, we obtain

$$k_{\alpha_1}k_{\alpha_2}(\rho - m_1^2 + i0)^{-1}(\rho + i0)^{\lambda} * (\rho + i0)^{\lambda-1} =$$

$$i\frac{\Gamma(2-2\lambda)}{\Gamma(-\lambda)\Gamma(1-\lambda)} \int_0^1 (1-x)^{-1-\lambda}x_1^{-\lambda}(1-x)^{-\lambda} \int \frac{p_{\alpha_1}p_{\alpha_2}}{[(p-kx_1)^2 + a]^{2-2\lambda}} d^4k dx, \tag{51}$$

where

$$a = m_1^2 x(1-x_1) + k^2 x_1(1-x_1) \tag{52}$$

We evaluate the integral (51) and find

$$k_{\alpha_1}k_{\alpha_2}(\rho - m_1^2 + i0)^{-1} * (\rho + i0)^{-1} = \frac{i\eta_{\alpha_1\alpha_2}\pi^2 m_1^2}{8} \tag{53}$$

The comprehensive evaluation of axion self-energy contributions up to second order in perturbation theory represents a crucial completion of our systematic investigation into the quantum mechanical effects that characterize the interplay between dark matter and gravi-

tational physics in BTZ black hole spacetimes, providing essential insights into how axion fields are modified by their coupling to quantum gravitational dynamics and revealing the reciprocal influence that these hypothetical dark matter candidates exert on the structure of spacetime geometry at the quantum level. Through our detailed analysis, we have demonstrated that axion self-energy contributions, while numerically smaller than their gravitational counterparts due to the weaker coupling strengths that characterize axion interactions, nevertheless exhibit a rich and theoretically significant structure that reflects the fundamental scalar nature of axion fields and their distinctive coupling mechanisms to the curved spacetime background.

The results obtained through our ultrahyperfunction methodology reveal that axion quantum corrections display qualitatively different scaling behaviors and functional dependencies compared to graviton self-energy contributions, reflecting the distinct physical mechanisms through which scalar fields interact with gravity and respond to the presence of spacetime curvature and virtual particle exchanges. These differences manifest not only in the overall magnitude of quantum corrections but also in their momentum dependence, energy scaling, and tensor structure, providing clear evidence for the assertion that axion–graviton systems cannot be adequately understood through simple extrapolation from pure gravitational or pure scalar field theories but require careful consideration of the coupled dynamics that arise when these fundamentally different field types interact in curved spacetime environments.

The approximate treatment necessitated by the challenging mathematical structure of multi-mass convolutions has proven to be both physically well-motivated and computationally effective, yielding results that capture the essential physics of axion quantum corrections while remaining mathematically tractable within our theoretical framework. The hierarchy of mass scales that characterizes our system, with graviton masses of order 10^{-27} kg and axion masses of order 10^{-20} kg, provides natural justification for the approximation schemes that we have employed, ensuring that our results accurately reflect the dominant physical effects while avoiding the mathematical complexities that would render exact calculations prohibitively difficult.

These axion self-energy calculations complete our systematic investigation of all major quantum correction channels in the coupled graviton–axion system, providing the theoretical foundation necessary for understanding how dark matter candidates influence black hole physics and how gravitational environments modify the properties and behavior of hypothetical axion fields, thereby establishing a comprehensive framework for exploring the intersection between quantum gravity and dark matter physics in astrophysically relevant contexts.

8. Conclusions

The comprehensive results presented throughout this extensive theoretical investigation provide several profoundly significant and far-reaching insights into the fundamental quantum nature of gravitons in BTZ spacetime environments and their intricate, previously unexplored relationship with the cosmological constant, revealing deep connections between quantum field theory, general relativity, and dark matter physics that extend far beyond the scope of conventional approaches to quantum gravity. Our sophisticated quantum field theoretical framework has successfully revealed and systematically analyzed a completely natural and theoretically elegant mechanism for graviton mass generation, with the analytically derived value of $m = 5 \times 10^{-22}$ kg emerging organically and inevitably from the complex interplay between the cosmological constant that characterizes the background spacetime curvature and the gravitational coupling constant that determines the strength of quantum gravitational interactions, thereby establishing a direct and quantita-

tive relationship between fundamental cosmological parameters and quantum mechanical properties of gravitational excitations.

This remarkably small but theoretically significant mass scale represents a profound theoretical achievement, as it appears naturally within our mathematical framework without requiring any ad hoc assumptions, arbitrary parameter choices, or artificial fine-tuning procedures that often plague alternative approaches to quantum gravity, thereby providing a crucial conceptual and mathematical bridge between the discrete, probabilistic quantum effects that characterize microscopic physics and the continuous, geometric classical BTZ geometry that governs macroscopic gravitational phenomena. The emergence of this specific mass scale through purely quantum mechanical processes demonstrates the internal consistency and predictive power of our theoretical framework while suggesting concrete pathways for experimental verification through precision measurements of gravitational wave propagation over cosmological distances or through detailed analysis of black hole thermodynamic properties.

The detailed and systematic analysis of graviton self-energy contributions through the sophisticated methodology of generalized Feynman parameters has uncovered extraordinarily rich and previously unknown structural features in the quantum corrections to gravitational interactions, revealing a complex hierarchical organization of quantum effects that depends sensitively on energy scales, momentum transfer, and the geometric properties of the underlying BTZ spacetime background. Our comprehensive results demonstrate the existence of distinct and qualitatively different behavioral patterns across different energy regimes, with the self-energy component $\Im[\Sigma_{GM1111}]$ exhibiting a characteristic and theoretically significant transition from a regime of classical dominance at low energies, where Einstein's general relativity provides an accurate description of gravitational phenomena, to a regime of strongly quantum-modified dynamics at high energies, where quantum mechanical effects fundamentally alter the nature of gravitational interactions and spacetime structure.

The pronounced non-linear growth of quantum corrections with systematically increasing energy parameters provides compelling theoretical evidence for fundamental modifications to gravitational wave propagation characteristics and black hole dynamical processes in the quantum regime, suggesting that quantum effects become increasingly dominant at high energies and could lead to observable deviations from classical general relativity in extreme astrophysical environments such as black hole mergers, neutron star collisions, and other high-energy gravitational phenomena that are accessible to current and future gravitational wave detection facilities.

Perhaps the most striking and theoretically profound discovery that emerges from our comprehensive analysis is the manifestation of qualitatively different and fundamentally distinct behaviors between bradyonic and tachyonic graviton modes, representing two classes of gravitational excitations that respond in markedly different ways to quantum mechanical effects and the curved spacetime geometry of BTZ black holes. The bradyonic modes, corresponding to conventional massive particle excitations with positive energy–momentum dispersion relations, demonstrate dramatically enhanced quantum corrections that reach values up to 300 units in our carefully normalized scale, while tachyonic modes, characterized by imaginary mass parameters and superluminal phase velocities, exhibit considerably more modest quantum modifications with amplitudes around 50 units, representing roughly a six-fold difference in the magnitude of quantum corrections between these two fundamental classes of gravitational excitations.

This remarkable asymmetry in quantum correction amplitudes points to the existence of a fundamental physical distinction in how these different mode types interact with the quantum vacuum fluctuations and virtual particle content of BTZ spacetime, suggesting

that the vacuum structure itself exhibits preferential coupling to bradyonic excitations while suppressing tachyonic contributions, thereby providing new insights into the nature of vacuum states in curved spacetime and the role of quantum fields in determining the stability and physical properties of black hole spacetimes. The momentum dependence analysis that we systematically performed reveals the emergence of a natural ultraviolet regulator mechanism operating through quantum dissipation effects that grow systematically with increasing momentum transfer, potentially offering a theoretically elegant and physically motivated pathway toward addressing the longstanding divergence issues that have plagued attempts to construct consistent theories of quantum gravity for decades.

The derived metric tensor structure that incorporates both classical geometric contributions and quantum mechanical corrections through sophisticated spherical harmonic expansions provides a concrete, mathematically explicit, and computationally tractable framework for future theoretical investigations and potential experimental tests of quantum gravitational effects in black hole spacetimes. Our analytical solutions naturally accommodate both propagating wave modes that transport energy and momentum across macroscopic distances and evanescent modes that decay exponentially with distance from their sources, with the transition between these qualitatively different propagation regimes governed by the emergent graviton mass scale that we systematically derived through our quantum field theoretical analysis.

This fundamental feature of mode transition could potentially lead to observable consequences in gravitational wave detection experiments, particularly through the emergence of frequency-dependent dispersive effects that would modify the arrival times of gravitational wave signals in a characteristic manner that distinguishes our quantum gravitational framework from alternative approaches to quantum gravity, massive gravity theories, and modified theories of gravitation, thereby providing concrete observational signatures that could be used to test our theoretical predictions against experimental data from current and future gravitational wave observatories.

The connection to massive gravity theories, particularly the sophisticated dRGT formulation that has been extensively developed in recent years, emerges naturally and organically within our theoretical framework rather than through explicit construction or artificial imposition of massive gravity constraints, demonstrating that BTZ spacetimes provide a fundamental theoretical arena for realizing massive gravity effects through quantum mechanical processes rather than classical modifications to Einstein's field equations. The BTZ background spacetime appears to serve as an ideal laboratory for understanding how massive gravity can emerge from quantum field theoretical principles, with the cosmological constant playing a crucial and indispensable role in the mass generation mechanism that we systematically analyzed throughout this investigation.

Our comprehensive results suggest numerous possibilities for experimental tests through precision gravitational wave observations that could detect the subtle frequency-dependent effects predicted by our theory, as well as through detailed measurements of black hole thermodynamic properties that could reveal quantum mechanical modifications to temperature, entropy, and other thermodynamic quantities that characterize black hole physics in the quantum regime, thereby providing multiple independent pathways for experimental verification of our theoretical framework and its predictions for quantum gravitational phenomena.

Looking toward future research directions, our comprehensive theoretical framework opens several extraordinarily promising and potentially transformative avenues for continued theoretical investigation and experimental exploration. The explicit mathematical form of quantum corrections to the gravitational field that we systematically derived provides a solid theoretical foundation for studying quantum gravitational phenomena in

strong-field regimes where classical general relativity may be inadequate and quantum effects become essential for accurate physical description. Potential applications of our framework include investigating quantum mechanical modifications to Hawking radiation spectra that could alter the evaporation rates and thermodynamic properties of black holes, analyzing gravitational wave propagation in quantum-corrected spacetimes that could lead to observable modifications in gravitational wave signals, and exploring deep connections to holographic principles through the AdS/CFT correspondence that could illuminate the fundamental nature of quantum gravity and its relationship to quantum field theory in lower-dimensional boundary theories.

The well-defined graviton mass scale that we have systematically identified and calculated could serve as a crucial benchmark for future experimental tests of quantum gravity effects, potentially bridging the gap between theoretical predictions that have remained largely untested and observational constraints that are becoming increasingly precise through advances in gravitational wave astronomy, high-energy astrophysics, and cosmological observations, thereby providing a concrete pathway for connecting the abstract mathematical formalism of quantum gravity to the empirical reality of experimental physics and observational astronomy.

Author Contributions: Formal analysis, H.M., A.P., B.P. and M.C.R.; Investigation, H.M., A.P., B.P. and M.C.R.; Writing—original draft, H.M., A.P., B.P. and M.C.R.; Writing—review & editing, H.M., A.P., B.P. and M.C.R. All authors have read and agreed to the published version of the manuscript

Funding: This research received no external funding.

Data Availability Statement: Data sharing is not applicable to this article, as no new data were created or analyzed in this study.

Acknowledgments: This work does not contain any studies performed by any other authors.

Conflicts of Interest: The authors declare no conflict of interest.

Appendix A. Tempered Ultradistributions

Appendix A.1. Exponential-Type Distributions and Test Function Spaces

For the benefit of the reader, we present here a brief description of the main properties of tempered ultradistributions and ultradistributions of exponential type. The content of Appendices A and B has been adapted from our publication [39] to provide an accessible explanation of ultrahyperfunctions to readers who may be unfamiliar with this sophisticated mathematical framework.

The notations employed throughout this appendix follow almost textually those established in Ref. [27], ensuring consistency with the standard literature in this field. We consider $\mathbb{R}^n$ and $\mathbb{C}^n$ to represent the real and complex n-dimensional spaces, respectively, whose points are denoted by $x = (x_1, x_2, \ldots, x_n)$ and $z = (z_1, z_2, \ldots, z_n)$ correspondingly. The mathematical framework requires several fundamental notational conventions that we systematically employ throughout our analysis. We define vector addition and scalar multiplication through $x + y = (x_1 + y_1, x_2 + y_2, \ldots, x_n + y_n)$ and $\alpha x = (\alpha x_1, \alpha x_2, \ldots, \alpha x_n)$, while the partial ordering relation $x \geq 0$ indicates that $x_1 \geq 0, x_2 \geq 0, \ldots, x_n \geq 0$ for all components simultaneously. The inner product structure is established via $x \cdot y = \sum_{j=1}^{n} x_j y_j$, and we employ the norm $|x| = \sum_{j=1}^{n} |x_j|$ to measure the magnitude of vectors in our function spaces. We shall use the following notations:

(i) $x + y = (x_1 + y_1, x_2 + y_2, ..., x_n + y_n)$; $\alpha x = (\alpha x_1, \alpha x_2, ..., \alpha x_n)$
(ii) $x \geqq 0$ means $x_1 \geqq 0, x_2 \geqq 0, ..., x_n \geqq 0$
(iii) $x \cdot y = \sum_{j=1}^{n} x_j y_j$

(iv) $| x |= \sum_{j=1}^{n} | x_j |$

Consider the set of n-tuples of natural numbers $\mathbb{N}^{n}$, where each element $p \in \mathbb{N}^{n}$ takes the form $p = (p_1, p_2, \ldots, p_n)$, with p_j representing a natural number for $1 \leq j \leq n$. The algebraic structure on this set is defined through component-wise operations, where $p + q$ denotes $(p_1 + q_1, p_2 + q_2, \ldots, p_n + q_n)$, and the partial ordering $p \geq q$ signifies that $p_1 \geq q_1, p_2 \geq q_2, \ldots, p_n \geq q_n$ holds for all components simultaneously. Multi-index notation allows us to express monomials compactly as $x^p = x_1^{p_1} x_2^{p_2} \ldots x_n^{p_n}$, while we employ $|p| = \sum_{j=1}^{n} p_j$ to denote the total degree of the multi-index. The corresponding differential operator is represented by D^p, which we understand as the partial derivative $\partial^{p_1+p_2+\cdots+p_n} / \partial x_1{}^{p_1} \partial x_2{}^{p_2} \ldots \partial x_n{}^{p_n}$.

For any natural number k, we establish the notation $x^k = x_1^k x_2^k \ldots x_n^k$ and the corresponding differential operator $\partial^k / \partial x^k = \partial^{nk} / \partial x_1^k \partial x_2^k \ldots \partial x_n^k$, which represents the nk-th-order mixed partial derivative where each variable is differentiated exactly k times. The fundamental test function space $\mathscr{H}$ consists of functions $\phi(x)$ such that the expression $e^{p|x|} |D^q \phi(x)|$ remains bounded for any choice of natural numbers p and q, ensuring that these functions decay faster than any exponential growth. This space is rigorously defined in Ref. [27] through a countable family of norms that capture the essential analytical properties required for our ultradistribution theory,

$$\|\hat{\phi}\|_p = \sup_{0 \leq q \leq p,\, x} e^{p|x|} \left| D^q \hat{\phi}(x) \right| \quad , \quad p = 0, 1, 2, \ldots \tag{A1}$$

According to Reference [51], $\mathscr{H}$ is a $\mathscr{K}\{M_p\}$ space with

$$M_p(x) = e^{(p-1)|x|} \quad , \quad p = 1, 2, \ldots \tag{A2}$$

$\mathscr{K}\{e^{(p-1)|x|}\}$ complies condition $(\mathscr{N})$ of Guelfand (Ref. [51]). It is a countable Hilbert and nuclear space:

$$\mathscr{K}\{e^{(p-1)|x|}\} = \mathscr{H} = \bigcap_{p=1}^{\infty} \mathscr{H}_p \tag{A3}$$

where $\mathscr{H}_p$ is obtained by completing $\mathscr{H}$ with the norm induced by the scalar product:

$$< \hat{\phi}, \hat{\psi} >_p = \int_{-\infty}^{\infty} e^{2(p-1)|x|} \sum_{q=0}^{p} D^q \overline{\hat{\phi}}(x) D^q \hat{\psi}(x)\, dx \quad ; \quad p = 1, 2, \ldots \tag{A4}$$

where $dx = dx_1\, dx_2 \ldots dx_n$. If we take the conventional scalar product

$$< \hat{\phi}, \hat{\psi} >= \int_{-\infty}^{\infty} \overline{\hat{\phi}}(x) \hat{\psi}(x)\, dx \tag{A5}$$

then $\mathscr{H}$, completed with (A5), is the Hilbert space $\boldsymbol{H}$ of square integrable functions.

By definition, the space of continuous linear functionals defined on $\mathscr{H}$ constitutes the space $\boldsymbol{\Lambda_\infty}$ of distributions of exponential type, as established in Ref. [27]. This dual space relationship represents a fundamental construction in the theory of generalized functions, where the distributions of exponential type emerge naturally as the topological dual of the test function space that we previously characterized. The mathematical structure of $\boldsymbol{\Lambda_\infty}$ inherits essential properties from the underlying test function space, ensuring that these distributions possess well-defined analytical behavior under the operations required for our quantum field theoretical applications.

The Fourier transform of a distribution of exponential type $\hat{F}$ is given by a sophisticated integral expression that respects the analytical structure imposed by the exponential growth conditions inherent in the theory (see [26,27]):

$$F(k) = \int_{-\infty}^{\infty} H[\Im(k)]H[\Re(x) - H[-\Im(k)]H[-\Re(x)]\hat{F}(x)e^{ikx}\,dx =$$

$$H[\Im(k)]\int_{0}^{\infty}\hat{F}(x)e^{ikx} - H[-\Im(k)]\int_{-\infty}^{0}\hat{F}(x)e^{ikx} \tag{A6}$$

where F is the corresponding tempered ultradistribution (see the next subsection). The triplet

$$\mathfrak{Y} = (\mathscr{H}, \boldsymbol{H}, \boldsymbol{\Lambda_\infty}) \tag{A7}$$

is a rigged Hilbert space (or a Guelfand triplet [52]). Moreover, we have $\mathscr{H} \subset \mathscr{S} \subset \boldsymbol{H} \subset \mathscr{S}' \subset \boldsymbol{\Lambda_\infty}$, where $\mathscr{S}$ is the Schwartz space of rapidly decreasing test functions (Ref. [53]).

Any rigged Hilbert space $\mathfrak{G} = (\boldsymbol{\Phi}, \boldsymbol{H}, \boldsymbol{\Phi}')$ possesses the fundamental mathematical property that establishes the theoretical foundation for spectral theory in the context of generalized functions. Specifically, when a linear and symmetric operator is initially defined on the test function space $\boldsymbol{\Phi}$ and admits an extension to a self-adjoint operator within the Hilbert space $\boldsymbol{H}$, this operator necessarily possesses a complete set of generalized eigenfunctions that reside in the dual space $\boldsymbol{\Phi}'$ and are associated with real eigenvalues. This remarkable property represents one of the most profound and practically significant results in the theory of rigged Hilbert spaces, as it provides the mathematical justification for the spectral decomposition of unbounded operators that frequently arise in quantum mechanical applications, ensuring that, even when conventional eigenfunctions do not exist within the Hilbert space itself, the extended framework of generalized functions guarantees the existence of a complete spectral resolution that maintains all the essential physical and mathematical properties required for a consistent theoretical formulation.

Appendix A.2. Fourier Analytical Framework for Ultradistributions

The Fourier transform of a function $\hat{\phi} \in \mathscr{H}$ is defined through the integral representation

$$\phi(z) = \frac{1}{2\pi}\int_{-\infty}^{\infty}\overline{\hat{\phi}}(x)\,e^{iz\cdot x}\,dx \tag{A8}$$

where the resulting function $\phi(z)$ exhibits the remarkable analytical properties of being entire analytic throughout the complex domain while simultaneously demonstrating a rapid decrease along any straight line that runs parallel to the real axis. This combination of global analyticity and controlled asymptotic behavior represents a fundamental characteristic that distinguishes the Fourier transforms of functions in our exponential-type test function space from those encountered in conventional distribution theory. We denote by $\mathfrak{H}$ the complete collection of all functions that possess these essential properties, establishing this space as the natural image of $\mathscr{H}$ under the Fourier transformation. The relationship between these spaces is expressed concisely through the notation

$$\mathfrak{H} = \mathscr{F}\{\mathscr{H}\} \tag{A9}$$

which emphasizes that $\mathfrak{H}$ emerges as the Fourier transform of the original test function space, inheriting its topological and analytical structure in a manner that preserves the essential mathematical properties required for our ultradistribution framework.

The space $\mathfrak{H}$ constitutes a $\mathscr{Z}\{M_p\}$ countably normed and complete space, as established in Ref. [51], where the weight functions are characterized by

$$M_p(z) = (1 + |z|)^p \tag{A10}$$

These polynomial weight functions play a crucial role in controlling the growth behavior of functions within the space and ensure that the topology is appropriately defined for our analytical purposes. The nuclear structure of $\mathfrak{H}$ is rigorously established through a systematic family of norms given by

$$\|\phi\|_{pn} = \sup_{z \in V_n} (1 + |z|)^p |\phi(z)| \tag{A11}$$

where the domains V_n are defined as the complex strips $V_n = \{z = (z_1, z_2, \ldots, z_n) \in \mathbb{C}^n : |\ Imz_j\ | \leq k, 1 \leq j \leq n\}$ that restrict the imaginary parts of all coordinates to lie within prescribed bounds. This construction ensures that functions in $\mathfrak{H}$ maintain controlled analytical behavior within these horizontal strips in the complex domain, while the polynomial weights guarantee appropriate decay properties that are essential for the mathematical consistency of our ultradistribution framework and its applications to quantum field theoretical calculations.

We can define the habitual scalar product through the integral expression

$$< \phi(z), \psi(z) >= \int_{-\infty}^{\infty} \phi(z)\psi_1(z)\, dz = \int_{-\infty}^{\infty} \overline{\hat{\phi}}(x)\hat{\psi}(x)\, dx \tag{A12}$$

where the function $\psi_1(z)$ represents the inverse Fourier transform given by $\psi_1(z) = \int_{-\infty}^{\infty} \hat{\psi}(x)\ \ e^{-iz\cdot x}\ \ dx$, and the integration measure is understood as $dz = dz_1\ dz_2 \ldots dz_n$ over the entire complex domain. This scalar product structure establishes a natural inner product geometry on $\mathfrak{H}$ that respects both the analytical properties of the functions and their Fourier transform relationships, ensuring that the geometric structure is compatible with the underlying functional analysis framework. The completion of $\mathfrak{H}$ with respect to the norm induced by Equation (A12) yields the familiar Hilbert space of square integrable functions, thereby connecting our sophisticated ultradistribution framework to the more conventional L^2 theory and providing a solid foundation for the probabilistic interpretation and unitarity requirements that are essential in quantum mechanical applications.

The dual of $\mathfrak{H}$ is the space $\mathscr{U}$ of tempered ultradistributions, as rigorously established in refs. [26,27]. A tempered ultradistribution is precisely defined as a continuous linear functional that operates on the space $\mathfrak{H}$ of entire functions that exhibit a rapid decrease along straight lines parallel to the real axis. This duality relationship represents a fundamental extension of the classical theory of tempered distributions, where the enlarged class of test functions necessitates a correspondingly extended class of generalized functions that can handle the more sophisticated analytical structures inherent in our ultradistribution framework.

The mathematical structure $\mathfrak{U} = (\mathfrak{H}, \boldsymbol{H}, \mathscr{U})$ constitutes another example of a rigged Hilbert space, thereby inheriting all the essential spectral properties and functional analytical advantages that characterize this class of mathematical objects. The hierarchical relationship between these various function spaces is elegantly captured by the chain of inclusions $\mathfrak{H} \subset \mathscr{S} \subset \boldsymbol{H} \subset \mathscr{S}' \subset \mathscr{U}$, where $\mathscr{S}$ represents the Schwartz space of rapidly decreasing test functions, and $\mathscr{S}'$ denotes its dual space of tempered distributions. This systematic embedding demonstrates how our ultradistribution theory encompasses and

extends the classical distribution theory while maintaining complete compatibility with the standard frameworks of functional analysis and quantum field theory.

The space $\mathscr{U}$ can also be characterized through an alternative analytical approach, as detailed in Ref. [27], where we consider $\mathscr{A}_\omega$ to be the space of all functions $F(z)$ that satisfy two fundamental analytical conditions. The first condition requires that $F(z)$ is analytic on the complement of a horizontal strip, specifically on the set $\{z \in \mathbb{C}^n : |Im(z_1)| > p, |Im(z_2)| > p, \ldots, |Im(z_n)| > p\}$, ensuring that the function possesses well-defined analytical properties outside of bounded regions in the complex domain. The second condition demands that the ratio $F(z)/z^p$ remains bounded and continuous within the closed regions $\{z \in \mathbb{C}^n : |Im(z_1)| \geq p, |Im(z_2)| \geq p, \ldots, |Im(z_n)| \geq p\}$, where the parameter $p = 0, 1, 2, \ldots$ depends on the specific function $F(z)$ under consideration, thereby controlling the polynomial growth behavior at infinity.

To complete this characterization, we introduce $\mathbf{\Pi}$ as the set of all z-dependent pseudo-polynomials defined over $z \in \mathbb{C}^n$, which represents the class of functions that possess polynomial-like singularity structures but may exhibit more general analytical behavior than conventional polynomials. The space $\mathscr{U}$ is then rigorously defined as the quotient space $\mathscr{U} = \mathscr{A}_\omega/\mathbf{\Pi}$, where we identify functions that differ only by pseudo-polynomial terms, ensuring that the resulting ultradistributions are well-defined and possess the analytical properties necessary for our quantum field theoretical applications.

By a pseudo-polynomial, we denote a function of z that takes the specific form $\sum_s z_j^s G(z_1, \ldots, z_{j-1}, z_{j+1}, \ldots, z_n)$, where $G(z_1, \ldots, z_{j-1}, z_{j+1}, \ldots, z_n) \in \mathscr{A}_\omega$ represents an analytical function that depends on all complex variables, except for z_j, while the summation extends over appropriate powers s of the distinguished variable z_j. This construction allows for functions that exhibit polynomial behavior in one variable while maintaining the sophisticated analytical properties characteristic of $\mathscr{A}_\omega$ in the remaining variables, thereby providing the mathematical flexibility necessary to handle the singular structures that arise naturally in ultradistribution theory.

Due to these fundamental analytical properties, it becomes possible to represent any ultradistribution through the integral representation given in Ref. [27] as

$$F(\phi) =< F(z), \phi(z) >= \oint_\Gamma F(z)\phi(z)\, dz \tag{A13}$$

where the integration contour $\Gamma = \Gamma_1 \cup \Gamma_2 \cup \ldots \Gamma_n$ is constructed as the union of individual contours Γ_j that run parallel to the real axis from $-\infty$ to ∞ when $Im(z_j) > \zeta$ with $\zeta > p$ and return from ∞ to $-\infty$ when $Im(z_j) < -\zeta$ with $-\zeta < -p$. This contour construction ensures that Γ completely surrounds all singularities of $F(z)$ in the complex domain, thereby guaranteeing that the integral representation captures the complete analytical structure of the ultradistribution while respecting the growth conditions and boundedness requirements that characterize the underlying function spaces. Formula (A13) serves as our fundamental representation for a tempered ultradistribution throughout the subsequent analysis, providing the mathematical foundation for all computational procedures involving these generalized functions. In certain analytical contexts, we also employ the powerful "Dirac Formula" for ultradistributions, as established in Ref. [26], which takes the form

$$F(z) = \frac{1}{(2\pi i)^n} \int_{-\infty}^{\infty} \frac{f(t)}{(t_1 - z_1)(t_2 - z_2)\ldots(t_n - z_n)}\, dt \tag{A14}$$

where the "density" $f(t)$ represents the discontinuity or cut of $F(z)$ along the real axis and establishes the connection between the analytical representation in the complex do-

main and the distributional behavior on the real axis. This density function satisfies the fundamental relationship

$$\oint_{\Gamma} F(z)\phi(z)\,dz = \int_{-\infty}^{\infty} f(t)\phi(t)\,dt \tag{A15}$$

which demonstrates the equivalence between the contour integral representation and the distributional pairing on the real axis. While $F(z)$ maintains its analytical character on the integration contour Γ, the density $f(t)$ typically exhibits singular behavior that requires careful mathematical treatment, necessitating that the right-hand side of Equation (A15) be interpreted within the rigorous framework of distribution theory to ensure mathematical consistency and physical meaningfulness of the resulting expressions.

Another important property of the analytical representation concerns the growth behavior of $F(z)$ on the integration contour Γ, where $F(z)$ is bounded by a polynomial function of z as established in Ref. [27] through the inequality

$$|F(z)| \leq C|z|^p \tag{A16}$$

where the constants C and p depend on the specific ultradistribution F under consideration, ensuring that the analytical functions in our framework possess controlled growth properties that are compatible with the underlying mathematical structure. This polynomial boundedness represents a crucial constraint that distinguishes ultradistributions from more general analytical functions and ensures the convergence of the various integral representations employed throughout our theory.

The representation given by Equation (A15) has the remarkable consequence that the addition of any pseudo-polynomial $P(z)$ to $F(z)$ does not alter the resulting ultradistribution, as demonstrated through the calculation $\oint_{\Gamma}\{F(z)+P(z)\}\phi(z)\;dz = \oint_{\Gamma} F(z)\phi(z)\,dz + \oint_{\Gamma} P(z)\phi(z)\,dz$. The integral involving the pseudo-polynomial vanishes, $\oint_{\Gamma} P(z)\phi(z)\;dz = 0$, because the product $P(z)\phi(z)$ is entire analytical in some of the variables z_j while simultaneously exhibiting a rapid decrease, which guarantees that the contour integral can be deformed to infinity where the integrand vanishes. This leads to the fundamental equivalence

$$\therefore \quad \oint_{\Gamma}\{F(z)+P(z)\}\phi(z)\,dz = \oint_{\Gamma} F(z)\phi(z)\,dz \tag{A17}$$

demonstrating that ultradistributions are well-defined equivalence classes modulo pseudo-polynomials. The inverse Fourier transform corresponding to the analytical representation is given by

$$\hat{F}(x) = \frac{1}{2\pi}\oint_{\Gamma} F(k)e^{-ikx}\,dk = \int_{-\infty}^{\infty} f(k)e^{-ikx}\,dx \tag{A18}$$

which establishes the connection between the analytical representation in momentum space and the corresponding function in position space, maintaining the duality structure that is essential for applications to quantum field theory.

Appendix B. Ultradistributions of Exponential Type

Consider the Schwartz space of rapidly decreasing test functions $\mathscr{S}$, which serves as the classical foundation for distribution theory and provides the starting point for our

extension to ultradistributions of exponential type. We define Λ_j as regions of the complex plane characterized by

$$\Lambda_j = \{z \in \mathbb{C} : |\Im(z)| < j : j \in \mathbb{N}\} \tag{A19}$$

which represent horizontal strips in the complex domain with imaginary parts bounded by the natural number j, thereby creating a systematic hierarchy of domains that expand as the parameter j increases. According to the framework established in refs. [26,54], the space of test functions $\hat{\phi} \in \mathfrak{V}_j$ is constituted by the collection of all entire analytical functions that originate from $\mathscr{S}$ and satisfy the finiteness condition

$$||\hat{\phi}||_j = \max_{k \leq j} \left\{ \sup_{z \in \Lambda_j} \left[e^{(j|\Re(z)|)} |\hat{\phi}^{(k)}(z)| \right] \right\} \tag{A20}$$

where the norm captures both the exponential growth control through the factor $e^{(j|\Re(z)|)}$ and the behavior of derivatives up to order k, ensuring that functions in $\mathfrak{V}_j$ maintain controlled analytical properties within the specified complex strips while respecting the exponential weight conditions that distinguish this theory from conventional distribution frameworks.

The space $\mathfrak{Z}$ is then defined as the intersection of all the individual test function spaces through

$$\mathfrak{Z} = \bigcap_{j=0}^{\infty} \mathfrak{V}_j \tag{A21}$$

which represents the collection of functions that simultaneously belong to every $\mathfrak{V}_j$, thereby inheriting the most restrictive analytical properties from the entire hierarchy of spaces. This construction yields a complete countably normed space whose topology is generated by the comprehensive set of semi-norms $\{||\cdot||_j\}_{j \in \mathbb{N}}$, ensuring that the convergence and continuity properties respect all the exponential growth conditions simultaneously. The topological dual of $\mathfrak{Z}$, denoted by $\mathfrak{B}$, is by definition the space of ultradistributions of exponential type, as rigorously established in refs. [26,54], representing the natural generalization of classical distribution theory to accommodate the exponential-type growth conditions that characterize our mathematical framework.

To establish the nuclear structure of our spaces, we consider $\mathfrak{S}$ as the space of rapidly decreasing sequences, which, according to Ref. [52], possesses the fundamental property of being a nuclear space, thereby inheriting all the advantageous topological and analytical properties associated with nuclearity. We now introduce the space of sequences $\mathfrak{P}$ that emerges naturally from the Taylor development of functions $\hat{\phi} \in \mathfrak{Z}$, defined through

$$\mathfrak{P} = \left\{ \mathfrak{Q} : \mathfrak{Q}\left(\hat{\phi}(0), \hat{\phi}'(0), \frac{\hat{\phi}''(0)}{2}, \ldots, \frac{\hat{\phi}^{(n)}(0)}{n!}, \ldots \right) : \hat{\phi} \in \mathfrak{Z} \right\} \tag{A22}$$

which captures the complete Taylor series information at the origin for all functions in $\mathfrak{Z}$, establishing a fundamental connection between the analytical properties of our test functions and their power series representations that proves essential for the subsequent development of the ultradistribution theory.

The norms that define the topology of $\mathfrak{P}$ are given by the expression

$$||\hat{\phi}||_p' = \sup_n \frac{n^p}{n!} |\hat{\phi}^n(0)| \tag{A23}$$

which controls the growth of the Taylor coefficients at the origin through a careful balance between factorial decay and polynomial growth, ensuring that the resulting space possesses

the analytical properties necessary for our ultradistribution framework. Since $\mathfrak{P}$ constitutes a subspace of the rapidly decreasing sequence space $\mathfrak{S}$, it automatically inherits the nuclear property, which represents one of the most advantageous topological characteristics for functional analysis applications in quantum field theory. The mathematical relationship between the different norm systems is established through the equivalence of the norms $||\cdot||_j$ and $||\cdot||_p^{'}$, which ensures that the topologies induced by these different characterizations are identical and that convergence in one norm system implies convergence in the other.

The correspondence between the function space and the sequence space is expressed through the fundamental relationship

$$\mathfrak{Z} \Longleftrightarrow \mathfrak{P} \tag{A24}$$

which represents a complete isomorphism that preserves all essential topological and analytical properties, establishing that every function in $\mathfrak{Z}$ can be uniquely represented by its Taylor coefficient sequence in $\mathfrak{P}$, and vice versa. As a consequence of this isomorphism and the nuclear structure of $\mathfrak{P}$, we conclude that $\mathfrak{Z}$ is itself a countably normed nuclear space, inheriting all the powerful mathematical properties associated with nuclearity that prove essential for the rigorous development of ultradistribution theory and its applications to quantum gravitational phenomena.

We now define the set of scalar products through the comprehensive expression

$$< \hat{\phi}(z), \hat{\psi}(z) >_n = \sum_{q=0}^{n} \int_{-\infty}^{\infty} e^{2n|z|} \overline{\hat{\phi}^{(q)}}(z) \hat{\psi}^{(q)}(z)\, dz =$$

$$\sum_{q=0}^{n} \int_{-\infty}^{\infty} e^{2n|x|} \overline{\hat{\phi}^{(q)}}(x) \hat{\psi}^{(q)}(x)\, dx \tag{A25}$$

where the scalar product incorporates both the exponential weight function $e^{2n|x|}$ that controls the growth behavior at infinity and the summation over derivatives up to order n, thereby creating a geometric structure that respects both the analytical properties of the test functions and their behavior under differentiation. The exponential weight ensures that functions with appropriate decay properties are properly incorporated into the inner product structure, while the inclusion of derivatives up to order n captures the smoothness requirements that characterize our test function spaces. This scalar product construction naturally induces the corresponding norm

$$||\hat{\phi}||_n^{''} = [< \hat{\phi}(x), \hat{\phi}(x) >_n]^{\frac{1}{2}} \tag{A26}$$

which provides a complete characterization of the geometric structure within each level of our hierarchical space construction, ensuring that the norm reflects both the exponential growth control and the derivative behavior that are essential for the mathematical consistency of our ultradistribution framework and its applications to quantum field theoretical calculations.

The norms $||\cdot||_j$ and $||\cdot||_n^{''}$ are equivalent, establishing that these different characterizations of the topology on $\mathfrak{Z}$ yield identical convergence properties and functional analytical structures, which ensures that $\mathfrak{Z}$ possesses the structure of a countably Hilbertian nuclear space. This equivalence is fundamental for the mathematical consistency of our framework, as it guarantees that the various analytical approaches to defining the space topology all yield the same geometric and topological properties. The nuclear and Hilbertian characteristics combine to provide $\mathfrak{Z}$ with exceptionally advantageous properties

for functional analysis applications, particularly in the context of spectral theory and the analysis of unbounded operators that arise naturally in quantum field theoretical contexts.

The hierarchical structure of our space construction becomes apparent when we consider $\mathfrak{Z}_p$ as the completion of $\mathfrak{Z}$ with respect to the norm p given in Equation (A26), which yields the fundamental decomposition

$$\mathfrak{Z} = \bigcap_{p=0}^{\infty} \mathfrak{Z}_p \tag{A27}$$

where each completed space $\mathfrak{Z}_p$ represents a different level of exponential growth control, and their intersection captures the most restrictive analytical properties from the entire hierarchy. The foundational level of this construction is characterized by

$$\mathfrak{Z}_0 = \boldsymbol{H} \tag{A28}$$

which identifies the base space as the familiar Hilbert space of square integrable functions, thereby connecting our sophisticated ultradistribution framework to the classical L^2 theory and ensuring compatibility with standard quantum mechanical formulations. As a consequence of this mathematical structure, the triplet

$$\mathfrak{U} = (\mathfrak{Z}, \boldsymbol{H}, \mathfrak{B}) \tag{A29}$$

constitutes a Gelfand triplet, inheriting all the powerful spectral properties and functional analytical advantages that characterize rigged Hilbert spaces and providing the mathematical foundation necessary for the rigorous treatment of unbounded operators and generalized eigenfunctions in our quantum gravitational applications.

The space $\mathfrak{B}$ can also be characterized through an alternative analytical approach, as detailed in refs. [26,54], where we consider $\mathfrak{C}_\omega$ to be the space of all functions $\hat{F}(z)$ that satisfy two fundamental analytical conditions governing their behavior in the complex domain. The first condition requires that $\hat{F}(z)$ is an analytic function for $\{z \in \mathbb{C} : |Im(z)| > p\}$, ensuring that the function possesses well-defined analytical properties outside of horizontal strips in the complex plane, thereby avoiding singularities in regions where the imaginary part exceeds the threshold parameter p. The second condition demands that the expression $\hat{F}(z)e^{-p|\Re(z)|}/z^p$ remains bounded and continuous within the closed regions $\{z \in \mathbb{C} : |Im(z)| \geq p\}$, where $p = 0, 1, 2, \ldots$ depends on the specific function $\hat{F}(z)$ under consideration, thereby controlling both the exponential growth along the real axis through the factor $e^{-p|\Re(z)|}$ and the polynomial behavior at infinity through the denominator z^p.

To complete this characterization, we introduce $\mathfrak{N}$ as the collection $\mathfrak{N} = \{\hat{F}(z) \in \mathfrak{C}_\omega : \hat{F}(z) \text{ is entire analytic}\}$, which represents the subset of functions in $\mathfrak{C}_\omega$ that are entire analytical throughout the complex plane and thus possess no singularities whatsoever. The space $\mathfrak{B}$ is then rigorously defined as the quotient space $\mathfrak{B} = \mathfrak{C}_\omega/\mathfrak{N}$, where we identify functions that differ only by entire analytical terms, ensuring that the resulting ultradistributions of exponential type are well-defined equivalence classes that capture the essential singular behavior while eliminating the ambiguity associated with the addition of entire functions that would not contribute to the distributional action on test functions.

Due to these fundamental analytical properties, it becomes possible to represent any ultradistribution of exponential type through the integral representation established in refs. [27,54] as

$$\hat{F}(\hat{\phi}) =< \hat{F}(z), \hat{\phi}(z) >= \oint_{\Gamma} \hat{F}(z)\hat{\phi}(z)\, dz \tag{A30}$$

where the integration contour Γ is constructed to run parallel to the real axis from $-\infty$ to ∞ when $Im(z) > \zeta$ with $\zeta > p$ and returns from ∞ to $-\infty$ when $Im(z) < -\zeta$ with $-\zeta < -p$, creating a closed contour that completely surrounds all singularities of $\hat{F}(z)$ in the complex domain. This contour construction is specifically designed to capture the complete analytical structure of the ultradistribution while respecting the exponential growth conditions and boundedness requirements that characterize the underlying function spaces, ensuring that the integral representation converges and provides a mathematically meaningful definition of the distributional action. The requirement that Γ surrounds all singularities of $\hat{F}(z)$ is essential for the consistency of the representation, as it guarantees that the contour integral captures all the relevant analytical information contained in the ultradistribution while avoiding any mathematical ambiguities that might arise from inappropriate contour choices or incomplete enclosure of the singular set.

Formula (A30) serves as our fundamental representation for an ultradistribution of exponential type throughout the subsequent mathematical development, providing the essential computational foundation for all analytical procedures involving these sophisticated generalized functions. The "Dirac Formula" for ultradistributions of exponential type, as rigorously established in refs. [26,54], takes the form

$$\hat{F}(z) \equiv \frac{1}{2\pi i} \int_{-\infty}^{\infty} \frac{\hat{f}(t)}{t-z}\, dt \equiv \frac{\cosh(\lambda z)}{2\pi i} \int_{-\infty}^{\infty} \frac{\hat{f}(t)}{(t-z)\cosh(\lambda t)}\, dt \tag{A31}$$

where the "density" $\hat{f}(t)$ represents the distributional cut or discontinuity of $\hat{F}(z)$ along the real axis, establishing the crucial connection between the analytical representation in the complex domain and the distributional behavior on the real line. This density function satisfies the fundamental consistency relation

$$\oint_{\Gamma} \hat{F}(z)\hat{\phi}(z)\, dz = \int_{-\infty}^{\infty} \hat{f}(t)\hat{\phi}(t)\, dt \tag{A32}$$

which demonstrates the equivalence between the contour integral representation and the distributional pairing on the real axis, ensuring mathematical consistency across different analytical approaches.

The application of Formula (A31) requires careful mathematical treatment and rigorous attention to the analytical properties of the functions involved. While $\hat{F}(z)$ maintains its analytical character on the integration contour Γ, the density $\hat{f}(t)$ typically exhibits singular behavior that necessitates interpretation within the framework of distribution theory, ensuring that the right-hand side of Equation (A32) is properly understood as a distributional pairing rather than a conventional Riemann or Lebesgue integral, thereby maintaining the mathematical rigor and physical meaningfulness required for applications to quantum field theoretical calculations.

Another important property of the analytical representation concerns the growth behavior of $\hat{F}(z)$ on the integration contour Γ, where $\hat{F}(z)$ is bounded by both an exponential function and a polynomial power of z as established in refs. [27,54] through the inequality

$$|\hat{F}(z)| \leq C|z|^{p} e^{p|\Re(z)|} \tag{A33}$$

where the constants C and p depend on the specific ultradistribution $\hat{F}$ under consideration, ensuring that the analytical functions in our exponential-type framework possess controlled growth properties that combine polynomial behavior with exponential growth along the real axis. This combined polynomial–exponential boundedness represents a fun-

damental characteristic that distinguishes ultradistributions of exponential type from their tempered counterparts and ensures the convergence of the various integral representations employed throughout our theory while maintaining compatibility with the exponential weight conditions that define the underlying test function spaces.

The representation given by Equation (A30) has the remarkable consequence that the addition of any entire function $\hat{G}(z) \in \mathfrak{N}$ to $\hat{F}(z)$ does not alter the resulting ultradistribution, as demonstrated through the calculation $\oint_\Gamma \{\hat{F}(z) + \hat{G}(z)\}\hat{\phi}(z)\ dz = \oint_\Gamma \hat{F}(z)\hat{\phi}(z)\ dz + \oint_\Gamma \hat{G}(z)\hat{\phi}(z)\ dz$. The integral involving the entire function vanishes, $\oint_\Gamma \hat{G}(z)\hat{\phi}(z)\ dz = 0$, because the product $\hat{G}(z)\hat{\phi}(z)$ is an entire analytical function throughout the complex domain, which allows the contour integral to be deformed to infinity where the rapidly decreasing nature of the test function ensures that the integrand vanishes. This fundamental property leads to the essential equivalence

$$\therefore \quad \oint_\Gamma \{\hat{F}(z) + \hat{G}(z)\}\hat{\phi}(z)\ dz = \oint_\Gamma \hat{F}(z)\hat{\phi}(z)\ dz \tag{A34}$$

demonstrating that ultradistributions of exponential type are well-defined equivalence classes modulo entire functions, ensuring that the mathematical structure is consistent and that the physical content of the theory is independent of the particular representative chosen from each equivalence class.

Another very important property of $\mathfrak{B}$ is that this space exhibits reflexivity under the Fourier transform, meaning that the space is preserved under both forward and inverse Fourier transformations, as expressed through the fundamental relationship

$$\mathfrak{B} = \mathscr{F}_c\{\mathfrak{B}\} = \mathscr{F}\{\mathfrak{B}\} \tag{A35}$$

where both the complex Fourier transform $\mathscr{F}_c$ and the standard Fourier transform $\mathscr{F}$ map the space $\mathfrak{B}$ onto itself, ensuring that the mathematical structure is preserved under these fundamental operations. The complex Fourier transform $F(k)$ of any ultradistribution $\hat{F}(z) \in \mathfrak{B}$ is given by the sophisticated expression

$$\begin{aligned} F(k) = H[\Im(k)] \int_{\Gamma_+} \hat{F}(z)e^{ikz}\ dz - H[-\Im(k)] \int_{\Gamma_-} \hat{F}(z)e^{ikz}\ dz = \\ \oint_\Gamma \{H[\Im(k)H[\Re(z)] - H[-\Im(k)H[-\Re(z)]\}\hat{F}(z)e^{ikz}\ dz = \\ H[\Im(k)] \int_0^\infty \hat{f}(x)e^{ikx}\ dx - H[-\Im(k)] \int_{-\infty}^0 \hat{f}(x)e^{ikx}\ dx \end{aligned} \tag{A36}$$

where H denotes the Heaviside function, Γ_+ represents the part of the contour Γ with $\Re(z) \geq 0$, and Γ_- corresponds to the part with $\Re(z) \leq 0$, ensuring that the Fourier transform respects the analytical structure and growth conditions characteristic of exponential-type ultradistributions.

Using the representation given by Equation (A36), we can interpret Dirac's Formula within this framework as

$$F(k) \equiv \frac{1}{2\pi i} \int_{-\infty}^{\infty} \frac{f(s)}{s-k}\ ds \equiv \mathscr{F}_c\Big\{\mathscr{F}^{-1}\{f(s)\}\Big\} \tag{A37}$$

which establishes the connection between the complex analytical representation and the distributional density on the real axis through the composition of forward and inverse

Fourier transforms. The corresponding inverse Fourier transform that recovers the original ultradistribution from its Fourier transform is given by

$$\hat{F}(z) = \frac{1}{2\pi} \oint_{\Gamma} \{H[\Im(z)]H[-\Re(k)] - H[-\Im(z)]H[\Re(k)]\} F(k) e^{-ikz}\, dk \tag{A38}$$

which completes the duality relationship and ensures that the Fourier transform constitutes a complete isomorphism on the space of exponential-type ultradistributions, providing the mathematical foundation necessary for momentum-space calculations and the treatment of quantum field theoretical problems within our ultradistribution framework.

The treatment for ultradistributions of exponential type defined on $\mathbb{C}^n$ follows a similar mathematical development to the case of one variable, with appropriate modifications to accommodate the multi-dimensional structure and the increased complexity that arises from the interaction between multiple complex variables. The regions Λ_j in the n-dimensional complex space are defined as

$$\Lambda_j = \{z = (z_1, z_2, \ldots, z_n) \in \mathbb{C}^n : |\Im(z_k)| \leq j \quad 1 \leq k \leq n\} \tag{A39}$$

which represent n-dimensional horizontal strips in the complex domain, where each coordinate z_k has its imaginary part bounded by the parameter j, creating a systematic hierarchy of domains that expand simultaneously in all directions as j increases. This construction ensures that the multi-dimensional framework preserves the essential analytical properties that characterize the one-dimensional theory while accommodating the tensor product structure that naturally arises in higher-dimensional contexts. The corresponding norm structure for the multi-dimensional case is given by

$$||\hat{\phi}||_j = \max_{k \leq j} \left\{ \sup_{z \in \Lambda_j} \left[e^{j\left[\sum_{p=1}^{n} |\Re(z_p)|\right]} \left| D^{(k)} \hat{\phi}(z) \right| \right] \right\} \tag{A40}$$

where the differential operator $D^{(k)} = \partial^{(k_1)} \partial^{(k_2)} \cdots \partial^{(k_n)}$ represents mixed partial derivatives with total order $k = k_1 + k_2 + \cdots + k_n$, and the exponential weight function $e^{j\left[\sum_{p=1}^{n} |\Re(z_p)|\right]}$ controls the growth behavior along all real directions simultaneously. This norm construction captures both the multi-dimensional exponential growth control and the behavior of all mixed partial derivatives up to order k, ensuring that functions in the multi-dimensional test function spaces maintain controlled analytical properties within the specified complex regions while respecting the exponential weight conditions that are essential for the mathematical consistency of the n-dimensional ultradistribution framework.

The n-dimensional space $\mathfrak{B}^n$ is characterized through a systematic extension of the one-dimensional framework that preserves the essential analytical properties while accommodating the increased complexity inherent in multi-variable complex analysis. We define $\mathfrak{C}_{\omega}^{n}$ as the space of all functions $\hat{F}(z)$ that satisfy two fundamental analytical conditions governing their behavior in the n-dimensional complex domain. The first condition requires that $\hat{F}(z)$ is analytic for $\{z \in \mathbb{C}^{\boldsymbol{n}} : |Im(z_1)| > p, |Im(z_2)| > p, \ldots, |Im(z_n)| > p\}$, ensuring that the function possesses well-defined analytical properties outside of n-dimensional horizontal strips in the complex space, thereby avoiding singularities in regions where all imaginary parts simultaneously exceed the threshold parameter p. This multi-dimensional analyticity requirement is more restrictive than simple analyticity in each variable separately, as it demands that the function be jointly analytic in all variables within the specified domain.

The second condition stipulates that the expression $\hat{F}(z)e^{-\left[p\sum_{j=1}^{n}|\Re(z_j)|\right]}/z^p$ remains bounded and continuous within the closed regions $\{z \in \mathbb{C}^{\boldsymbol{n}} : |Im(z_1)| \geq p, |Im(z_2)| \geq p, \ldots, |Im(z_n)| \geq p\}$, where $p = 0, 1, 2, \ldots$ depends on the specific function $\hat{F}(z)$ under consideration. This condition controls both the exponential growth along all real directions simultaneously through the factor $e^{-\left[p\sum_{j=1}^{n}|\Re(z_j)|\right]}$ and the polynomial behavior at infinity through the denominator z^p, ensuring that the multi-dimensional ultradistributions possess the controlled growth properties necessary for mathematical consistency while respecting the tensor product structure that characterizes the n-dimensional framework and maintaining compatibility with the exponential weight conditions that define the underlying multi-dimensional test function spaces.

To complete the characterization of the n-dimensional framework, we introduce $\mathfrak{N}^n$, as the collection

$$\mathfrak{N}^n = \left\{\hat{F}(z) \in \mathfrak{C}_{\omega}^{n} : \hat{F}(z)\right.$$

is an entire analytic function at minus in one of the variables $z_j \quad 1 \leq j \leq n\Big\}$, which represents the subset of functions in $\mathfrak{C}_{\omega}^{n}$ that are entire analytical in at least one of the complex variables z_j, thereby possessing no singularities with respect to that particular variable throughout the complex plane. This construction is essential for defining the quotient structure, as these entire functions represent the equivalence class elements that must be factored out to obtain well-defined ultradistributions. The space $\mathfrak{B}^n$ is then rigorously defined as the quotient space $\mathfrak{B}^n = \mathfrak{C}_{\omega}^{n}/\mathfrak{N}^n$, where we identify functions that differ only by elements of $\mathfrak{N}^n$, ensuring that the resulting n-dimensional ultradistributions of exponential type are well-defined equivalence classes that capture the essential multi-dimensional singular behavior while eliminating ambiguities associated with the addition of functions that are entire in at least one variable.

The fundamental representation for n-dimensional ultradistributions of exponential type is given by

$$\hat{F}(\hat{\phi}) =< \hat{F}(z), \hat{\phi}(z) >= \oint_{\Gamma} \hat{F}(z)\hat{\phi}(z)\, dz \tag{A41}$$

where the integration contour $\Gamma = \Gamma_1 \cup \Gamma_2 \cup ...\Gamma_n$ is constructed as the union of individual contours Γ_j that run parallel to the real axis from $-\infty$ to ∞ when $Im(z_j) > \zeta$ with $\zeta > p$ and return from ∞ to $-\infty$ when $Im(z_j) < -\zeta$ with $-\zeta < -p$, ensuring that the path Γ completely surrounds all singularities of $\hat{F}(z)$ in the n-dimensional complex domain. The corresponding n-dimensional Dirac Formula takes the form

$$\hat{F}(z) = \frac{1}{(2\pi i)^n} \int_{-\infty}^{\infty} \frac{\hat{f}(t)}{(t_1 - z_1)(t_2 - z_2)\ldots(t_n - z_n)}\, dt \tag{A42}$$

where the "density" $\hat{f}(t)$ satisfies the fundamental consistency relation

$$\oint_{\Gamma} \hat{F}(z)\hat{\phi}(z)\, dz = \int_{-\infty}^{\infty} \hat{f}(t)\hat{\phi}(t)\, dt \tag{A43}$$

demonstrating the equivalence between the multi-dimensional contour integral and the distributional pairing on the real domain. The growth behavior of $\hat{F}(z)$ is controlled by the bound

$$|\hat{F}(z)| \leq C|z|^p e^{\left[p\sum\limits_{j=1}^{n}|\Re(z_j)|\right]} \tag{A44}$$

where C and p depend on $\hat{F}$, ensuring that the n-dimensional ultradistributions possess the polynomial–exponential growth properties necessary for mathematical consistency while respecting the multi-dimensional structure of the underlying complex domain.

Appendix C. Mathematical Prerequisites and Foundational Framework

In this paper, we will not employ the functional integral approach to quantify the gravitational field due to two fundamental mathematical and physical limitations that render this method incompatible with our ultrahyperfunction framework. The first limitation arises from the fact that functional integral methods cannot adequately treat ultrahyperfunctions, since these sophisticated mathematical objects possess essential singularities located within a strip that surrounds the real axis, and conventional path integral techniques are not designed to handle such complex analytical structures that extend into the complex domain with specific growth and singularity patterns. The second limitation stems from the structure of our interacting Lagrangian, which contains derivative couplings of the graviton field that create additional technical complications when attempting to implement functional integral quantization procedures, as these derivative interactions require careful treatment of boundary terms and integration by parts that can compromise the mathematical rigor of the path integral approach.

Instead, we adopt the variational Schwinger–Feynman method [55], which represents the most general and mathematically robust quantization procedure currently available in quantum field theory, possessing the remarkable capability to handle even high-order supersymmetric theories, as demonstrated in the exemplary applications presented in [56,57]. This method proves particularly valuable because it can successfully quantize theoretical frameworks that cannot be treated using the conventional Dirac bracket technique, thereby providing the mathematical flexibility and generality necessary for our sophisticated ultrahyperfunction approach to quantum gravity while maintaining the rigorous analytical control required for handling the complex singularity structures and derivative couplings that characterize our gravitational field theory in the BTZ spacetime background.

For that purpose, we write the action for a set of fields in the form

$$\mathscr{S}[\sigma(x),\sigma_0,\phi_A(x)] = \int_{\sigma_0}^{\sigma(x)} \mathscr{L}[\phi_A(\xi),\partial_\mu\phi_A(\xi),\xi]d\xi, \tag{A45}$$

where $\sigma(x)$ if a space-like surface passes through the point x. σ_0 is a surface in the remote past, at which all field variations vanish. The Schwinger–Feynman variational principle establishes the following:

"Any Hermitian infinitesimal variation $\delta\mathscr{S}$ of the action induces a canonical transformation of the vector space in which the quantum system is defined, and the generator of this transformation is this same operator $\delta\mathscr{S}$".

As a consequence of this statement, we obtain [55]

$$\delta\phi_A = i[\delta\mathscr{S},\phi_A]. \tag{A46}$$

Thus, for a Poincare transformation, we have

$$\delta\mathscr{S} = a^\mu\mathscr{P}_\mu + \frac{1}{2}a^{\mu v}\mathscr{M}_{\mu v}, \tag{A47}$$

Therefore, the variation of the field is given by

$$\delta\phi_a = a^\mu\hat{P}_\mu\phi_A + \frac{1}{2}a^{\mu v}\hat{M}_{\mu v}\phi_A. \tag{A48}$$

From (A46)–(A48), we obtain

$$\partial_\mu \phi_A = i[\mathscr{P}_\mu, \phi_A]. \tag{A49}$$

In particular, when $\mu = 0$, we have

$$\partial_0 \phi_A = i[\mathscr{P}_0, \phi_A]. \tag{A50}$$

This result is used to quantize the QFTs. In particular, we will use it to quantize the EG.

Appendix D. The Correct Quantization of the Theory

We need to remember some usual definitions. The energy–momentum tensor is given by

$$T_\rho^\lambda = \frac{\partial \mathscr{L}}{\partial \partial^\rho \phi^{\mu v}} \partial^\lambda \phi^{\mu v} - \delta_\rho^\lambda \mathscr{L}, \tag{A51}$$

From this definition, we obtain the time component of the four-momentum vector

$$\mathscr{P}_0 = \int T_0^0 \, d^3x. \tag{A52}$$

Using Expression (12) of the Lagrangian of the free fields, we obtain

$$T_0^0 = \frac{1}{4}\Big[\partial_0 \phi_{\mu v} \partial^0 \phi^{\mu v} + \partial_j \phi_{\mu v} \partial^j \phi^{\mu v} - 2\partial_\alpha \phi_{\mu 0} \partial^0 \phi^{\mu \alpha} - 2\partial_\alpha \phi_{\mu j} \partial^j \phi^{\mu \alpha} +$$

$$2\partial_\alpha \phi^{\mu \alpha} \partial_0 \phi_\mu^0 + 2\partial_\alpha \phi^{\mu \alpha} \partial_j \phi_\mu^j - \frac{\Lambda}{2} \phi_{\mu v} \phi^{\mu v}\Big]. \tag{A53}$$

Consequently, from this last equation, we arrive at

$$\mathscr{P}_0 = \frac{1}{4} \int k_0 \Big[a_{\mu v}(\vec{k}) a^{+\mu v}(\vec{k}) + a^{+\mu v}(\vec{k}) a_{\mu v}(\vec{k})\Big] d^3k. \tag{A54}$$

We now use Equation (A50), and we have

$$[\mathscr{P}_0, a_{\mu v}(\vec{k})] = k_0 a_{\mu v}(\vec{k})$$

$$[\mathscr{P}_0, a^{+\mu v}(\vec{k})] = -k_0 a^{+\mu v}(\vec{k}). \tag{A55}$$

Replacing (A54) in (A55), we obtain the integral equation

$$k_0 a^{+\rho\lambda}(\vec{k'}) = \frac{1}{2} \int k_0 [a_{\mu v}(\vec{k}), a^{+\rho\lambda}(\vec{k'})] a^{+\mu v}(\vec{k}) \, d^3k. \tag{A56}$$

The solution of this equation is

$$\Big[a_{\mu v}(\vec{k}), a^{+\rho\lambda}(\vec{k'})\Big] = \Big[\delta_\mu^\rho \delta_v^\lambda + \delta_v^\rho \delta_\mu^\lambda\Big] \delta(\vec{k} - \vec{k'}). \tag{A57}$$

As customary, in the Gupta quantization for the graviton, the physical state $|\psi>$ of the theory is defined via the equation

$$\phi_\mu^\mu |\psi> = 0. \tag{A58}$$

We now use the usual definition for the graviton's propagator:

$$\Delta_{\mu\nu}^{\rho\lambda}(x - y) = <0|T[\phi_{\mu\nu}(x) \phi^{\rho\lambda}(y)]|0> . \tag{A59}$$

Thus, the propagator then turns out to be

$$\Delta^{\rho\lambda}_{\mu\nu}(x-y) = -\frac{i}{(2\tau)^4}(\delta^{\rho}_{\mu}\delta^{\lambda}_{v} + \delta^{\rho}_{v}\delta^{\lambda}_{\mu}) \int \frac{e^{ik_{\mu}(x^{\mu}-y^{\mu})}}{k^2 - m^2 + i0} d^4k. \tag{A60}$$

The tensor field of the graviton is defined as

$$\Phi(x) = \phi^{\rho\lambda}(x) dx_{\rho} \otimes dx_{\lambda} \tag{A61}$$

The corresponding propagator results in

$$\Delta(x-y) = < 0|T[\Phi(x) \otimes \Phi(y)]|0 > \tag{A62}$$

This is

$$\Delta(x-y) = \Delta^{\rho\lambda}_{\mu\nu}(x-y) dx_{\rho} \otimes dx_{\lambda} \otimes dy^{\mu} \otimes dy^{\nu} \tag{A63}$$

Using (A54), we can write

$$\mathscr{P}_0 = -\frac{1}{4} \int k_0 \left[a_{\mu v}(\vec{k}) a^{+\mu v}(\vec{k'}) + a^{+\mu v}(\vec{k'}) a_{\mu v}(\vec{k}) \right] \delta(\vec{k} - \vec{k'}) d^3k d^3k', \tag{A64}$$

According (A57), we get

$$\mathscr{P}_0 = -\frac{1}{4} \int k_0 \left[2a^{+\mu v}(\vec{k'}) a_{\mu v}(\vec{k}) + \delta(\vec{k} - \vec{k'}) \right] \delta(\vec{k} - \vec{k'}) d^3k d^3k'. \tag{A65}$$

We then obtain

$$\mathscr{P}_0 = -\frac{1}{2} \int k_0 a^{+\mu v}(\vec{k}) a_{\mu v}(\vec{k}) d^3k, \tag{A66}$$

Here, we utilized the fundamental property that the product of two delta functions with identical arguments vanishes [28], specifically $\delta(\vec{k} - \vec{k'})\delta(\vec{k} - \vec{k'}) = 0$, which represents a crucial mathematical result in the theory of ultrahyperfunctions that distinguishes our approach from conventional distribution theory, where such products are typically undefined or require additional regularization procedures. This remarkable property demonstrates that the employment of ultrahyperfunctions in our theoretical framework is mathematically equivalent to adopting normal ordering in the definition of the time component of the four-momentum, yielding the expression

$$\mathscr{P}_0 = -\frac{1}{4} \int k_0 : \left[a_{\mu v}(\vec{k}) a^{+\mu v}(\vec{k}) + a^{+\mu v}(\vec{k}) a_{\mu v}(\vec{k}) \right] : d^3k. \tag{A67}$$

where the colons denote normal ordering, and the automatic emergence of this ordering from our ultrahyperfunction treatment eliminates the need for ad hoc prescriptions that are typically required in conventional approaches to quantum field theory.

We must emphasize the critical requirement that physical states should satisfy not only the constraint given by Equation (A58) but also the additional relation established in [45–47] through

$$\partial_{\mu}\phi^{\mu v}|\psi >= 0. \tag{A68}$$

The resulting theoretical framework exhibits remarkable similarities to quantum electrodynamics when formulated using the Gupta–Bleuler quantization method, demonstrating that our obtained theory maintains unitarity at any finite perturbative order, which represents a fundamental requirement for any physically meaningful quantum field theory. When we carefully analyze the degrees of freedom present in our theory, we conclude that there exists only one type of free graviton ϕ^{12}, which corresponds to a single graviton species possessing exactly two possible transverse polarizations, as expected for a massless spin-2 particle

in four-dimensional spacetime. This result occurs specifically for the non-interacting theory, as originally observed by Gupta, and provides the essential foundation upon which our more complex interacting gravitational theory is systematically constructed.

Unitarity Violation in the Absence of the Additional Constraint

If we do not implement the new constraint given by Equation (A58), our theoretical framework undergoes a fundamental transformation that leads to significantly different mathematical and physical consequences, with the four-momentum taking the alternative form

$$\mathscr{P}_0 = -\frac{1}{2}\int k_0 \left[a^{+\mu v}(\vec{k}) a_{\mu v}(\vec{k}) - \frac{1}{2} a_{\mu}^{+\mu}(\vec{k}) a_{v}^{v}(\vec{k}) \right] d^3k, \tag{A69}$$

which differs substantially from our previous result by including additional terms that involve the trace components of the graviton field operators, thereby introducing extra degrees of freedom that prove to be problematic for the physical consistency of the theory. The application of the Feynman–Schwinger variational principle [55] to this modified four-momentum expression leads to the integral equation

$$k_0 a_{\rho\lambda}^{+}(\vec{k'}) =$$

$$\frac{1}{2}\int k_0 \left\{ a^{+\mu v}(\vec{k}) [a_{\mu v}(\vec{k}), a_{\rho\lambda}^{+}(\vec{k'})] - \frac{1}{2} a_{\mu}^{+\mu}(\vec{k}) [a_{v}^{v}(\vec{k}), a_{\rho\lambda}^{+}(\vec{k'})] \right\} d^3k, \tag{A70}$$

which incorporates both the standard graviton field commutators and additional terms involving the trace components that arise from the modified four-momentum structure.

The solution of this integral equation yields the commutation relations

$$\left[a_{\mu v}(\vec{k}), a_{\rho\lambda}^{+}(\vec{k'}) \right] = \left[\eta_{\mu\rho}\eta_{v\lambda} + \eta_{v\rho}\eta_{\mu\lambda} - \eta_{\rho\lambda}\eta_{\mu v} \right] \delta(\vec{k} - \vec{k'}). \tag{A71}$$

which represents the conventional graviton quantization procedure that has been extensively studied in the literature and is well-known to possess serious theoretical deficiencies. This standard approach to graviton quantification, while mathematically consistent at the level of canonical quantization, leads to a fundamental physical problem in that the resulting theory produces an S-matrix that fails to satisfy the unitarity requirement, as demonstrated in [45–47,58], thereby rendering the theory physically unacceptable for describing realistic gravitational interactions and highlighting the crucial importance of our modified constraint structure for maintaining the physical consistency and mathematical coherence of quantum gravitational theories.

Appendix E. The Correct Quantization of the Theory

We clarify that the content of this appendix has been adapted from the References [29,30] to simplify the reading of the paper and provide essential background material for readers who may be unfamiliar with the sophisticated mathematical techniques employed throughout our analysis. This appendix presents the fundamental theoretical framework for convolution operations involving Lorentz invariant ultrahyperfunctions, which represents one of the most technically challenging and mathematically demanding aspects of our ultradistribution approach to quantum field theory in curved spacetime environments.

In [29] Formula (7.34), we obtained a conceptually simple but rather lengthy expression for the convolution of two Lorentz invariant tempered ultradistributions, which serves as the mathematical foundation for evaluating the complex loop integrals that arise naturally in our quantum gravitational calculations and provides the analytical tools necessary

for handling the sophisticated singular structures that characterize graviton self-energy contributions in BTZ spacetime backgrounds. This convolution formula represents a significant mathematical achievement that extends far beyond conventional distribution theory to encompass the broader class of ultradistributions, thereby enabling us to handle the complex analytical structures and singular behaviors that would otherwise render our quantum field theoretical calculations mathematically ill-defined or physically meaningless,

$$H_\lambda(\rho,\Lambda)=\frac{1}{8\pi^2\rho}\int_{\Gamma_1}\int_{\Gamma_2}F(\rho_1)G(\rho_2)\rho_1^\lambda\rho_2^\lambda\{\Theta[\Im(\rho)]\{[\ln(-\rho_1+\Lambda)-\ln(-\rho_1-\Lambda)]\times$$

$$[\ln(-\rho_2+\Lambda)-\ln(-\rho_2-\Lambda)]\sqrt{4(\rho_1+\Lambda)(\rho_2+\Lambda)-(\rho-\rho_1-\rho_2-2\Lambda)^2}\times$$

$$\ln\left[\frac{\sqrt{4(\rho_1+\Lambda)(\rho_2+\Lambda)-(\rho-\rho_1-\rho_2-2\Lambda)^2}-i(\rho-\rho_1-\rho_2-2\Lambda)}{2\sqrt{(\rho_1+\Lambda)(\rho_2+\Lambda)}}\right]+$$

$$[\ln(\rho_1+\Lambda)-\ln(\rho_1-\Lambda)][\ln(\rho_2+\Lambda)-\ln(\rho_2-\Lambda)]\times$$

$$\sqrt{4(\rho_1-\Lambda)(\rho_2-\Lambda)-(\rho-\rho_1-\rho_2+2\Lambda)^2}\times$$

$$\ln\left[\frac{\sqrt{4(\rho_1-\Lambda)(\rho_2-\Lambda)-(\rho-\rho_1-\rho_2+2\Lambda)^2}-i(\rho-\rho_1-\rho_2+2\Lambda)}{2\sqrt{(\rho_1-\Lambda)(\rho_2-\Lambda)}}\right]+$$

$$[\ln(\rho_1+\Lambda)-\ln(\rho_1-\Lambda)][\ln(-\rho_2+\Lambda)-\ln(-\rho_2-\Lambda)]\times$$

$$\left\{\frac{i\pi}{2}\left[\sqrt{4(\rho_1+\Lambda)(\rho_2-\Lambda)-(\rho-\rho_1-\rho_2)^2}-i(\rho-\rho_1-\rho_2)\right]+\right.$$

$$\sqrt{4(\rho_1+\Lambda)(\rho_2-\Lambda)-(\rho-\rho_1-\rho_2)^2}\times$$

$$\left.\ln\left[\frac{\sqrt{4(\rho_1+\Lambda)(\rho_2-\Lambda)-(\rho-\rho_1-\rho_2)^2}-i(\rho-\rho_1-\rho_2)}{2i\sqrt{-(\rho_1+\Lambda)(\rho_2-\Lambda)}}\right]\right\}+$$

$$[\ln(-\rho_1+\Lambda)-\ln(-\rho_1-\Lambda)][\ln(\rho_2+\Lambda)-\ln(\rho_2-\Lambda)]\times$$

$$\left\{\frac{i\pi}{2}\left[\sqrt{4(\rho_1-\Lambda)(\rho_2+\Lambda)-(\rho-\rho_1-\rho_2)^2}-i(\rho-\rho_1-\rho_2)\right]+\right.$$

$$\sqrt{4(\rho_1-\Lambda)(\rho_2+\Lambda)-(\rho-\rho_1-\rho_2)^2}\times$$

$$\left.\left.\ln\left[\frac{\sqrt{4(\rho_1-\Lambda)(\rho_2+\Lambda)-(\rho-\rho_1-\rho_2)^2}-i(\rho-\rho_1-\rho_2)}{2i\sqrt{-(\rho_1-\Lambda)(\rho_2+\Lambda)}}\right]\right\}\right\}-$$

$$\Theta[-\Im(\rho)]\{[\ln(-\rho_1+\Lambda)-\ln(-\rho_1-\Lambda)][\ln(-\rho_2+\Lambda)-\ln(-\rho_2-\Lambda)]\times$$

$$\sqrt{4(\rho_1-\Lambda)(\rho_2-\Lambda)-(\rho-\rho_1-\rho_2+2\Lambda)^2}\times$$

$$\ln\left[\frac{\sqrt{4(\rho_1-\Lambda)(\rho_2-\Lambda)-(\rho-\rho_1-\rho_2+2\Lambda)^2}-i(\rho-\rho_1-\rho_2+2\Lambda)}{2\sqrt{(\rho_1-\Lambda)(\rho_2-\Lambda)}}\right]+$$

$$[\ln(\rho_1+\Lambda)-\ln(\rho_1-\Lambda)][\ln(\rho_2+\Lambda)-\ln(\rho_2-\Lambda)]\times$$

$$\sqrt{4(\rho_1+\Lambda)(\rho_2+\Lambda)-(\rho-\rho_1-\rho_2-2\Lambda)^2}\times$$

$$\ln\left[\frac{\sqrt{4(\rho_1+\Lambda)(\rho_2+\Lambda)-(\rho-\rho_1-\rho_2-2\Lambda)^2}-i(\rho-\rho_1-\rho_2-2\Lambda)}{2\sqrt{(\rho_1+\Lambda)(\rho_2+\Lambda)}}\right]+$$

$$[\ln(\rho_1+\Lambda)-\ln(\rho_1-\Lambda)][\ln(-\rho_2+\Lambda)-\ln(-\rho_2-\Lambda)]\times$$

$$\left\{\frac{i\pi}{2}\left[\sqrt{4(\rho_1-\Lambda)(\rho_2+\Lambda)-(\rho-\rho_1-\rho_2)^2}-i(\rho-\rho_1-\rho_2)\right]+\right.$$
$$\sqrt{4(\rho_1-\Lambda)(\rho_2+\Lambda)-(\rho-\rho_1-\rho_2)^2}\times$$
$$\left.\ln\left[\frac{\sqrt{4(\rho_1-\Lambda)(\rho_2+\Lambda)-(\rho-\rho_1-\rho_2)^2}-i(\rho-\rho_1-\rho_2)}{2i\sqrt{-(\rho_1-\Lambda)(\rho_2+\Lambda)}}\right]\right\}+$$
$$[\ln(-\rho_1+\Lambda)-\ln(-\rho_1-\Lambda)][\ln(\rho_2+\Lambda)-\ln(\rho_2-\Lambda)]\times$$
$$\left\{\frac{i\pi}{2}\left[\sqrt{4(\rho_1+\Lambda)(\rho_2-\Lambda)-(\rho-\rho_1-\rho_2)^2}-i(\rho-\rho_1-\rho_2)\right]+\right.$$
$$\sqrt{4(\rho_1+\Lambda)(\rho_2-\Lambda)-(\rho-\rho_1-\rho_2)^2}\times$$
$$\left.\left.\ln\left[\frac{\sqrt{4(\rho_1+\Lambda)(\rho_2-\Lambda)-(\rho-\rho_1-\rho_2)^2}-i(\rho-\rho_1-\rho_2)}{2i\sqrt{-(\rho_1+\Lambda)(\rho_2-\Lambda)}}\right]\right\}\right\}-\frac{i}{2}\times$$
$$\{[\ln(-\rho_1+\Lambda)-\ln(-\rho_1-\Lambda)][\ln(-\rho_2+\Lambda)-\ln(-\rho_2-\Lambda)]\times$$
$$(\rho_1-\rho_2)\left[\ln\left(i\sqrt{\frac{\rho_1+\Lambda}{\rho_2+\Lambda}}\right)+\ln\left(-i\sqrt{\frac{\rho_1-\Lambda}{\rho_2-\Lambda}}\right)\right]+$$
$$[\ln(\rho_1+\Lambda)-\ln(\rho_1-\Lambda)][\ln(\rho_2+\Lambda)-\ln(\rho_2-\Lambda)]\times$$
$$(\rho_1-\rho_2)\left[\ln\left(-i\sqrt{\frac{\Lambda-\rho_1}{\Lambda-\rho_2}}\right)+\ln\left(i\sqrt{\frac{\Lambda+\rho_1}{\Lambda+\rho_2}}\right)\right]+$$
$$[\ln(\rho_1+\Lambda)-\ln(\rho_1-\Lambda)][\ln(-\rho_2+\Lambda)-\ln(-\rho_2-\Lambda)]\times$$
$$\left\{(\rho_1-\rho_2)\left[\ln\left(\sqrt{\frac{\Lambda+\rho_1}{\Lambda-\rho_2}}\right)+\ln\left(\sqrt{\frac{\Lambda-\rho_1}{\Lambda+\rho_2}}\right)\right]+\right.$$
$$\frac{(\rho_1-\rho_2)}{2}[\ln(-\rho_1-\rho_2+\Lambda)-\ln(-\rho_1-\rho_2-\Lambda)-$$
$$\ln(\rho_1+\rho_2+\Lambda)+\ln(\rho_1+\rho_2-\Lambda)]+\rho_2[\ln(-\rho_1-\rho_2+\Lambda)-$$
$$\ln(-\rho_1-\rho_2-\Lambda)]+\rho_1[\ln(\rho_1+\rho_2+\Lambda)-\ln(\rho_1+\rho_2-\Lambda)]\}$$
$$[\ln(-\rho_1+\Lambda)-\ln(-\rho_1-\Lambda)][\ln(\rho_2+\Lambda)-\ln(\rho_2-\Lambda)]\times$$
$$\left\{(\rho_1-\rho_2)\left[\ln\left(\sqrt{\frac{\Lambda-\rho_1}{\Lambda+\rho_2}}\right)+\ln\left(\sqrt{\frac{\Lambda+\rho_1}{\Lambda-\rho_2}}\right)\right]+\right.$$
$$\frac{(\rho_1-\rho_2)}{2}[\ln(\rho_1+\rho_2+\Lambda)-\ln(\rho_1+\rho_2-\Lambda)-$$
$$\ln(-\rho_1-\rho_2+\Lambda)+\ln(-\rho_1-\rho_2-\Lambda)]+\rho_1[\ln(-\rho_1-\rho_2+\Lambda)-$$
$$\left.\left.\ln(-\rho_1-\rho_2-\Lambda)]+\rho_2[\ln(\rho_1+\rho_2+\Lambda)-\ln(\rho_1+\rho_2-\Lambda)]\}\right\}\right\}\,d\rho_1\,d\rho_2 \tag{A72}$$

This defines an ultradistribution in the variables ρ and Λ for $|\Im(\rho)|>\Im(\Lambda)>|\Im(\rho_1)|+|\Im(\rho_2)|$ Let $\mathfrak{B}$ be a vertical band contained in the complex λ-plane $\mathfrak{P}$. Integral (A72) is an analytic function of λ defined in the domain $\mathfrak{B}$. Moreover, it is bounded by a power of $|\rho\Lambda|$. Then, $H_\lambda(\rho,\Lambda)$ can be analytically continued to other parts of $\mathfrak{P}$. Thus, we define

$$H(\rho)=H^{(0)}(\rho,i0^+) \tag{A73}$$

$$H_\lambda(\rho,i0^+)=\sum_{-m}^{\infty}H^{(n)}(\rho,i0^+)\lambda^n \tag{A74}$$

As in the other cases, we now define

$$\{F * G\}(\rho) = H(\rho) \tag{A75}$$

as the convolution of two Lorentz invariant tempered ultradistributions. Alternatively, we can use the formula obtained in [30], Formula (10.1), for ultrahyperfunctions of exponential type:

$$H_{\gamma\lambda}(\rho,\Lambda) = \frac{1}{8\pi^2\rho}\int_{\Gamma_1}\int_{\Gamma_2}[2\cosh(\gamma\rho_1)]^{-\lambda}F(\rho_1)[2\cosh(\gamma\rho_2)]^{-\lambda}G(\rho_2)$$
$$\{\Theta[\Im(\rho)]\{[\ln(-\rho_1+\Lambda)-\ln(-\rho_1-\Lambda)]\times$$
$$[\ln(-\rho_2+\Lambda)-\ln(-\rho_2-\Lambda)]\sqrt{4(\rho_1+\Lambda)(\rho_2+\Lambda)-(\rho-\rho_1-\rho_2-2\Lambda)^2}\times$$
$$\ln\left[\frac{\sqrt{4(\rho_1+\Lambda)(\rho_2+\Lambda)-(\rho-\rho_1-\rho_2-2\Lambda)^2}-i(\rho-\rho_1-\rho_2-2\Lambda)}{2\sqrt{(\rho_1+\Lambda)(\rho_2+\Lambda)}}\right]+$$
$$[\ln(\rho_1+\Lambda)-\ln(\rho_1-\Lambda)][\ln(\rho_2+\Lambda)-\ln(\rho_2-\Lambda)]\times$$
$$\sqrt{4(\rho_1-\Lambda)(\rho_2-\Lambda)-(\rho-\rho_1-\rho_2+2\Lambda)^2}\times$$
$$\ln\left[\frac{\sqrt{4(\rho_1-\Lambda)(\rho_2-\Lambda)-(\rho-\rho_1-\rho_2+2\Lambda)^2}-i(\rho-\rho_1-\rho_2+2\Lambda)}{2\sqrt{(\rho_1-\Lambda)(\rho_2-\Lambda)}}\right]+$$
$$[\ln(\rho_1+\Lambda)-\ln(\rho_1-\Lambda)][\ln(-\rho_2+\Lambda)-\ln(-\rho_2-\Lambda)]\times$$
$$\left\{\frac{i\pi}{2}\left[\sqrt{4(\rho_1+\Lambda)(\rho_2-\Lambda)-(\rho-\rho_1-\rho_2)^2}-i(\rho-\rho_1-\rho_2)\right]+\right.$$
$$\sqrt{4(\rho_1+\Lambda)(\rho_2-\Lambda)-(\rho-\rho_1-\rho_2)^2}\times$$
$$\left.\ln\left[\frac{\sqrt{4(\rho_1+\Lambda)(\rho_2-\Lambda)-(\rho-\rho_1-\rho_2)^2}-i(\rho-\rho_1-\rho_2)}{2i\sqrt{-(\rho_1+\Lambda)(\rho_2-\Lambda)}}\right]\right\}+$$
$$[\ln(-\rho_1+\Lambda)-\ln(-\rho_1-\Lambda)][\ln(\rho_2+\Lambda)-\ln(\rho_2-\Lambda)]\times$$
$$\left\{\frac{i\pi}{2}\left[\sqrt{4(\rho_1-\Lambda)(\rho_2+\Lambda)-(\rho-\rho_1-\rho_2)^2}-i(\rho-\rho_1-\rho_2)\right]+\right.$$
$$\sqrt{4(\rho_1-\Lambda)(\rho_2+\Lambda)-(\rho-\rho_1-\rho_2)^2}\times$$
$$\left.\left.\ln\left[\frac{\sqrt{4(\rho_1-\Lambda)(\rho_2+\Lambda)-(\rho-\rho_1-\rho_2)^2}-i(\rho-\rho_1-\rho_2)}{2i\sqrt{-(\rho_1-\Lambda)(\rho_2+\Lambda)}}\right]\right\}\right\}-$$
$$\Theta[-\Im(\rho)]\{[\ln(-\rho_1+\Lambda)-\ln(-\rho_1-\Lambda)][\ln(-\rho_2+\Lambda)-\ln(-\rho_2-\Lambda)]\times$$
$$\sqrt{4(\rho_1-\Lambda)(\rho_2-\Lambda)-(\rho-\rho_1-\rho_2+2\Lambda)^2}\times$$
$$\ln\left[\frac{\sqrt{4(\rho_1-\Lambda)(\rho_2-\Lambda)-(\rho-\rho_1-\rho_2+2\Lambda)^2}-i(\rho-\rho_1-\rho_2+2\Lambda)}{2\sqrt{(\rho_1-\Lambda)(\rho_2-\Lambda)}}\right]+$$
$$[\ln(\rho_1+\Lambda)-\ln(\rho_1-\Lambda)][\ln(\rho_2+\Lambda)-\ln(\rho_2-\Lambda)]\times$$
$$\sqrt{4(\rho_1+\Lambda)(\rho_2+\Lambda)-(\rho-\rho_1-\rho_2-2\Lambda)^2}\times$$
$$\ln\left[\frac{\sqrt{4(\rho_1+\Lambda)(\rho_2+\Lambda)-(\rho-\rho_1-\rho_2-2\Lambda)^2}-i(\rho-\rho_1-\rho_2-2\Lambda)}{2\sqrt{(\rho_1+\Lambda)(\rho_2+\Lambda)}}\right]+$$

$$[\ln(\rho_1+\Lambda)-\ln(\rho_1-\Lambda)][\ln(-\rho_2+\Lambda)-\ln(-\rho_2-\Lambda)]\times$$
$$\left\{\frac{i\pi}{2}\left[\sqrt{4(\rho_1-\Lambda)(\rho_2+\Lambda)-(\rho-\rho_1-\rho_2)^2}-i(\rho-\rho_1-\rho_2)\right]+\right.$$
$$\sqrt{4(\rho_1-\Lambda)(\rho_2+\Lambda)-(\rho-\rho_1-\rho_2)^2}\times$$
$$\left.\ln\left[\frac{\sqrt{4(\rho_1-\Lambda)(\rho_2+\Lambda)-(\rho-\rho_1-\rho_2)^2}-i(\rho-\rho_1-\rho_2)}{2i\sqrt{-(\rho_1-\Lambda)(\rho_2+\Lambda)}}\right]\right\}+$$
$$[\ln(-\rho_1+\Lambda)-\ln(-\rho_1-\Lambda)][\ln(\rho_2+\Lambda)-\ln(\rho_2-\Lambda)]\times$$
$$\left\{\frac{i\pi}{2}\left[\sqrt{4(\rho_1+\Lambda)(\rho_2-\Lambda)-(\rho-\rho_1-\rho_2)^2}-i(\rho-\rho_1-\rho_2)\right]+\right.$$
$$\sqrt{4(\rho_1+\Lambda)(\rho_2-\Lambda)-(\rho-\rho_1-\rho_2)^2}\times$$
$$\left.\left.\ln\left[\frac{\sqrt{4(\rho_1+\Lambda)(\rho_2-\Lambda)-(\rho-\rho_1-\rho_2)^2}-i(\rho-\rho_1-\rho_2)}{2i\sqrt{-(\rho_1+\Lambda)(\rho_2-\Lambda)}}\right]\right\}\right\}-\frac{i}{2}\times$$
$$\{[\ln(-\rho_1+\Lambda)-\ln(-\rho_1-\Lambda)][\ln(-\rho_2+\Lambda)-\ln(-\rho_2-\Lambda)]\times$$
$$(\rho_1-\rho_2)\left[\ln\left(i\sqrt{\frac{\rho_1+\Lambda}{\rho_2+\Lambda}}\right)+\ln\left(-i\sqrt{\frac{\rho_1-\Lambda}{\rho_2-\Lambda}}\right)\right]+$$
$$[\ln(\rho_1+\Lambda)-\ln(\rho_1-\Lambda)][\ln(\rho_2+\Lambda)-\ln(\rho_2-\Lambda)]\times$$
$$(\rho_1-\rho_2)\left[\ln\left(-i\sqrt{\frac{\Lambda-\rho_1}{\Lambda-\rho_2}}\right)+\ln\left(i\sqrt{\frac{\Lambda+\rho_1}{\Lambda+\rho_2}}\right)\right]+$$
$$[\ln(\rho_1+\Lambda)-\ln(\rho_1-\Lambda)][\ln(-\rho_2+\Lambda)-\ln(-\rho_2-\Lambda)]\times$$
$$\left\{(\rho_1-\rho_2)\left[\ln\left(\sqrt{\frac{\Lambda+\rho_1}{\Lambda-\rho_2}}\right)+\ln\left(\sqrt{\frac{\Lambda-\rho_1}{\Lambda+\rho_2}}\right)\right]+\right.$$
$$\frac{(\rho_1-\rho_2)}{2}[\ln(-\rho_1-\rho_2+\Lambda)-\ln(-\rho_1-\rho_2-\Lambda)-$$
$$\ln(\rho_1+\rho_2+\Lambda)+\ln(\rho_1+\rho_2-\Lambda)]+\rho_2[\ln(-\rho_1-\rho_2+\Lambda)-$$
$$\ln(-\rho_1-\rho_2-\Lambda)]+\rho_1[\ln(\rho_1+\rho_2+\Lambda)-\ln(\rho_1+\rho_2-\Lambda)]\}$$
$$[\ln(-\rho_1+\Lambda)-\ln(-\rho_1-\Lambda)][\ln(\rho_2+\Lambda)-\ln(\rho_2-\Lambda)]\times$$
$$\left\{(\rho_1-\rho_2)\left[\ln\left(\sqrt{\frac{\Lambda-\rho_1}{\Lambda+\rho_2}}\right)+\ln\left(\sqrt{\frac{\Lambda+\rho_1}{\Lambda-\rho_2}}\right)\right]+\right.$$
$$\frac{(\rho_1-\rho_2)}{2}[\ln(\rho_1+\rho_2+\Lambda)-\ln(\rho_1+\rho_2-\Lambda)-$$
$$\ln(-\rho_1-\rho_2+\Lambda)+\ln(-\rho_1-\rho_2-\Lambda)]+\rho_1[\ln(-\rho_1-\rho_2+\Lambda)-$$
$$\left.\ln(-\rho_1-\rho_2-\Lambda)]+\rho_2[\ln(\rho_1+\rho_2+\Lambda)-\ln(\rho_1+\rho_2-\Lambda)]\}\right\}\,d\rho_1\,d\rho_2 \tag{A76}$$
$$|\Im(\rho)|>\Im(\Lambda)>|\Im(\rho_1)|+|\Im(\rho_2)|\;;\;\gamma<\min\left(\frac{\pi}{2\mid\Im(\rho_1)\mid};\frac{\pi}{2\mid\Im(\rho_2)\mid}\right)$$

We define

$$H(\rho)=H^{(0)}(\rho,i0^+)=H^{(0)}_{\gamma}(\rho,i0^+) \tag{A77}$$

$$H_{\gamma\lambda}(\rho,i0^+)=\sum_{-m}^{\infty}H^{(n)}_{\gamma}(\rho,i0^+)\lambda^n \tag{A78}$$

If we take into account that singularities (in the variable Λ) are contained in a horizontal band of width $|\sigma_0|$, we have

$$H_{\gamma\lambda}(\rho, i0^+) = \sum_{-m}^{\infty} H_{\gamma\lambda}^{(n)}(\rho, i\sigma)\frac{(-i\sigma)^n}{n!} \qquad \sigma > |\sigma_0| \tag{A79}$$

As in the other cases, we now define

$$\{F * G\}(\rho) = H(\rho) \tag{A80}$$

as the convolution of two Lorentz invariant ultradistributions of exponential type. Let $\hat{H}_{\gamma\lambda}(x)$ be the Fourier antitransform of $H_{\gamma\lambda}(\rho, i0^+)$:

$$\hat{H}_{\gamma\lambda}(x) = \sum_{n=-m}^{\infty} \hat{H}_{\gamma}^{(n)}(x)\lambda^n \tag{A81}$$

If we define

$$\begin{aligned} \hat{f}_{\gamma\lambda}(x) &= \mathscr{F}^{-1}\{F_{\gamma\lambda}(\rho)\} = \mathscr{F}^{-1}\{[\cosh(\gamma\rho)]^{-\lambda}F(\rho)\} \\ \hat{g}_{\gamma\lambda}(x) &= \mathscr{F}^{-1}\{G_{\gamma\lambda}(\rho)\} = \mathscr{F}^{-1}\{[\cosh(\gamma\rho)]^{-\lambda}G(\rho)\} \end{aligned} \tag{A82}$$

then

$$\hat{H}_{\gamma\lambda}(x) = (2\pi)^4\hat{f}_{\gamma\lambda}(x)\hat{g}_{\gamma\lambda}(x) \tag{A83}$$

and, taking into account Laurent's developments of $\hat{f}$ and $\hat{g}$,

$$\begin{aligned} \hat{f}_{\gamma\lambda}(x) &= \sum_{n=-m_f}^{\infty} \hat{f}_{\gamma}^{(n)}(x)\lambda^n \\ \hat{g}_{\gamma\lambda}(x) &= \sum_{n=-m_f}^{\infty} \hat{g}_{\gamma}^{(n)}(x)\lambda^n \end{aligned} \tag{A84}$$

we can write

$$\sum_{n=-m}^{\infty} \hat{H}_{\gamma}^{(n)}(x)\lambda^n = (2\pi)^4 \sum_{n=-m}^{\infty} \left(\sum_{k=-m}^{n} \hat{f}_{\gamma}^{(k)}(x)\hat{g}_{\gamma}^{(n-k)}(x) \right) \lambda^n \tag{A85}$$

$(m = m_f + m_g)$ and, as a consequence,

$$\hat{H}^{(0)}(x) = \sum_{k=-m}^{0} \hat{f}_{\gamma}^{(k)}(x)\hat{g}_{\gamma}^{(n-k)}(x) \tag{A86}$$

The Feynman propagators corresponding to a massless particle F and a massive particle G are, respectively, the following ultrahyperfunctions:

$$\begin{aligned} F(\rho) &= -\Theta[-\Im(\rho)]\rho^{-1} \\ G(\rho) &= -\Theta[-\Im(\rho)](\rho + m^2)^{-1} \end{aligned} \tag{A87}$$

where ρ is the complex variable such that, on the real axis, one has $\rho = k_1^2 + k_2^2 + k_3^2 - k_0^2$. On the real axis, the previously defined propagators are given by

$$\begin{aligned} f(\rho) &= F(\rho + i0) - F(\rho - i0) = (\rho - i0)^{-1} \\ g(\rho) &= G(\rho + i0) - G(\rho - i0) = (\rho + m^2 - i0)^{-1} \end{aligned} \tag{A88}$$

These are the usual expressions for Feynman propagators.

Consider first the convolution of two massless propagators. We use (A88), since, here, the corresponding ultrahyperfunctions do not have singularities in the complex plane. We obtain from (A72) a simplified expression for the convolution:

$$h_\lambda(\rho) = \frac{\pi}{2\rho} \iint_{-\infty}^{\infty} (\rho_1 - i0)^{\lambda-1} (\rho_2 - i0)^{\lambda-1} \left[(\rho - \rho_1 - \rho_2)^2 - 4\rho_1\rho_2 \right]_+^{\frac{1}{2}} d\rho_1 \, d\rho_2 \tag{A89}$$

This expression is nothing other than the usual convolution:

$$h_\lambda(\rho) = (\rho - i0)^{\lambda-1} * (\rho - i0)^{\lambda-1} \tag{A90}$$

Appendix F. A Mathematical Proof

According to the ultrahyperfunctions theory, we can write

$$\oint_\Gamma \ln(a-z)\phi(z)dz = \int_{-\infty}^{\infty} [\ln(a-x-i0) - \ln(a-x+i0)]\phi(x)dx = -2i\pi \int_{-\infty}^{\infty} H(x-a)\phi(x)dx \tag{A91}$$

So, we have the correspondence:

$$-\frac{1}{2\pi i} \ln(a-z) \longleftarrow H(x-a) \tag{A92}$$

Now using the Dirac formula for ultrahyperfunctions, we obtain

$$-\frac{1}{2\pi i} \ln(a-z) = \frac{1}{2\pi i} \int_{-\infty}^{\infty} \frac{H(x-a)}{x-z} dx = \frac{1}{2\pi i} \int_{a}^{\infty} \frac{1}{x-z} dx \tag{A93}$$

Thus,

$$\ln(a-z) = -\int_{a}^{\infty} \frac{1}{x-z} dx \tag{A94}$$

We then have for $a > 0$

$$\ln a = -\int_{a}^{\infty} \frac{1}{x} dx \tag{A95}$$

According to the result obtained by Guelfand in [49],

$$\int_{0}^{\infty} \frac{1}{x} dx = 0 \tag{A96}$$

and, therefore,

$$\ln a = \int_{0}^{a} \frac{1}{x} dx \tag{A97}$$

Appendix G. Essentials of the Tempered Ultrahyperfunction Framework

This brief overview summarizes the basic elements of ultrahyperfunction and tempered ultradistribution theory needed for the main text. It is intended to make the paper self-contained for readers who are not specialists in this mathematical area.

(i) Definition.

The Fourier transform of a distribution of exponential type $\hat{F}$ is given by the integral

$$F(k) = \int_{-\infty}^{\infty} H[\Im(k)]H[\Re(x) - H[-\Im(k)]H[-\Re(x)]\hat{F}(x)e^{ikx}\,dx =$$

$$H[\Im(k)]\int_{0}^{\infty}\hat{F}(x)e^{ikx} - H[-\Im(k)]\int_{-\infty}^{0}\hat{F}(x)e^{ikx} \tag{A98}$$

where F is the corresponding tempered ultradistribution. Let $\mathfrak{H}$ denote the space of analytic functions on $\mathbb{C}$, with norms given by

$$\|\phi\|_{pn} = \sup_{z\in V_n}(1+|z|)^p|\phi(z)| \tag{A99}$$

The dual of $\mathfrak{H}$ is the space $\mathscr{U}$ of tempered ultradistributions

(ii) Boundary value representation.

Every $F \in \mathscr{U}$ can be represented as

$$F(\phi) =< F(z), \phi(z) >= \oint_{\Gamma} F(z)\phi(z)\,dz \tag{A100}$$

where the integration contour $\Gamma =$ is the contour that runs parallel to the real axis from $-\infty$ to ∞ when $Im(z_j) > p$ with and returns from ∞ to $-\infty$ when $Im(z_j) < -p$. This contour construction ensures that Γ completely surrounds all singularities of $F(z)$ in the complex domain, thereby guaranteeing that the integral representation captures the complete analytical structure of the ultradistribution while respecting the growth conditions and boundedness requirements that characterize the underlying function spaces.

(iii) Operations and convolution.

Derivatives and convolutions are continuous in this topology:

$$\{F * G\}(\rho) = H(\rho) = (\text{E.4}) \tag{A101}$$

$F' \in \mathscr{U}$. This ensures that products of fields and Green functions remain well-defined without ad hoc regulators.

(iv) Relation to other spaces.

The inclusion chain

$$\mathfrak{H} \subset \mathcal{S}(\mathbb{R}^n) \subset \mathcal{S}'(\mathbb{R}^n) \subset \mathscr{U} \tag{A102}$$

shows that ultrahyperfunctions extend distributions while retaining control of analytic and growth properties.

(v) Comparison of spaces.

To see a comparison of the distribution spaces used in quantum field theory, see Table A1.

Table A1. Comparison of distribution spaces used in quantum field theory.

Property	**Schwartz $\mathscr{S}'$**	**Hadamard/Microlocal**	**Ultrahyperfunction $\mathscr{U}$**
Domain	$\mathbb{R}^n$	Local	**Outside of Analytic boundary**
Singularities	Polynomial	Conic	**Analytic boundary**
Growth control	Polynomial	Polynomial	**Polynomial**
Regularization need	Yes	Partial	**No (intrinsic)**
Curved-space covariance	Moderate	Local	**Global analytic**

(vi) Relevance to this work.

The use of $\mathscr{U}$ as the test-function dual space guarantees microcausality, covariance, and the finiteness of all loop integrals. Readers seeking further mathematical details may consult refs. [26,51,54,59].

References

1. Bañados, M.; Teitelboim, C.; Zanelli, J. Black hole in three-dimensional spacetime. *Phys. Rev. Lett.* **1992**, *69*, 1849–1851. [CrossRef]
2. Maldacena, J. The Large-N Limit of Superconformal Field Theories and Supergravity. *Int. J. Theor. Phys.* **1999**, *38*, 1113–1133. [CrossRef]
3. Witten, E. Anti De Sitter Space And Holography. *Adv. Theor. Math. Phys.* **1998**, *2*, 253–291. [CrossRef]
4. Sa, P.M.; Kleber, A.; Lemos, J.P. Black holes in three-dimensional dilaton gravity theories. *Quantum Gravity* **1996**, *13*, 125–138. [CrossRef]
5. de Rham, C.; Gabadadze, G. Generalization of the Fierz-Pauli action. *Phys. Rev. D* **2010**, *82*, 044020. [CrossRef]
6. de Rham, C.; Gabadadze, G.; Tolley, A.J. Resummation of Massive Gravity. *Phys. Rev. Lett.* **2011**, *106*, 231101. [CrossRef] [PubMed]
7. Hinterbichler, K. Theoretical aspects of massive gravity. *Rev. Mod. Phys.* **2012**, *84*, 671–710. [CrossRef]
8. de Rham, C. Massive Gravity. *Living Rev. Rel.* **2014**, *17*, 7–189. [CrossRef]
9. Strominger, A. Black hole entropy from near-horizon microstates. *J. High Energy Phys.* **1998**, *1998*, JHEP02. [CrossRef]
10. Birmingham, D. Choptuik scaling and quasinormal modes in the anti–de Sitter spaceÕconformal-field theory correspondence. *Phys. Rev.* **2001**, *D64*, 064024.
11. Carlip, S. Entropy versus action in the (2 + 1)-dimensional Hartle-Hawking wave function. *Phys. Rev. D* **1992**, *46*, 4387–4395. [CrossRef] [PubMed]
12. Singh, D.V.; Sachan, S. How are the degrees of freedom responsible for entropy in BTZ spacetime? *J. Hologr. Appl. Phys.* **2022**, *2*, 93–100.
13. Cai, R.-G.; Zhang, Y.-Z. Black plane solutions in four-dimensional spacetimes. *Phys. Rev. D* **1996**, *54*, 4891–4898. [CrossRef] [PubMed]
14. Mann, R.B.; Stelea, C. New Taub-NUT-Reissner-Nordström spaces in higher dimensions. *Phys. Lett. B* **2006**, *632*, 537–542. [CrossRef]
15. Sadekov, D. Effective graviton mass in de Sitter space. *Phys. Rev. D* **2024**, *109*, 085001. [CrossRef]
16. Tan, L.; Tsamis, N.C.; Woodard, R.P. Graviton Self-Energy from Gravitons in Cosmology. *Class. Quantum Gravity* **2021**, *38*, 145024. [CrossRef]
17. Leonard, K.E.; Park, S.; Prokopec, T.; Woodard, R.P. Representing the graviton self-energy on de Sitter background. *Phys. Rev. D* **2014**, *90*, 024032. [CrossRef]
18. Novello, M.; Neves, R.P. The mass of the graviton and the cosmological constant. *Class. Quantum Gravity* **2003**, *20*, L67–L73. [CrossRef]
19. Burns, D.; Pilaftsis, A. Matter quantum corrections to the graviton self-energy and the Newtonian potential. *Phys. Rev. D* **2015**, *91*, 064047. [CrossRef]
20. Chen, W. Semi-automatic calculations of multi-loop Feynman amplitudes with AmpRed. *Comput. Phys. Commun.* **2025**, *312*, 109607. [CrossRef]
21. Isaev, A.P. Multi-loop Feynman integrals and conformal quantum mechanics. *Nucl. Phys. B* **2003**, *662*, 461–475. [CrossRef]
22. Britto, R. Generalized Cuts of Feynman Integrals in Parameter Space. *Phys. Rev. Lett.* **2023**, *131*, 091601. [CrossRef]
23. Bjerrum-Bohr, N.E.J.; Donoghue, J.F.; Holstein, B.R. Quantum corrections to the Schwarzschild and Kerr metrics. *Phys. Rev. D* **2003**, *68*, 084005-1–084005-16; Erratum in *Phys. Rev. D* **2005**, *D71*, 069904. [CrossRef]

24. Knorr, B.; Schiffer, M. Non-Perturbative Propagators in Quantum Gravity. *Universe* **2021**, *7*, 216. [CrossRef]
25. Caron-Huot, S.; Li, Y.-Z. Gravity and a universal cutoff for field theory. *J. High Energy Phys.* **2025**, *2025*, 115. [CrossRef]
26. Sebastiao e Silva, J. Les fonctions analytiques comme ultra-distributions dans le calcul opérationnel. *Math. Ann.* **1958**, *136*, 58–96. [CrossRef]
27. Hasumi, M. Note on the N-Dimensional Tempered Ultra-Distributions. *Tôhoku Math. J.* **1961**, *13*, 94–104. [CrossRef]
28. Bollini, C.G.; Escobar, T.; Rocca, M.C. Convolution of Ultradistributions and Field Theory. *Int. J. Theor. Phys.* **1999**, *38*, 2315–2332. [CrossRef]
29. Bollini, C.G.; Rocca, M.C. Convolution of Lorentz Invariant Ultradistributions and Field Theory. *Int. J. Theor. Phys.* **2004**, *43*, 1019–1053. [CrossRef]
30. Bollini, C.G.; Marchiano, P.; Rocca, M.C. Convolution of Ultradistributions, Field Theory, Lorentz Invariance and Resonances. *Int. J. Theor. Phys.* **2007**, *46*, 3030–3059. [CrossRef]
31. Franco, D.H.T.; Renoldi, L.H. A note on Fourier–Laplace transform and analytic wave front set in theory of tempered ultrahyperfunctions. *J. Math. Anal. Appl.* **2007**, *325*, 819–829. [CrossRef]
32. Daniel, H.T. Holomorphic extension theorem for tempered ultrahyperfunctions. *Port. Math.* **2009**, *66*, 175–190. [CrossRef]
33. Franco, D.H.; Lourenço, J.A.; Renoldi, L.H. The ultrahyperfunctional approach to non-commutative quantum field theory. *J. Phys. A Math. Theor.* **2008**, *41*, 095402; Erratum in *J. Phys. A Math. Theor.* **2009**, *42*, 369801. [CrossRef]
34. Plastino, A.; Rocca, M.C. Quantum field theory, Feynman-, Wheeler propagators, dimensional regularization in configuration space and convolution of Lorentz Invariant Tempered Distributions. *J. Phys. Commun.* **2018**, *2*, 115029. [CrossRef]
35. Hameeda, M.; Plastino, A.; Rocca, M.C. Galaxies' clustering generalized theory. *Phys. Dark Universe* **2021**, *32*, 100816. [CrossRef]
36. Hameeda, M.; Gani, Q.; Pourhassan, B.; Rocca, M.C. Boltzmann and Tsallis statistical approaches to study quantum corrections at large distances and clustering of galaxies. *Int. J. Mod. Phys. A* **2022**, *37*, 2250116. [CrossRef]
37. Gani, Q.; Hameeda, M.; Pourhassan, B.; Rocca, M.C. Revisiting the Schwarzschild black hole solution: A distributional approach. *Phys. Dark Universe* **2024**, *46*, 101604. [CrossRef]
38. Hameeda, M.; Rocca, M.C. Supercoherent states of the open NS world sheet superstring. *J. Hologr. Appl. Phys.* **2021**, *1*, 57–70.
39. Rocca, M.C.; Plastino, A.R.; Plastino, A.; Ferri, G.L.; Paoli, A.L.D. New Solution of Diffusion–Advection Equation for Cosmic-Ray Transport Using Ultradistributions. *J. Stat. Phys.* **2015**, *161*, 986–1009. [CrossRef]
40. Paoli, A.L.D.; Estevez, M.; Vucetich, H.; Rocca, M.C. Study of Gamow States in the Rigged Hilbert Space with Tempered Ultradistributions. *Infin. Dimens. Anal. Quantum Probab. Relat. Top.* **2001**, *4*, 511–520. [CrossRef]
41. Bollini, C.G.; Rocca, M.C. Bosonic String and String Field Theory: A Solution Using Ultradistributions of Exponential Type. *Int. J. Theor. Phys.* **2008**, *47*, 1409–1423. [CrossRef]
42. Bollini, C.G.; Rocca, M.C. A Solution to Non-Linear Equations of Motion of Nambu-Goto String. *Open Nuc. Part. Phys. J.* **2011**, *4*, 4–12. [CrossRef]
43. Hameeda, M.; Plastino, A.; Rocca, M.C. Quantum Theory of 3+1 Gravity and Dark Matter: A New Formulation of the Gupta-Feynman based Quantum Field Theory of 3+1 Einstein Gravity. *J. Hologr. Appl. Phys.* **2024**, *4*, 21–58. [CrossRef]
44. Upadhyay, S.; Islam, N.U.; Ganai, P.A. A modified thermodynamics of rotating and charged BTZ black hole. *J. Hologr. Appl. Phys.* **2022**, *2*, 25–48.
45. Gupta, S.N. Quantization of Einstein's Gravitational Field: Linear Approximation. *Proc. Pys. Soc. A* **1952**, *65*, 161–169. [CrossRef]
46. Gupta, S.N. Quantization of Einstein's Gravitational Field: General Treatment. *Proc. Pys. Soc. A* **1952**, *65*, 608–619. [CrossRef]
47. Gupta, S.N. Supplementary Conditions in the Quantized Gravitational Theory. *Phys. Rev.* **1968**, *172*, 1303–1307. [CrossRef]
48. Plastino, A.; Rocca, M.C. *Dimensional Regularization and Non-Renormalizable Quantum Field Theories*; Cambridge Scholars Publishing: Newcastle upon Tyne, UK, 2021.
49. Gel'fand, I.M.; Shilov, G.E. *Generalized Functions*; Academic Press: Cambridge, MA, USA, 1964; Volume 1.
50. Peccei, R.D. The Strong CP Problem and Axions. In *Axions: Theory, Cosmology, and Experimental Searches*; Lecture Notes in Physics; Markus, K., Georg, R., Berta, B., Eds.; Springer: Berlin/Heidelberg, Germany, 2008; Volume 741, pp. 3–17.
51. Gel'fand, I.M.; Shilov, G.E. *Generalized Functions*; Academic Press: Cambridge, MA, USA, 1968; Volume 2.
52. Gel'fand, I.M.; Vilenkin, N.Y. *Generalized Functions*; Academic Press: Cambridge, MA, USA, 1968; Volume 4.
53. Schwartz, L. *Théorie des Distributions*; Hermann: Paris, France, 1966.
54. Hoskins, R.F.; Pinto, J.S. *Distributions, Ultradistributions and Other Generalised Functions*; Ellis Horwood: Chichester, UK, 1994.
55. Visconti, A. *Quantum Field Theory*; Pergamon Press: Oxford, UK, 1969.
56. Delbourgo, R.; Prasad, V.B. Supersymmetry in the four-dimensional limit. *J. Phys. G Nucl. Phys.* **1975**, *1*, 377–380. [CrossRef]
57. Barci, D.G.; Bollini, C.G.; Rocca, M.C. Quantization of a Six-Dimensional Wess-Zumino Model. *Il Nuovo C.* **1995**, *108*, 797–808. [CrossRef]

58. Feynman, R.P. Quantum Theory If Gravitation. *Acta Phys. Pol.* **1963**, *24*, 841–866.
59. Kawata, T. *Fourier Analysis in Probability Theory*; Academic Press: New York, NY, USA, 1972.